(E77-10027) USE OF SATELLITE PICTURES FOR DETERMINING MAJOR SHIELD FRACTURES RELEVANT FOR ORE PROSPECTING, NORTHERN FINLAND (Helsinki Univ.) 101 p HC A06/MF A01 CSCL 08G G3/43

N77-11490

Unclas
00027

1580B

SR No. 580-03

USE OF SATELLITE PICTURES FOR DETERMINING MAJOR SHIELD FRACTURES RELEVANT FOR ORE PROSPECTING, NORTHERN FINLAND

by Jussi Aarnisalo
Outokumpu Oy, Exploration
P.O. Box 27
SF-02101 Espoo 10
Finland

for Heikki V. Tuominen, Principal Investigator
Department of Geology
University of Helsinki
Snellmaninkatu 5
SF-00170 Helsinki 17
Finland

September 1976

Type III Report

Ore-geological Commission
of Northern Finland, Ministry
of Commerce and Industry
of Finland

Aleksanterinkatu 10
SF-00170 Helsinki 17
Finland

Goddard Space Flight Center
Greenbelt, Maryland 20771

1.	SR No. 580-03 2. Type of Report Type III Report	3.	Recipient's Catalog. No.
4.	Title Use of Satellite Pictures for Determining Major Shield Fractures Relevant for Ore Prospecting, Northern Finland	5.	Report Date First Draft: May 11, 1974 Final Draft: Sept. 30, 1976
		6.	Period Covered
7.	Principal Investigator Dr. Heikki V. Tuominen	8.	No. of Pages 92
9.	Name and Address of Principal Investigator's Organization Dept. of Geology, Univ. of Helsinki Snellmaninkatu 5 SF-00170 Helsinki 17, Finland	10.	Principal Investigator's Report No.
		11.	GSFC Technical Monitor Ensor, G.
12.	Sponsoring Agency Name and Address Ore-geological Commission of Northern Finland, Ministry of Commerce and Industry of Finland Aleksanterinkatu 10 SF-00170 Helsinki 17, Finland	13.	Key Words (Selected by Principal Investigator) Structural Survey (3K)
14.	Supplementary Notes Report Prepared by Jussi Aarnisalo, Co-investigator Outokumpu Oy, Exploration P.O. Box 27 SF-02101 Espoo 10, Finland		

15. Abstract

Applicability of LANDSAT-1 imagery to detection of major fractures of the Baltic Shield has been studied in northern Finland. Comparison of the MSS bands and their various photographic versions with extensive other data obtained by analysis of aerial photos, aeromagnetic maps and other maps indicates that the major fracture zones are represented by long lineaments in the imagery. These zones divide the bedrock into a mosaic of blocks which in many cases coincide with areas of distinctive rock units. The fracture trends and patterns of the Svecokarelian formations and their Archean basement, the main tectonic/lithologic units of the region, are characteristically different. Differences of this sort seem to occur also between the major rock units or blocks of the area. The known base metal occurences of the area show a tendency to concentrate along the fracture zones. An association of different types of mineralizations with fractures of different trends seems possible in the light of the data available.

PREFACE

Application of satellite imagery to regional geological and other studies has been a subject of growing interest in Finland since the early days of weather satellites. When the participation in ERTS-1 (now LANDSAT-1) program of NASA became available, three Finnish programs of different disciplines were suggested and became accepted by NASA. One of these was the geological program (No. SR-530-03), the results of which are discussed in the present paper.

The program was accomplished by the Department of Geology of the University of Helsinki in years 1972-1974 and later jointly by this institute and the Outokumpu Exploration. The Geological Survey of Finland assisted at the work. The research was carried out under the sponsorship of the Ore-geological Commission of Northern Finland, Ministry of Commerce and Industry of Finland.

Aside Dr. Heikki V. Tuominen, the principle investigator, the program staff was formed by Mr. Jussi Aarnisalo, M.Sc., Mr. Kaj Österlund, Ph.Lic., Mr. Viljo Kuosmanen, B.Sc., Mr. Aimo Kuivamäki, B.Sc. and Mr. Jorma Räsänen, B.Sc. A number of geology students of the University of Helsinki also took part in the work. Dr. Jorma Kujansuu and Dr. Raimo Lauerma from the Geological Survey of Finland assisted at the initial study of the imagery. Dr. Jouko Talvitie, Geophysics Department of the University of Oulu, studied the imagery covering the surroundings of the city of Oulu. Professor Aimo Mikkola, Helsinki University of Technology, kindly gave his personal ore data file to be used in the program. The Ore Data File Project of northern Finland gave additional information for the map of base metal deposits and mineralizations of northern Finland.

In his comments of the first draft of this report, the Scientific Monitor pointed out, for instance, that the use of the presented fracture map to aid ore prospecting was treated only superficially and that the lineaments

and fractures had not been classified according to their structural significance. Attempts to complement the report in these respects has required extensive additional investigations, which have delayed the finishing of the report.

USE OF SATELLITE PICTURES FOR DETERMINING MAJOR SHIELD FRACTURES RELEVANT FOR ORE PROSPECTING, NORTHERN FINLAND

by Jussi Aarnisalo

Outokumpu Oy, Exploration
P.O. Box 27
SF-02101 Espoo 10
Finland

for Heikki V. Tuominen, Principal Investigator

Department of Geology
University of Helsinki
Snellmaninkatu 5
SF-00170 Helsinki 17
Finland

September 1976

Type III Report

. TABLE OF CONTENTS

Section			Page
LIST OF ILLUSTRATIONS, TABLES AND PLATES			3
1.0	SUMMARY REPORT		
	1.1	General	7
	1.2	Significant results	8
	1.3	Recommendations	10
2.0	TECHNICAL REPORT		
	2.1	Image processing	10
	2.2	Processing of background data	15
	2.3	Field surveys	16
	2.4	Published articles and papers	17
3.0	RESULTS		
	3.1	General	19
	3.2	Linears of central Finnish Lapland	26
		3.2.1 Comparison between photolinears and LANDSAT-linears	27
		3.2.2 Map of linears	37
		3.2.3 LANDSAT-linears discarded	42
		3.2.4 Classification and trend analysis of the linears	45
	3.3	Fracture zones of central Finnish Lapland	62
	3.4	Major fracture zones of northern Finland	68
	3.5	Mineralizations and major fracture zones	75
4.0	CONCLUSIONS		81
REFERENCES			84
NOTES ON THE PLATES			92
PLATES			

LIST OF ILLUSTRATIONS, TABLES AND PLATES

Figures		Page
Fig. 1.	Test site of the program and the coverage of the LANDSAT scenes mainly used in the study.	11
Fig.2.	Examples of density level gradients in variously enhanced images.	13
Fig.3.	A mosaic of LANDSAT winter images of an area around the city of Oulu, Finland, processed with the equidensity method.	14
Fig.4.	LANDSAT image (1039-09315-5) of central Finnish Lapland.	20
Fig.5.	Bedrock features discernible on LANDSAT images in Finnish Lapland.	21
Fig.6.	A masking enhancement picture (5/7) of scene 1039-09315.	22
Fig.7.	Layering in the granulite complex in northern Finnish Lapland.	25
Fig.8.	Map of photolinears of central Finnish Lapland.	28
Fig.9.	LANDSAT-linears interpreted from LANDSAT-1 scene 1039-09315.	29
Fig.10.	Comparison of photolinears and LANDSAT-linears.	31
Fig.11.	The test areas for comparison of strike-frequency distribution of the photo-linears, LANDSAT-linears, and the corresponding LANDSAT-image.	34

Fig.12.	Relative strike-frequency curves obtained by optical filtering of an equivalent circular area of the maps of LANDSAT-linears, LANDSAT image 1039-09315-7 and photolinears.	35
Fig.13.	LANDSAT-linears interpreted from scene 1215-09102 and 1216-09160.	38
Fig.14.	Linears interpreted from the map of bogs and watercourses of central Finnish Lapland.	39
Fig.15.	Map of linears in central Finnish Lapland.	41
Fig.16.	a) LANDSAT-linears of scene 1039-09315, or parts of them, not included in Fig. 15. b) the relative strike-frequency curve of the LANDSAT-linears shown in (a).	43
Fig.17.	Class I linears, representing fracture and fault zones.	47
Fig.18.	Class II linears, representing bedrock trends.	48
Fig.19.	Class III linears, representing minor faults, fractures, jointing, dikes, etc.	49
Fig.20.	Strike-frequency analysis of different classes of linears.	51
Fig.21.	Main trends of crustal shear in the Baltic Shield according to Tuominen et al. (1973) and main trends of Class I linears of central Finnish Lapland.	52
Fig.22.	Areal distributions of Class I linears of different maximum trends in central Finnish Lapland.	56 57

Fig.23.	Relative strike frequency curves of Class I linears for E and W parts of the study area.	59
Fig.24.	Azimuthal sector combinations revealing different patterns of Class I linears within S ecokarelidic formations and their basement complex.	61
Fig.25.	Trends of the aeromagnetic anomalies.	63
Fig.26.	Class I linears combined with Class II linears representing bedrock trends in central Finnish Lapland.	64
Fig.27.	Generalized bedrock map of central Finnish Lapland.	65
Fig.28.	Basic and ultrabasic rocks of central Finnish Lapland.	66
Fig.29.	Uncontrolled mosaic of LANDSAT-1 images obtained over northern Finland and vicinity in winter 1973.	70
Fig.30.	Lineaments derived from the LANDSAT imagery shown in the mosaic of Fig.29.	71
Fig.31.	Aeromagnetic anomalies of northern Finland.	72
Fig.32.	Generalized geological map of northern Finland.	73
Fig.33.	Gravimetric map of northern Finland.	74
Fig.34.	Base metal ore deposits and mineralizations in northern Finland.	77

Fig.35. Strike frequency rosettes of the fractures correlating with base metal ore deposits and mineralizations of different types in northern Finland. 80

Tables

Table 1. Summary of the relationships of the mineral occurences shown in Fig.34. with the fracture zones of northern Finland (Plate III). 78

Plates

I Class I linears representing fracture and fault zones.

II Prominent fractures of central Finnish Lapland.

III Significant lineaments of northern Finland representing major fractures, or their component parts.

IV Main blocks of northern Finland.

1.0 SUMMARY REPORT

1.1 General

The main objective of the program was to study the applicability of LANDSAT-1 imagery to the detection of major crustal fractures in the Baltic Shield. The test area was situated in Finnish Lapland, north of the Arctic Circle.

In addition to the study of the main problem, a quick evaluation of the imagery for the survey of both Quaternary (glacial) deposits and Precambrian basement rocks and formations was made (Tuominen 1973).

The investigation was carried out by analyzing various ground and airborne data in different ways. This material was compared with the LANDSAT imagery, which was studied both visually and by other means such as photographic processing, optical filtering and densitometric studies.

To obtain the background data for the program, an extensive analysis of linears from about 1000 aerial photos (scale 1 : 60 000, alt. 9 300 m) covering about 44 5000 sq. km in the area of scene 1039-09315 and vicinity was made. For the same purpose, also the aeromagnetic maps and the maps of bogs and watercources of northern Finland were compiled into respective small-scale maps. LANDSAT-1 took MSS images over Finland and vicinity in three periods during June 1972 - Sept. 1973. Of these 108 have been listed in a separate paper as an index of LANDSAT-1 scenes of Finland for future users in Finland (Aarnisalo 1974). The project has been concentrated mainly on the analysis of two scenes, 1039-09315 and 1040-09371, covering the

test site and vicinity. In addition, winter imagery obtained in February - March 1973 and covering most of northern Finland was used in the study. The images were processed by various photographic methods, including enlarged B&W and color composite prints, density-sliced copies and both B&W and color-coded masking enhancement pictures.

Technical problems were caused by some defects in the 70 mm copies (Tuominen 1973) and gradients in the density level in all the processed images. Unavoidable delays resulted from reconstruction of our optical filter laboratory.

A number of field trips and low-altitude flights were made to study the features discerned in the LANDSAT-1 imagery. During the summer of 1973 and 1974, also field surveys were carried out in a test area in central Lapland. The purposes of the survey was to study the correlations between the bedrock, glacial deposits, vegetation and the density variations of LANDSAT imagery. The analysis of the field data obtained is under way and will be discussed in a separate M Sc. thesis.

Six papers dealing with the LANDSAT-1 imagery of Finland and with the major crustal fractures of the Baltic Shield have been published.

1.2 Significant Results

Study of the MSS scenes 1039-09315 and 1040-09371 and of the winter imagery obtained in 1973, has led, after various processing, to the following main results. Cultural features show up distinctly in LANDSAT imagery. Color-coded masking enhancement pictures (band 5-pos-blue/band 7-neg.-yellow) appear to be especially suitable in this respect. Various Quaternary features are revealed by the different bands.

It seems evident that LANDSAT imagery will be a great help in mapping such features. The analysis of the bedrock features has shown that schist belts can be discerned from areas occupied by their basement rocks or major plutons. Frequently, however, the boundaries of the formation remain obscured by thick glaciogenic deposits. The masking enhancement pictures appear to facilitate distinquishing between different rock formations on LANDSAT imagery.

A combined analysis of LANDSAT-1 imagery, aeromagnetic and other maps and aerial photos has revealed a dense network of bedrock fractures in northern Finland. They form several fracturing zones, which obviously represent surficial manifestations of major fractures. The fractures follow, in general, the eight main trends of crustal shear characteristic of the Baltic Shield (Tuominen, Aarnisalo and Söderholm, 1973), but show distinct deviations from them in detail.

The major fracture zones divide the bedrock into a mosaic of polygonal blocks, which in many cases coincide with the main rock units of the area and are characterized by different patterns of internal fracturing.

The known mineralizations in the study area show a tendency to concentrate along the fracture zones. The association of different types of mineralizations with fractures of different trends seem possible in the light of the data available.

Preliminary results of trend analysis made by optical filtering of LANDSAT image 1039-09315-7, of the linears interpreted from the image, and of the map of linears interpreted from aerial photos suggest that optical filtering of original LANDSAT images might provide a rapid tool for the analysis of major structural trends in extensive areas such as shields or entire continents.

1.3 Recommendations

The results obtained are tentative, but they will obviously cause some revisions in earlier interpretations of the major fracture zones of the Baltic Shield. They require further testing based on various remote sensing data and extensive field work. The significance of these zones from the standpoint of ore prospecting, especially Ni and Cr, requires more study. The optical filtering of LANDSAT imagery for analysis of structural trends should be developed further. The possibilities of its use as a tool in studies of tectonic patterns in more extensive areas should be tested.

2.0 TECHNICAL REPORT

2.1 Image Processing

LANDSAT-1 took MSS-images of Finland in three periods during June 1972 - September 1973. Of these images 108 were recorded from the Standard Catalogs (NDPF/ NASA User Services 1972, 1973) and listed in a separate paper (Aarnisalo 1974, see p. 18, paper 4).

Since the test site of the program is situated in Lapland (Fig. 1), the work was concentrated mostly on the analysis of two scenes, 1039-09315 and 1040-09371. During the image-processing studies, the images of scene 1039-09315 were mostly used, since this scene covers about half of the proposed test area. However, also the other images were processed by various methods. All the processing was done by using 9.5"-transparencies, since various defects were found in the 70 mm products (Tuominen 1973).

The following processing methods were used:

- Contact copying and enlargements for producing B&W copies of each band on the scales 1 : 1 000 000 and

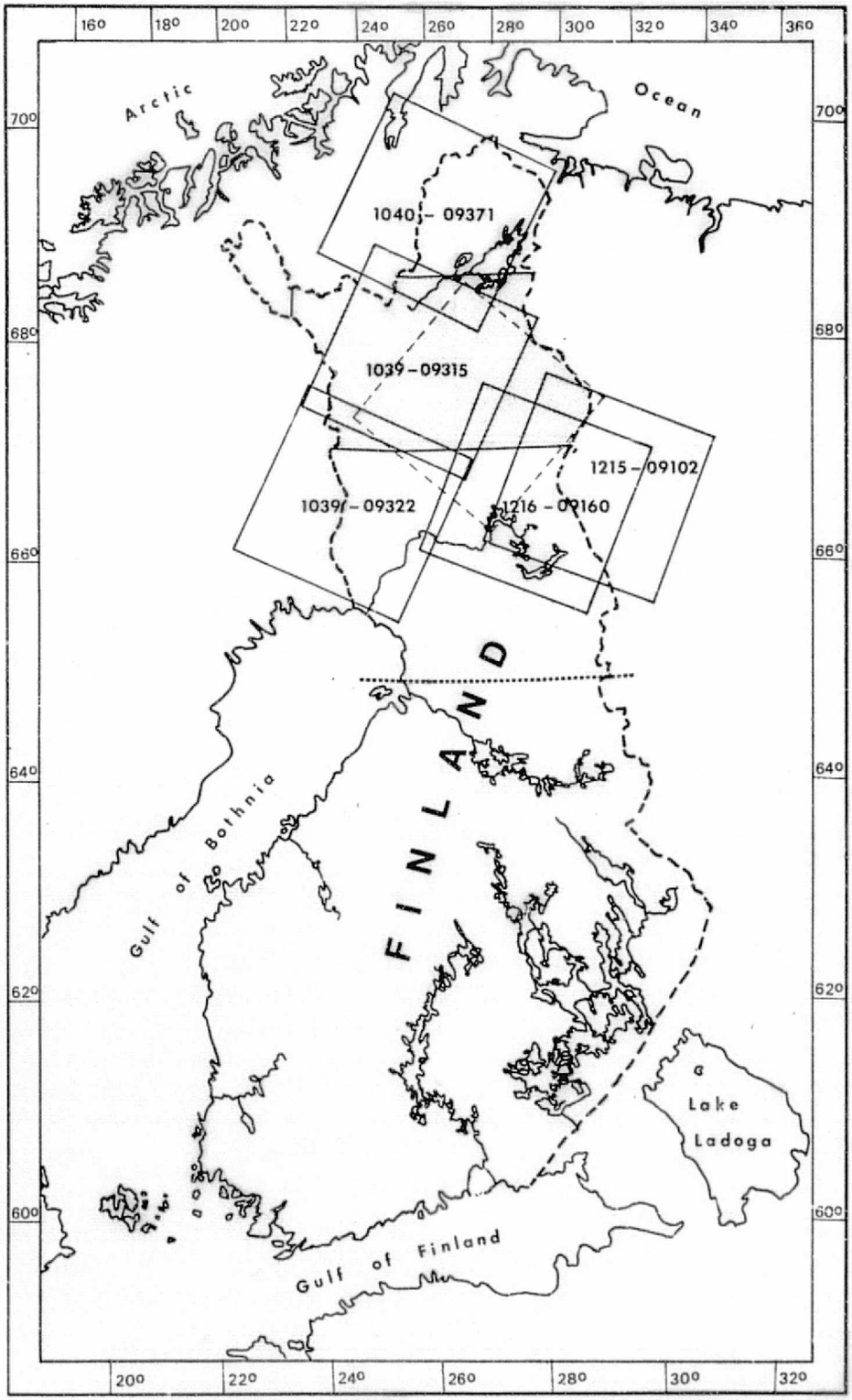

Fig. 1. Test site of the program (thin broken line) and the coverage of the ERTS scenes mainly used in the study. The identification numbers of the scenes are shown in the picture. Shaded area shows the coverage of aerial photos used in the study. Southern border of the area studied from the ERTS-scenes obtained mainly in the winter of 1973, is also indicated by dotted line.

1 : 400 000 and negative copies (1 : 1 000 000) of band 7. (Tuominen 1973).

- Color composite prints on scales 1 : 1 000 000 and 1 : 400 000 (Tuominen op.cit.)
- Density-sliced copies (1 : 1 000 000) of bands 7, 5 and 4 for scene 1039-09315 and of band 7 for scenes 1039-09322 and 1040-09371.
- Masking methods for producing masking enhancement pictures of scene 1039-09315 with spectral band combination 5/7 and 6/7, scales 1 : 1 000 000 and 1 : 400 000.
- Color processing of the masking enhancement pictures of scene 1039-09315 (1 : 1 000 000).
- Equidensity processing (Agfa Contour-method) of scene 1039-09315 (1 : 1 000 000).

Uncontrolled photomosaics (1 : 1 000 000) were produced from the images of band 5 as well as from the density-sliced copies of the images of band 7. A 1 : 400 000 uncontrolled photomosaic was also prepared using the color composite prints. Further, the original paper prints of the imagery obtained mainly in winter were laid into an uncontrolled photomosaic (1 : 1 000 000), which covers northern Finland and its vicinity and extends from the Gulf of Bothnia to the northernmost parts of Finland in Lapland.

The processing of transparencies for optical filtering was performed from the images of bands 5 and 7 as well as from the masking enhancement pictures.

The technical problems encountered in the processings have been mostly caused by the gradients in the density level found to exist in all the processed images. (Fig. 2, a through d). In general, the left halves of the

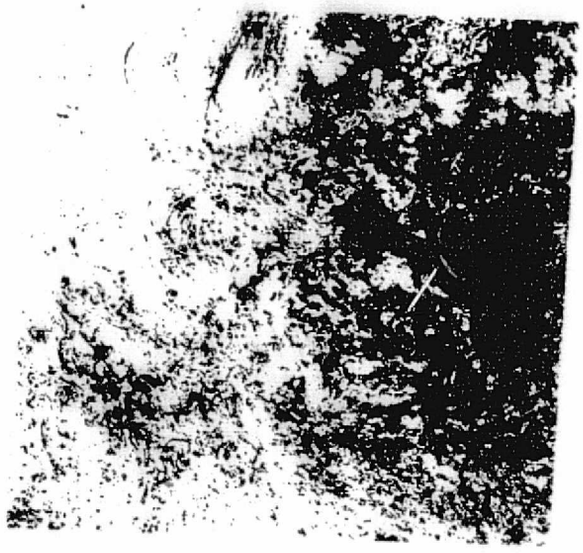

a) An equidensity copy of image 1039-09315-5

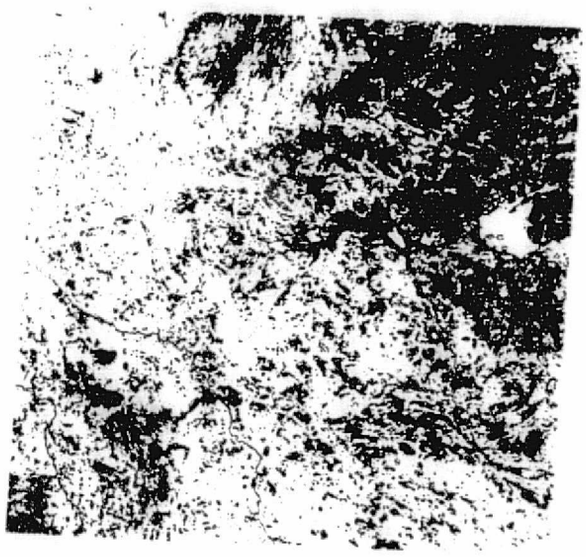

b) An equidensity copy of image 1039-09315-7

c) A high-contrast copy of image 1039-09322-7

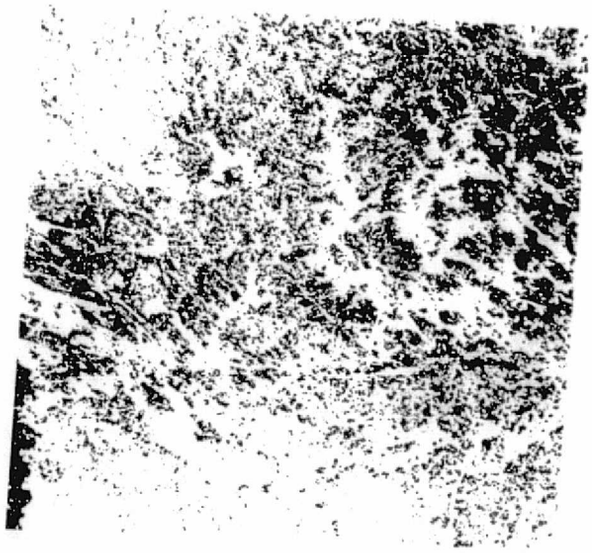

d) A high-contrast copy of image 1216-09174-6

Fig.2. Examples of density level gradients in variously enhanced images. The upper central parts of the right halves of the images studied generally have the highest density values, as shown here by images processed by both the equidensity method and density slicing with high-contrast copying.

Fig.3. A mosaic of LANDSAT winter images of an area around the city of Oulu, Finland, processed by the equidensity method (Talvitie 1974). Several distinct lineaments (indicated by arrows with azimuthal trends) can be discerned.

images appear to have a lower density level than the right halves, the upper left corners having the lightest tones. Also a narrow stripe on the lower edges of the images seems to have lower density values than the central parts of the images. The area with the highest density values appears to occur in the upper central parts of the right halves of the images. These features resemble the shading effect existing in the RBV-system (NASA/ GSFC 1972). They have hampered especially the use of the equidensity method in the study of summer imagery, since the objects having the same reflectance appear on different levels of grey tones in different parts of a scene. Thus the results of the equidensity processing were not uniform over the whole scene. The same effect has been found to occur also in the winter imagery (Fig. 2 d), which has been corrected for the linear grey scale in NDPF. There the effect is, however, essentially weaker, so that the equidensity method can be used in the analysis of large areas. Fig. 3 shows a mosaic of LANDSAT winter images of an area around the city of Oulu, Finland, processed by the equidensity method (Talvitie 1974).

2.2 Processing of Background Data

For the evalution of the results of the analyses of LANDSAT imagery, the following background data were used:

- aeromagnetic maps, profile intervals 400 m, flying alt. 150 m, scale 1 : 400 000,
- aerial photos (total about 1 000), alt. 9 300 m, scale 1 : 60 000.
- general topographic maps, scales 1 : 400 000 and 1 : 100 000.
- general geologic maps for basement rocks, scales 1 : 400 000 and 1 : 1 000 000,
- general gravity maps, scale 1 : 400 000.

The aeromagnetic maps were reduced to the scale of 1 : 1 000 000. This was done to produce a small-scale

aeromagnetic map of northern Finland. A stereoscopic lineament interpretation was made from the aerial photos. The results were compiled to produce a map of photolinears of central Lapland, which extends over most of the area of scene 1039-09315 (Fig.1).

The general topographic maps were used to produce a small-scale map of the bogs and watercourses in northern Finland. This map was used to study the topographic manifestations of the major fractures. Also the height-contour elements of the topographic maps (1 : 100 000 and 1 : 400 000) were used in the fracture analysis.

New general gravity maps (Bouguer anomalies) of northern Finland (scale 1 : 400 000) made by the Geodetic Institute of Finland at the beginning of 1974 were also reduced to the scale of 1 : 1 000 000 for comparison with other data.

2.3 Field surveys

During the summer of 1973, a number of field trips and lowaltitude flights were made to study the features discerned in the different bands and color composite prints (1 : 400 000) of LANDSAT imagery and to investigate the appearance of different ground features in the imagery. Special attention was paid to the border zone of the granulite complex of Lapland, where the occurence of large-scale bedrock layering was suggested by the LANDSAT imagery (see p.26 and Tuominen 1973).

Oblique false-color photos of different features discernible in the LANDSAT imagery were taken on low-altitude flights.

During the summers of 1973 and 1974 a field survey was also carried out in a test area common to the geologic

(SR 580-03) and forestry (SR 580-02) programs of Finland. The size of the area is about 96 x 16 Sq.km and it is situated in central Lapland. The area consists of different metamorphic and plutonic rocks, which are extensively covered by glacial deposits. The purpose of the study was to obtain information on possible correlations between the bedrock, glacial deposits, vegetation and the density variations in the different spectral bands of the LANDSAT imagery. The work was carried out by collecting soil samples, studying the possible outcrops and observing the species of vegetation at statistically defined sampling points, which were situated on profiles analyzed microdensitometrically from the LANDSAT imagery (scene 1039-09315). The results of this field work were analyzed by, for example, grouping the density values of different spectral bands according to the field observation variables and by using cluster analysis. The collection of the field data was started in the summer of 1973 and completed during the summer of 1974. The results of this study will be discussed in a M.Sc. thesis under preparation in the Dept. of Geology, University of Helsinki.

2.4 Published Articles and Papers

The following papers dealing with satellite imagery and major crustal fractures of Finland have been published during the project:

1) Aarnisalo, J. (1973) ERTS-tekokuututkimukset Suomessa (" ERTS-satellite studies in Finland ", English abstract). Geofysiikan päivät Helsingissä 29-30-05-1973 (Ed. E Jatila).

   (The paper was read at a meeting of the Geophysical Society in Helsinki May 29-30,1973. The general objectives of NASA's LANDSAT program are stated and the

LANDSAT-system is briefly explained. The main objectives of the Finnish LANDSAT-1 programs are stated and some preliminary results of these programs reported by Kuittinen 1973, Kuusela 1973 and Tuominen 1973 are summarized.)

2) Tuominen, H.V., Aarnisalo, J. and Söderholm, B., (1973).
Tectonic patterns in the central Baltic Shield. Bull. Geol.Soc.Finland 45, 205 - 217.

3) Paarma, H., Aarnisalo, J. and Talvitie, J. (1974).
On the tectonic control of weathered iron formations in Finnish Lapland. Abstract. XI Nordiska Geologiska Vinermötet, Oulu/Uleåborg,1974 January 3-5, B. Abstracts, program, deltagarlista och allmänna instruktioner.
(Abstract of paper presented to the XI Nordic Geologic Winter Meeting. Attention is drawn to the fact that in northern Finland the occurence of supergene iron ore seems to correlate with lineaments detected in LANDSAT imagery and small-scale (1 : 400 000) aerial photomosaics).

4) Aarnisalo, J. (1974) ERTS-kuvia Suomesta (Summary: ERTS-scenes of Finland) Geologi 26, 73-81.
(The paper lists 108 LANDSAT scenes (former ERTS) obtained over Finland and vicinity during the period June 1972 - September 1973, and deals briefly with the cloud cover of the scenes. Also three index maps of these images are presented and the possibilities of ordering images from the EROS Data Center and LANDSAT reports from NTIS are mentioned.)

5) Talvitie, J. (1974): ERTS imagery as a tool for tectonic and tectonophysical studies in the Baltic Shield.
Photogram.J. Finland, 6, 2, 174 - 184.

6) Aarnisalo, J. and Mikkola, A.K. (1975): Fracture patterns of Finnish Lapland and their relation to ore deposits. Abstract. Abstracts of keynote adresses and short communications. Meeting of European Geological Societies, Reading, U.K., Sept. 1975.

3.0 RESULTS

3.1 General

In the first phase of the project, a brief study was made of the types of information LANDSAT imagery over Finland might, in general, provide to an Earth scientist (Tuominen 1973). It was noted that cultural features are easily detected from the imagery. Urban, agricultural, timbering and forest improvement areas, highways and, occasionally, even side roads only some 10 - 20 m wide can be discerned. In this respect, band 5 seems to provide the best information (Fig. 4.) of all the bands. Color-coded masking enhancement pictures (band 5-positive-blue/band 7-negative-yellow) appeared to be especially suitable for the analysis of cultural features. Even small gravel pits and the yards of isolated roadside houses are discernible. In Fig. 4. they appear as small light dots by the roads. Fig. 4 reveals also the effect of the timbering areas on the photo textures. The timbering and forest improvement areas of different ages appear to have different grey tones, the youngest being the lightest. It is evident that numerous wide areas of this kind disturb the natural photo textures and grey tones, thus making geological interpretations difficult. This applies to the images of bands 4 and 5 in particular.

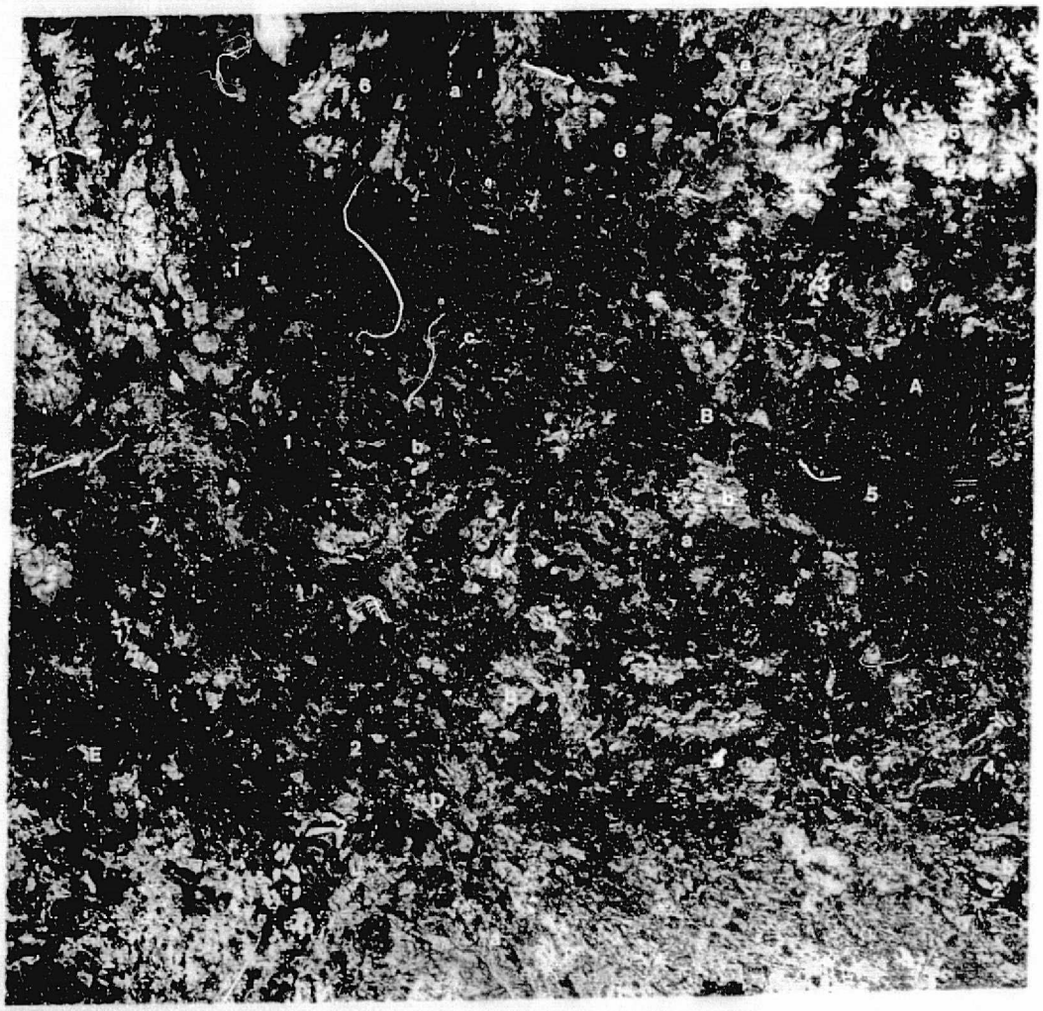

Fig.4. LANDSAT image (1039-09315-5) of Central Lapland. Different cultural features are readily discerned: A: Lokka Reservoir, B: Porttipahta Reservoir, C: Sodankylä, D: Kittilä, E: Muonio, a) highways and sideroads, b) timbering and forest improvement areas, c) gravel pits and house yards by the roads. Geologic information, as contained in general geological maps and previous studies, is also abundant: 1. amphibolite ridge, 2. quartzite, 3. granite, 4. mica schists and a distnct fold, 5. gabbro, 6. granulite complex, 7. gneiss granite. Arrows point at some distinct fracture zones in the area.

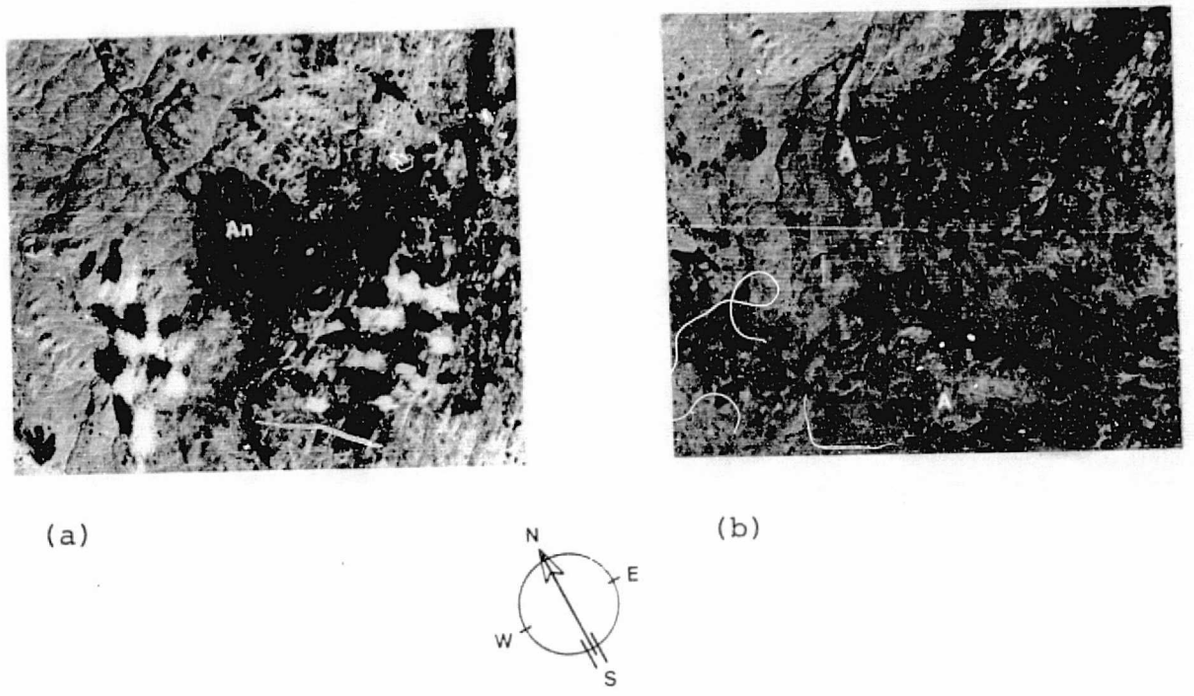

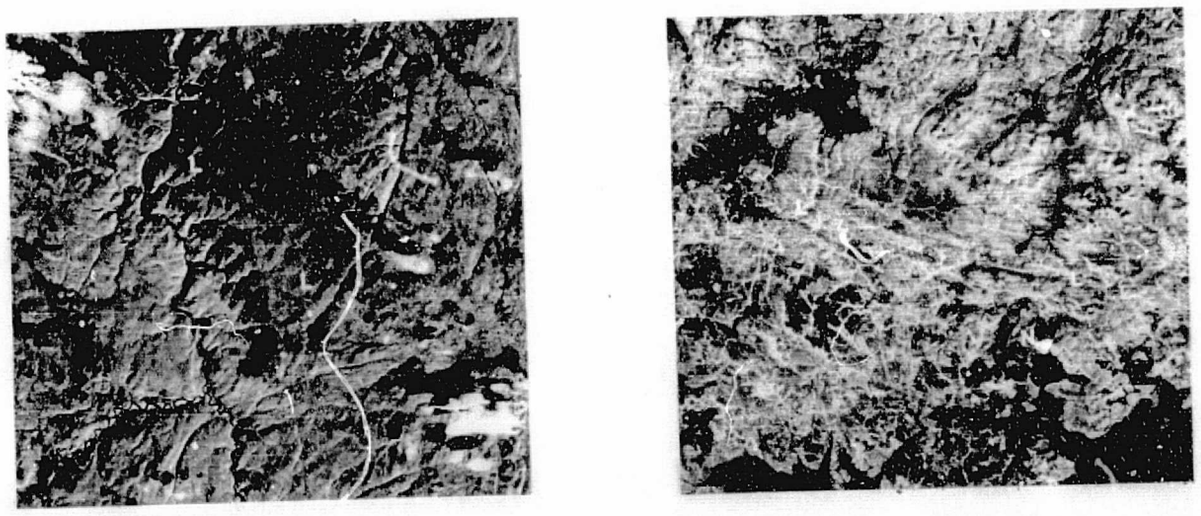

Fig. 5. Bedrock features discernable on LANDSAT images in Finnish Lapland.

a) Angeli anorthosite massif (An) (image 1040-09371; band 7).
b) An amphibolite belt (A), see also Figs. 4 and 6 (image 1039-09315; band 7).
c) Layering (L) in the granulite complex (image 1040-09371; band 7).
d) Layering (L) in the granulite comples and Nattanen granite massif (N) (image 1039-09315; band 7).

Angeli Anorthosite massif (a), the amphibolite belt (b) and Nattanen granite (d) are shown on the general geological maps, but they give only hints on the layering of the granulite complex clearly detectable on the LANDSAT imagery (c) and (d). Scale 1:1 000 000. North is indicated by an arrow.

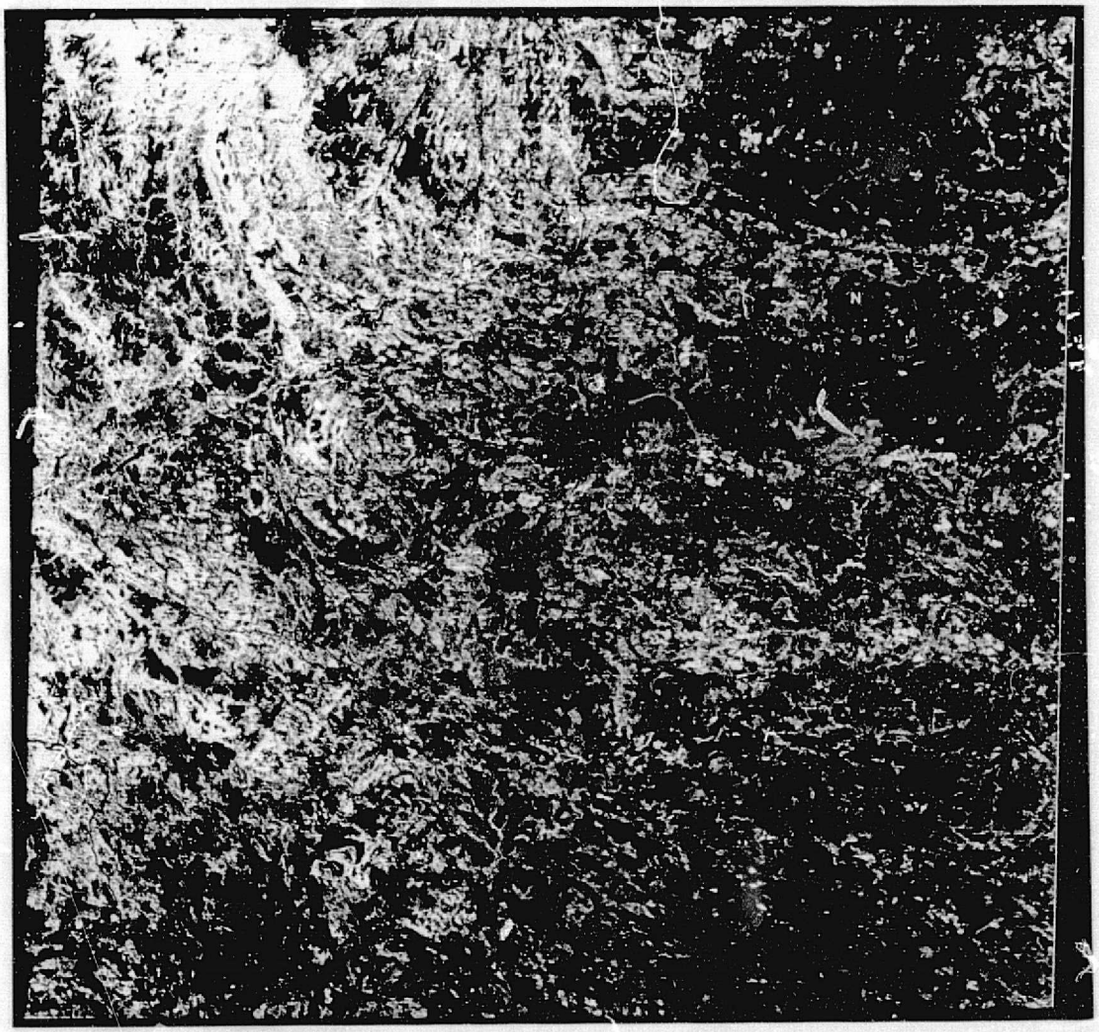

Fig. 6. A masking enhancement picture (5/7) of scene 1030-09315. Several rock bodies and bedrock structures are better revealed than in the images of the single bands (compare Figs. 5 and 7).

The amphibolite ridge (A) seen in Fig. 5b is clearly visible. The dark and light stripes in the upper right part of the image correspond to bedrock layering (L) (see also Figs. 5 and 7).

A quick evaluation of LANDSAT imagery for the survey of Quaternary features was also carried out. This was done mainly by using ground data provided by the Geological Survey of Finland (Dr. Raimo Kujansuu). It was established that several different types of glaciogenic and other formations can be detected from LANDSAT imagery. Especially drumlin terrains, glacial fluting, eskers, glaciofluvial deposits and deltas were discerned. Also different types of bogs were discernible as well as the blockfields common in Lapland. It was concluded that LANDSAT imagery is useful in mapping glaciogenic Quaternary features.

The analysis of the bedrock features has shown that schist belts, as known from ground surveys, can be discerned from the areas occupied by their basement rocks or major plutons. These bedrock units have a rather specific morphographic appearance and thus different phototextures so that they are easily located in the images. However, the details of the boundaries between different formations are usually hard to detect. They are often masked by Quaternary features - thick soils and glaciogenic structures. Also the cultural features hamper the detection of these boundaries. In several places, rock bodies are revealed by specific grey tones caused by the vegetation growing on them. The best examples are the Angeli anorthosite massif in scene 1040-09371 and an amphibolite belt in scene 1030-09315 (Fig. 5.). A certain grey-tone criterion cannot, however, be applied to the whole area studied, since in Lapland the vegetation is highly dependent on latitude and elevation. The timber line runs roughly E-W over the upper parts of scene 1039-09315. This causes marked variations in the general type of vegetation within differences in elevation of a few dozen meters. Relief of this magnitude is common in wide parts of Lapland, and thus the grey tones of the same rock types may differ greatly in neighbouring areas. However, several different rock formations are discernible on the combined basis

of the morphography and the grey tones (Tuominen 1973).

For the delineation of different rock formations from LANDSAT imagery, the masking enhancement pictures (Fig. 6) may provide a considerably better tool than the images of individual bands alone. For instance, the amphibolite ridge is more clearly visible in Fig 6 than in Figs. 4 and 5.

Fig. 7. (On the following page). Layering in the granulite complex in northern Finnish Lapland.

a) Part of scene 1040-09371, processed by masking enhancement (5/7).

b) Features interpreted from (a). Dark grey areas in LANDSAT image, possibly indicating bedrock layers; Medium grey areas in LANDSAT image, possibly indicating bedrock layers; Anorthosite; —— Possible rock boundaries; ····· Bedrock trends; — — — ---- Prominent linears; Clouds.

c) Geological map of the area covered by (a), modified from Meriläinen (1965). Granulite complex; Granulites in general; Fine-grained garnet-quartz-feldspar gneisses; Coarse-grained garnet-quartz-feldspar gneisses; Garnet-cordierite gneisses; Coarse-grained garnet-cordierite-quartz-feldspar gneisses. Other rock types; Quartz-feldspar gneisses (arkose gneisses) with amphibolites as bands and intercalations, mica gneisses; Granitic gneisses, migmatitic granitic gneisses and hornblende gneisses; Anorthosites; Various other rock types (mainly hypersthene bearing quartz diorites and granodiorites within the granulite complex and amphibolites or greenstones elsewhere).

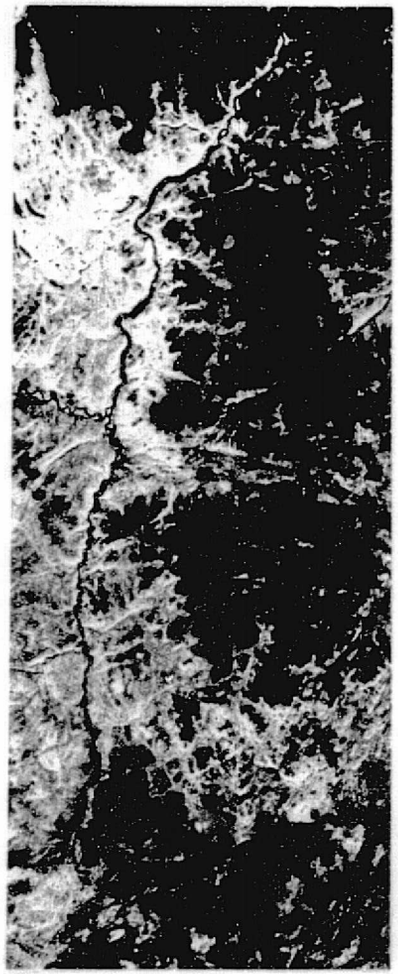

A

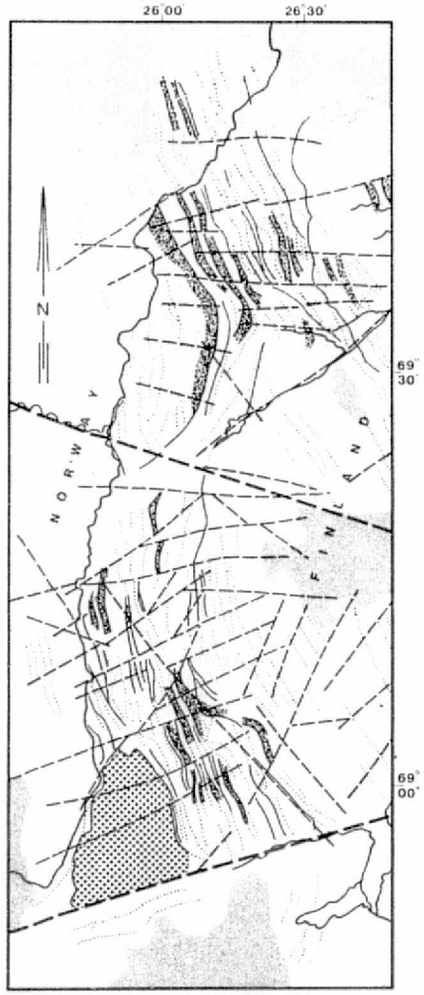

B

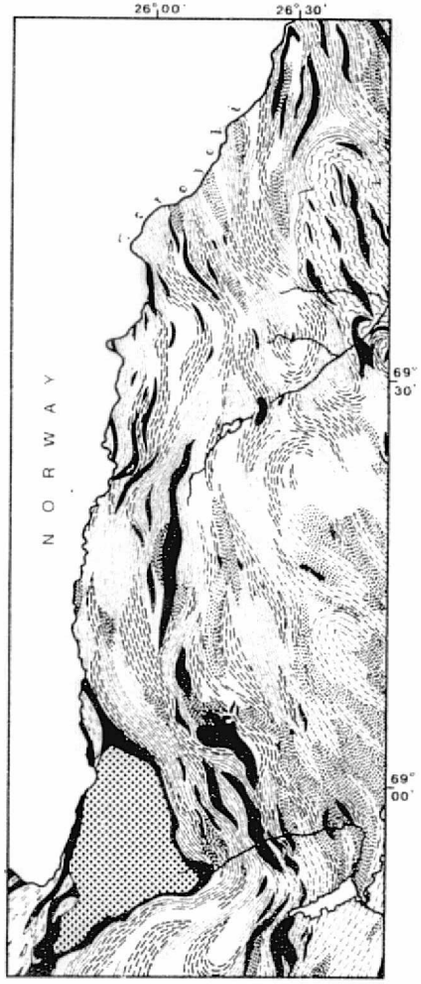

C

Fig. 7. Notes on preceding page.

Within the granulite complex of northern Lapland, LANDSAT imagery (scenes 1039-09315 and 1040-09371) reveals bedrock features not clearly shown on existing geological maps. In Figs. 5c and 6, several parallel darker and lighter stripes can be discerned. They have approximately the same strike as that mapped for the granulite complex (Mikkola 1937 and Meriläinen 1965).

Fig. 7a is a modified map of the northern parts of the complex. Fig. 7b shows the same area in masking enhancement picture of scene 1040-09371. Fig. 7c is a sketch map showing layering bedrock trends and more prominent linears suggested by Fig. 7b. By comparing the different pictures, it becomes evident that the features visible on the LANDSAT image correlate with the ground data and appear to reveal a layering in the granulite complex.

3.3 Linears of central Finnish Lapland

The main objective of the project was to study the major fracture and fault zones of northern Finland and their relationships to mineral deposits. The problem was approached in two steps. First, an area in central Lapland (see p. 10) was studied by producing various background data maps on the scale of 1 : 400 000 and comparing these maps with derivatives of LANDSAT-1 imagery on the same scale. The study was concentrated mainly in the area of scene 1039-09315 (Figs. 1 and 4). The winter imagery (scenes 1215-09102 and 1216-09160) covering the eastern parts of the area (Figs. 1 and 13) were also used. Second, a lineament analysis was performed on the LANDSAT imagery obtained in the winter of 1973 and on an scene of Sept. 1972. This study covered the parts of Finland situated north of the 65th parallel and was done on images on the scale

of 1 : 1 000 000. The results were then compared with various background data maps on the same scale for compiling a general fracture and fault zone map for northern Finland.

The terms linear and lineament are used in this report in much the sense defined by Hoppin (1974). This usage was adopted to avoid confusion between features of different magnitudes and, perhaps differing in importance. Thus, linears are single lines on aerial photos, topographic maps or LANDSAT imagery, being usually only a few kilometers or tens of kilometers long, while lineaments are lines or zones of structural discordance of more regional extent (appearing in different types of data). For clarity, in the following comparisons the linears interpreted from aerial photos will be called photolinears, and those interpreted on a scale of 1 : 400 000 from LANDSAT imagery as LANDSAT-linears. More regional linear features interpreted from LANDSAT imagery on a scale of 1 : 1 000 000 are correspondingly called lineaments.

3.2.1 Comparison between photolinears and LANDSAT-linears

Since orbital imagery had, even before the launching of LANDSAT-1, proven useful in detecting major fractures and lineaments (e.g., Sabatini et.al. 1971, Lathram 1972), it was considered necessary to compare the map of linears, compiled by conventional interpretation of aerial photos, with the linears seen in LANDSAT imagery. This was expected to provide information on how the linear patterns detected in aerial photos would appear in LANDSAT imagery.

A map of photolinears (Fig. 8) was made by stereoscopic interpretation of about 1 000 photos on the scale of 1 : 60 000.

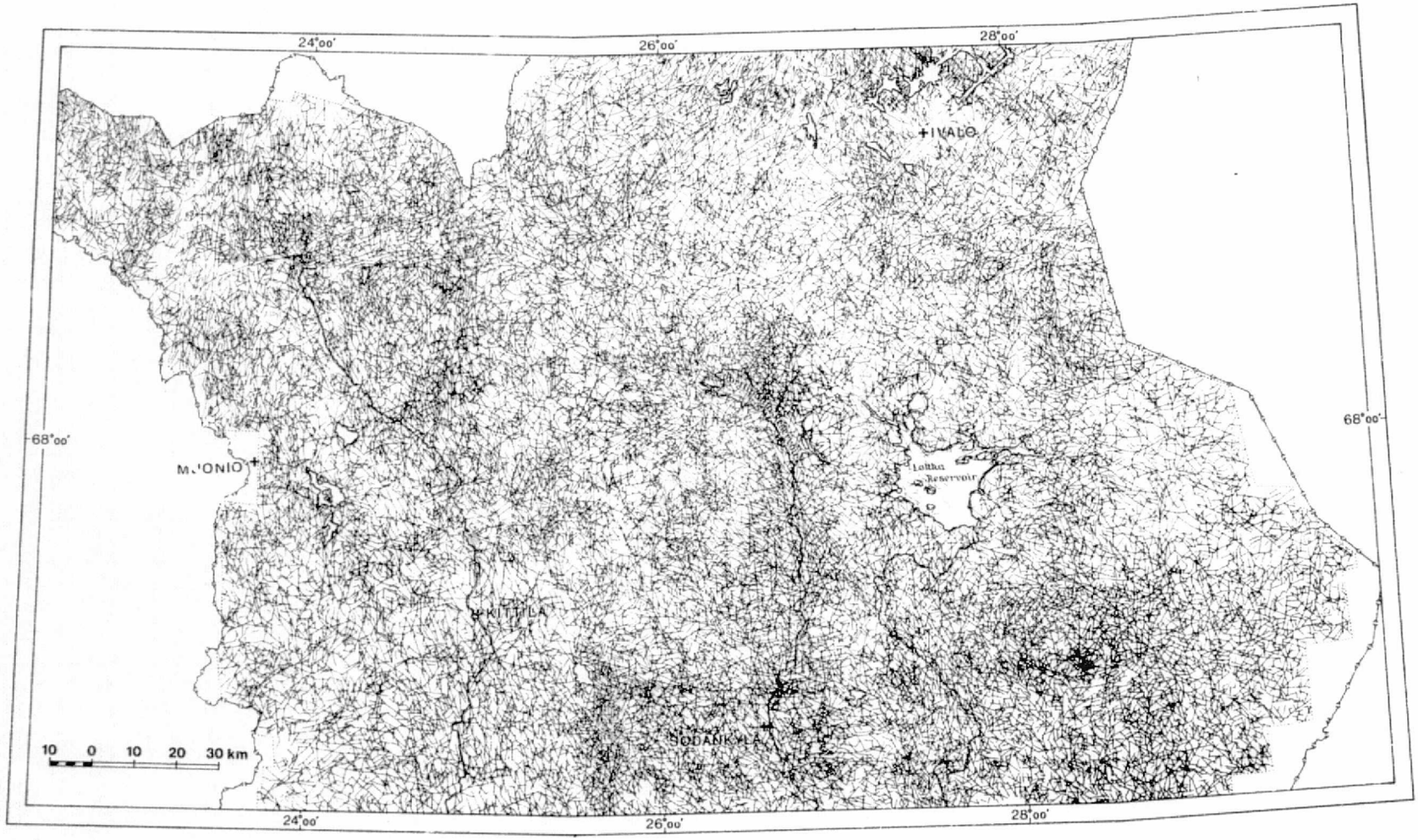

Fig. 8. Map of photolinears of central Finnish Lapland.

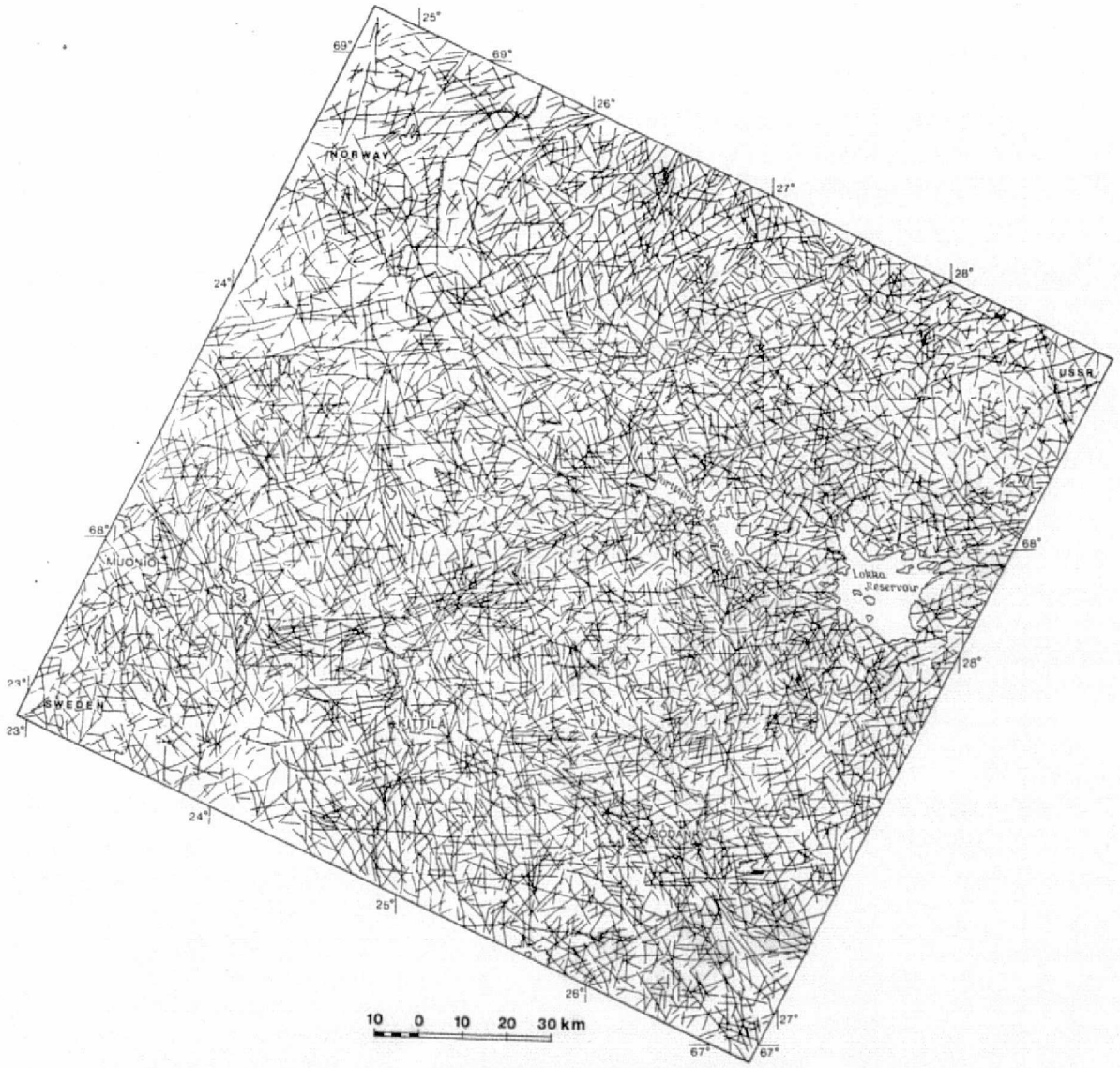

Fig. 9. LANDSAT-linears interpreted from LANDSAT-1 scene 1039-09315.

The work was carried out by several persons, each of whom interpreted a given area, usually 60 x 65 sg.km. Their results were then checked and revised by the author. This was essential, because each person has his own style of interpretation and the results would have been heterogeneous. In the map of photolinears (Fig. 8), the areas dealt with by different interpreters are still detectable but, as a whole, the map is fairly homogeneous. The analysis of the aerial photos and the compilation of the map took more than 1 500 man hours. The total size of the area thus studied is about 44 500 sq.km.

Fig. 10 (On the following page). Comparison of the photolinears and LANDSAT-linears. Three example areas are shown from different parts of Figs. 8 and 9. The size of each of the areas is 36 x 36 sq.kms. Different relationships between the photolinears and LANDSAT linears can be noticed:

1) Photolinears arranged in en echélon pattern along a zone of long LANDSAT-linears.
2) A zone of short discrete subparallel photolinears, detected as a long LANDSAT-linear.
3) Long photolinears detected also as long LANDSAT-linears.
4) A zone of short discrete photolinears, discernible as a zone of longer LANDSAT-linears.
5) East-westerly running zone of higher photolinear density, composed of subparallel and en echélon photolinears. Detected as a zone of subparallel east-westerly running LANDSAT-linears.
6) LANDSAT-linears only partly detected also as photolinears.

Photolinears

LANDSAT-linears

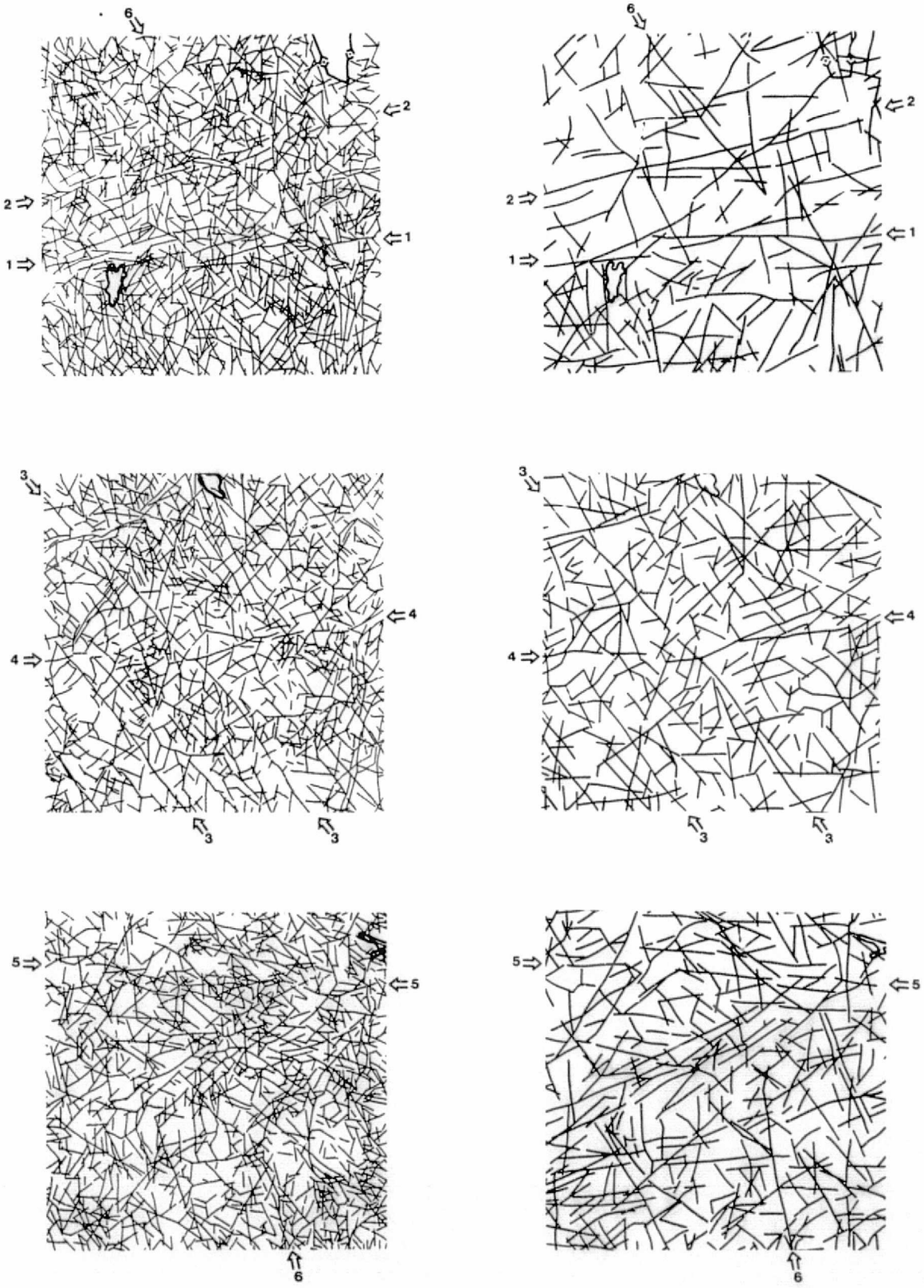

Fig. 10. Notes on preceding page.

Different types of photolinears were not separated in the work. Thus the photolinears in Fig. 8 may be due to morphographic and vegetational features, watercouses and bogs, as well as to faults, fractures and bedrock textures. Obvious glaciogenic features were avoided.

A thorough search for LANDSAT linears was made on scene 1039-09315. The interpretation was performed mainly from 1 : 400 000 images of bands 7 and 5, but color-composite prints on the same scale and other variously processed LANDSAT images were also used. This work was carried out by the author within just a few days. Figure 9 shows the LANDSAT linears compiled from these data.

The distribution of the photolinears in Fig. 8 reveals zones of subparallel photolinears or of photolinears arranged in en echélon patterns (Figs. 8 and 10), several of which can be traced through the entire map. The longer photolinears (Fig. 8) frequently exist also as LANDSAT-linears indicated in Fig. 9. Many of the shorter ones are also discernible. On the other hand, there are other LANDSAT-linears, which do not appear on the photolinear map or, more often, can be traced on it as a line of short discrete photolinears after being first observed as an LANDSAT-linear (Fig. 10). In addition, the LANDSAT imagery has revealed zones of subparallel LANDSAT-linears, which appear on the photolinear map merely as zones of higher photolinear density. In these cases, the photolinears often show no clear orientational patterns parallel to the LANDSAT-linears. The east-westerly LANDSAT-linears, particularly, show up in this way on the photolinear map.

To compare the strike-frequency distributions of the photolinears (Fig. 8) and LANDSAT-linears (Fig. 9), an equivalent

circular sample area (Ø about 140 km) was taken from both maps of linears (Fig. 11, a and b). A corresponding area was also directly taken from LANDSAT image 1039-09315-7 (Fig. 11c). The IR band was selected because it shows least cultural effects. The analysis was done with an automatic scanning optical filter (originally French FO-100, with automatic scanning facilities developed during the program) using a 5^{o}-sector filter. This means that the diffraction pattern of the input is scanned by a rotating 5^{o} opening in the focal plane. The relative intensities of the 5^{o}-sectors of the diffraction pattern were detected continuosly by a photomultiplier and fed to a plotter. The curve thus obtained is analogous to the relative strike-frequency distribution of the input elements weighted with the length of the elements. A circular area was used because otherwise the rectangular screen of the holder of the input image would have caused unwanted rectangular " coordinate axes " in the diffraction patterns. The results are shown in Fig. 12.

The results show similar general trends in the 270^{o}-360^{o} range, but appear to differ in the 0^{o} - 90^{o} range. The linears interpreted from LANDSAT scene 1039-09315 (Fig. 12a) show two distinct maxima areas. In the azimuths 320^{o} - 10^{o}, the strike-frequency curve of the linears has the same general form as in the other two curves (b and c in Fig. 12), except that the linears with a northerly orientation seem to have relatively more weight in the interpretation than in the original LANDSAT image (Fig. 12 a and b).

In the 30^{o} - 90^{o} range, the general trends of the curves are different. In these directions, the relative quantity of LANDSAT-linears is markedly higher than that obtained from aerial photos (Fig. 12 a and b). This difference is is evidently due to the direction of the illumination

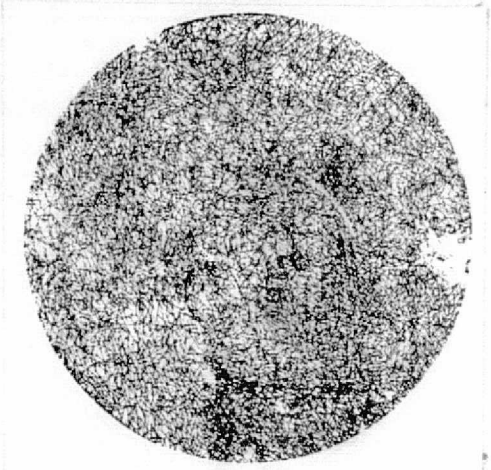

(a) photolinears

(b) LANDSAT-linears

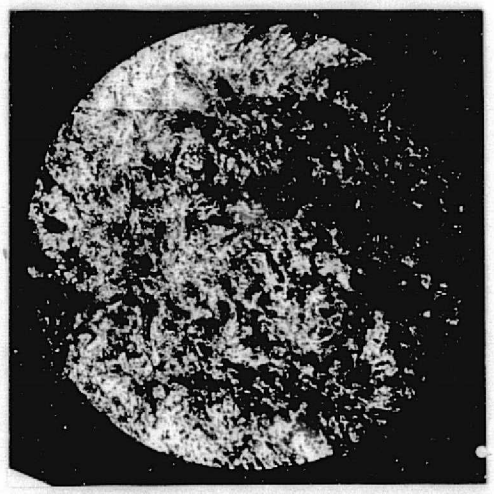

(c) LANDSAT image 1039-09315, band 7

Fig. 11. The test areas for comparison of the strike-frequency distributions of the photolinears, LANDSAT-linears and of the corresponding LANDSAT image.

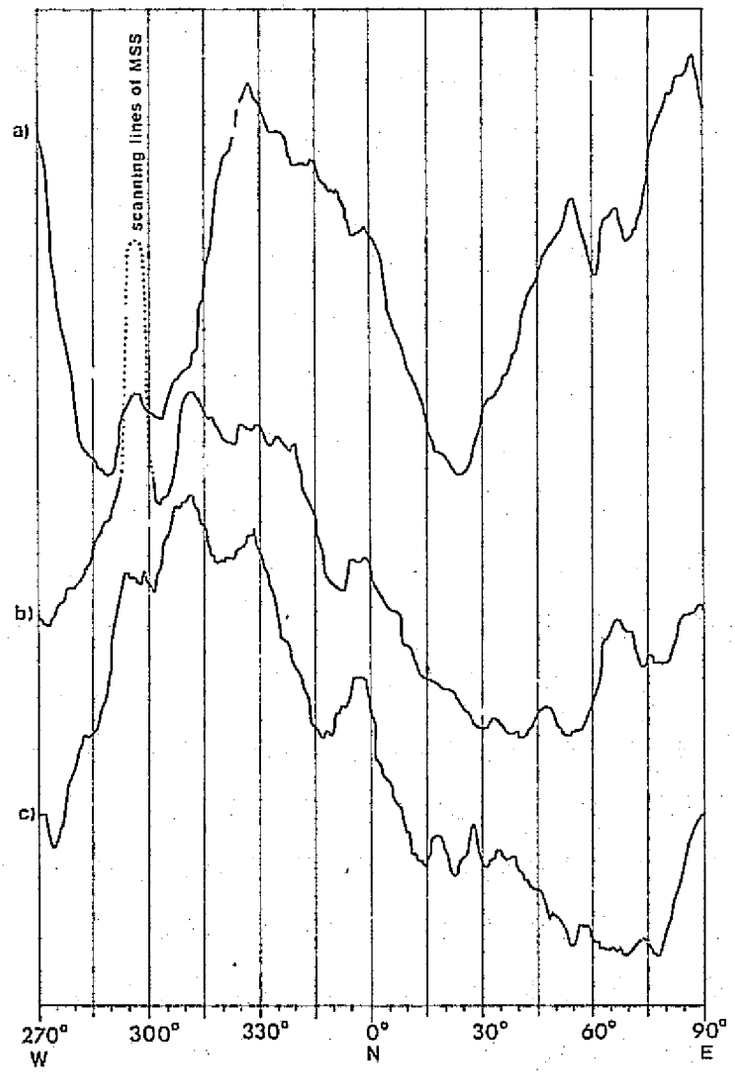

Fig. 12. The relative strike-frequency curves obtained by the optical filtering of an equivalent circular area (Ø about 140 km) of

a) the linears interpreted from LANDSAT scene 1039-09315 (Fig. 9),
b) LANDSAT image 1039-09315-7,
c) the photolinear map of central Finnish Lapland

The curves are not normalized and they may contain some instrumental drift.

during imaging time. The azimuth of the sun has been 167° (sun elevation 30°) or roughly perpendicular to the 35° - 90° trends. In the LANDSAT images, the shadows of the relief have strengthened the linears of these trends. This can be noticed also in the strike-frequency curve obtained directly from the image (Fig. 12b).

The directions near the MSS-scanning lines have clearly less relative weight in the LANDSAT image interpretation than in the aerial photo interpretation when compared with respective neighbouring directions (Fig. 12, a and b). The obvious neglect of the LANDSAT-linears of these trends (280° - 315°) is possibly due to the fact that the scanning lines in the LANDSAT image form a line raster the direction of which has tended to be avoided in the search for linears.

The curve obtained directly from the LANDSAT image shows the same trends and maxima as the curve for the photo-linear map (Fig. 12 b and c).

The major differences appear in the 30° -90° range showing the illumination effect. Five of the peaks (290° - 300°, 305° - 315°, 325° - 335°, 355° - 05° and 85° - 95°) are clearly common in both curves. Also three minor maxima (15° - 20°, 30° - 40°, 45° - 50°) appear to occur as small peaks or bulges in both curves.

In general, each of the curves shows minor peaks that do not seem to appear in, or merge into, the wider peaks of the other curves. Differences of this sort may result from the different fine textures in the input pictures or from the instrumental noise. At any rate, more work is needed to find the sources of these differences.

It seems possible that in many areas the linear patterns can be analyzed directly from the LANDSAT imagery by optical filtering. This would reduce the need of photo-interpretation, which is expensive, time-consuming and,

generally, subjective.

3.2.2 Map of linears

Though interpretation of linears and lineaments have for a long time been used in the study of geological structures, especially fractures and faults, the procedure used by different authors vary considerably. Even the definitions of these and related terms are rather heterogeneous (e.g., Hobbs 1911, Wilson 1941, Brock 1957, Lattman 1958, Haman 1961). Hoppin (1974) has recently discussed this subject and states that lineaments and linears are different rather than equivalent features (see also p. 27) Nevertheless, the nature of linears and lineaments as well as the procedures generally used in mapping them from aerial or orbital photos, topographic maps or other similar data, leads to the inclusion of linear features that do not necessarily have structural correlations. Moreover, complete field checks of the interpretations are usually impossible in practice. For this reason, the results of the interpretations are commonly biased-being influenced by, among other things, the experience of the interpreter and his expectations about the results, as well as by the grid systems caused by cultural features (e.g., fields, roads, timbering areas; see Lattman 1958), and the geological, vegetational and climatological history of the study area. In Finland, for instance, Quaternary glacial features such as fluting, drumlins and eskers, etc., often complicate the interpretation by strengthening the linear features in the directions of the ice flow and covering with drift those of other trends.

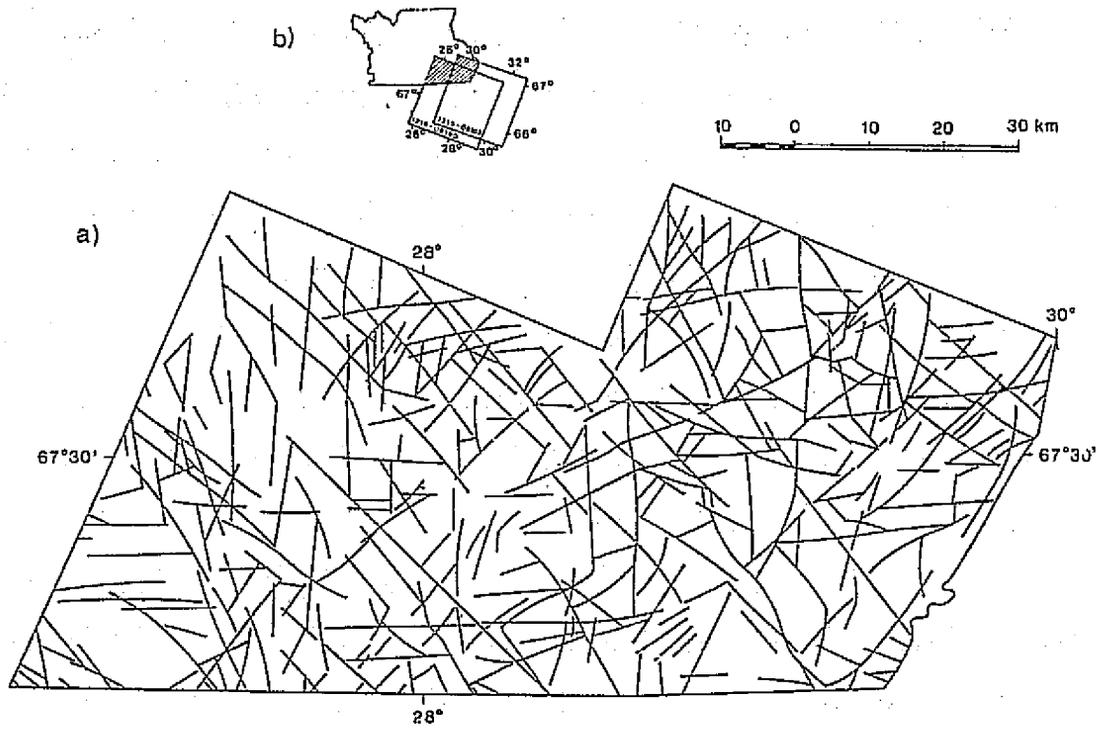

Fig. 13. Linears interpreted from LANDSAT-1 scenes 1215-09102 and 1216-09160 obtained in the winter of 1973 (a). Index map (b) shows the coverage of the interpreted area on the map of photolinears (Fig. 8).

This kind of bias is obviously difficult to avoid. However, the bias, or the misinterpretation of linears, apparently tends to differ with different types of data. As a consequence, the bias might be reduced by tracing the linears from several types of data, and including in the final result only those linears found from more than one source. This method evidently leads to the detection of the most distinct and, perhaps, geologically most significant linears.

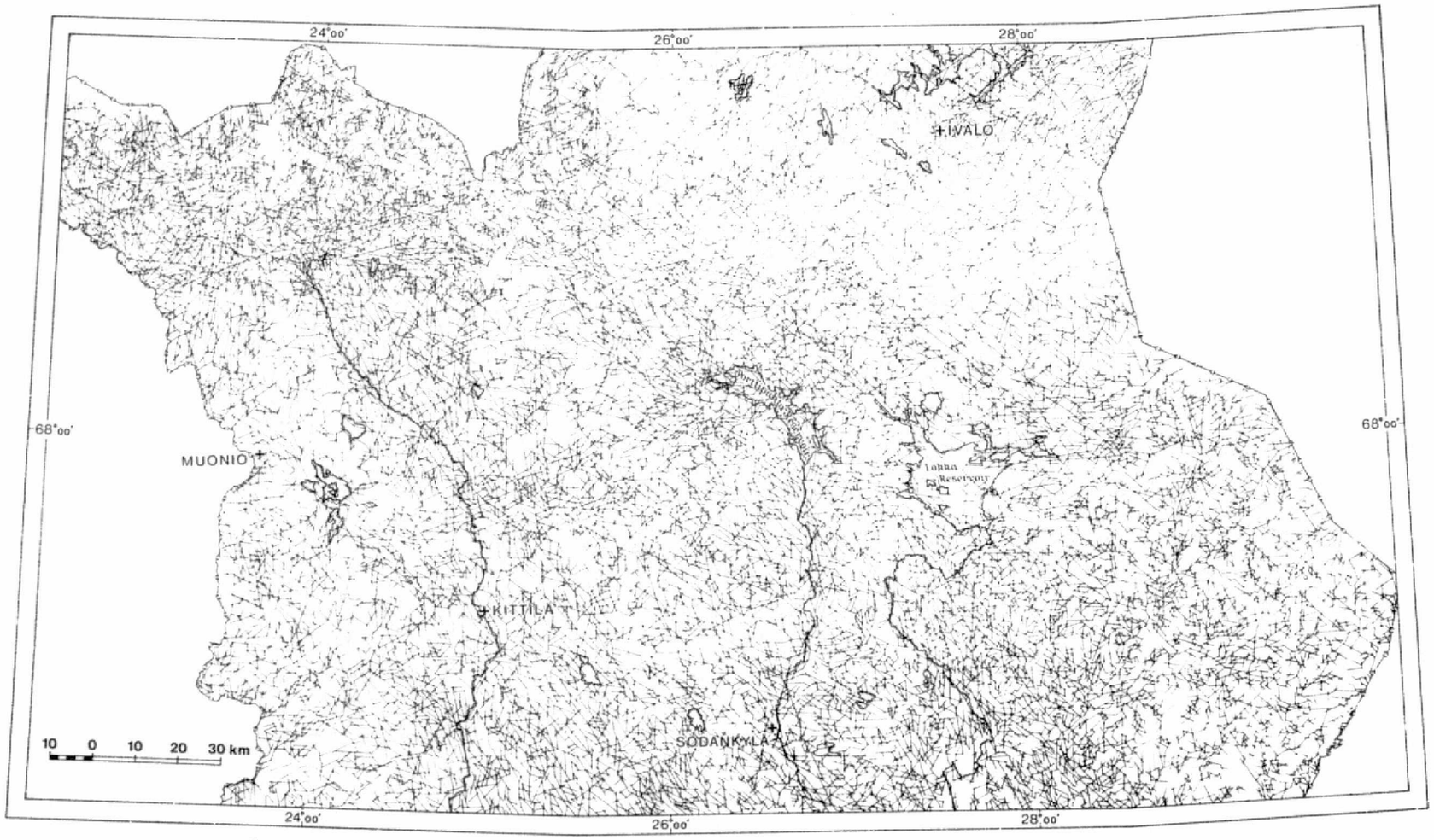

Fig. 14. Linears interpreted from the map of bogs and watercourses on a scale of 1 : 400 000.

On the other hand, some true linears will obviously be excluded, but, in most cases, they probably come from minor geological structures, such as joints, small fractures, etc.

A procedure of this kind was used in making a map of linears for central Finnish Lapland (Fig. 15). The handling of two of the data sources needed, aerial photos and LANDSAT imagery, has already been discussed in the previous chapter. The map of LANDSAT-linears (Fig. 9), which is based on summer imagery, covers only the western and central parts of the area of the photolinear map (Fig. 8, see also Fig. 1, p. 11). Winter imagery, scenes 1215-09102 and 1216-09160, was used to obtain a wider coverage for the LANDSAT-linear map (Fig. 13.). At third interpretation of linears in the same area was done from the map of bogs and watercourses on the scale of 1 : 400 000. The result of this interpretation is shown in Fig. 14.

The three separate maps of linears were superposed on each other and all the linears, or parts of them, that were detected in at least two of the maps, were redrawn on an overlay to obtain the final result of the interpretation procedure. In addition, areas where several closely situated subparallel linears were located and areas of numerous linears crossing each other were delineated as zones of high linear density. The map of linears obtained (Fig. 15) is considered to contain the reliably detectable linears of the area.

When studying Fig. 15 it must be remembered that in the original interpretations of the different data, no structural classification was used. Thus the linears obtained evidently represent structural features, such as faults and fractures, bedding or

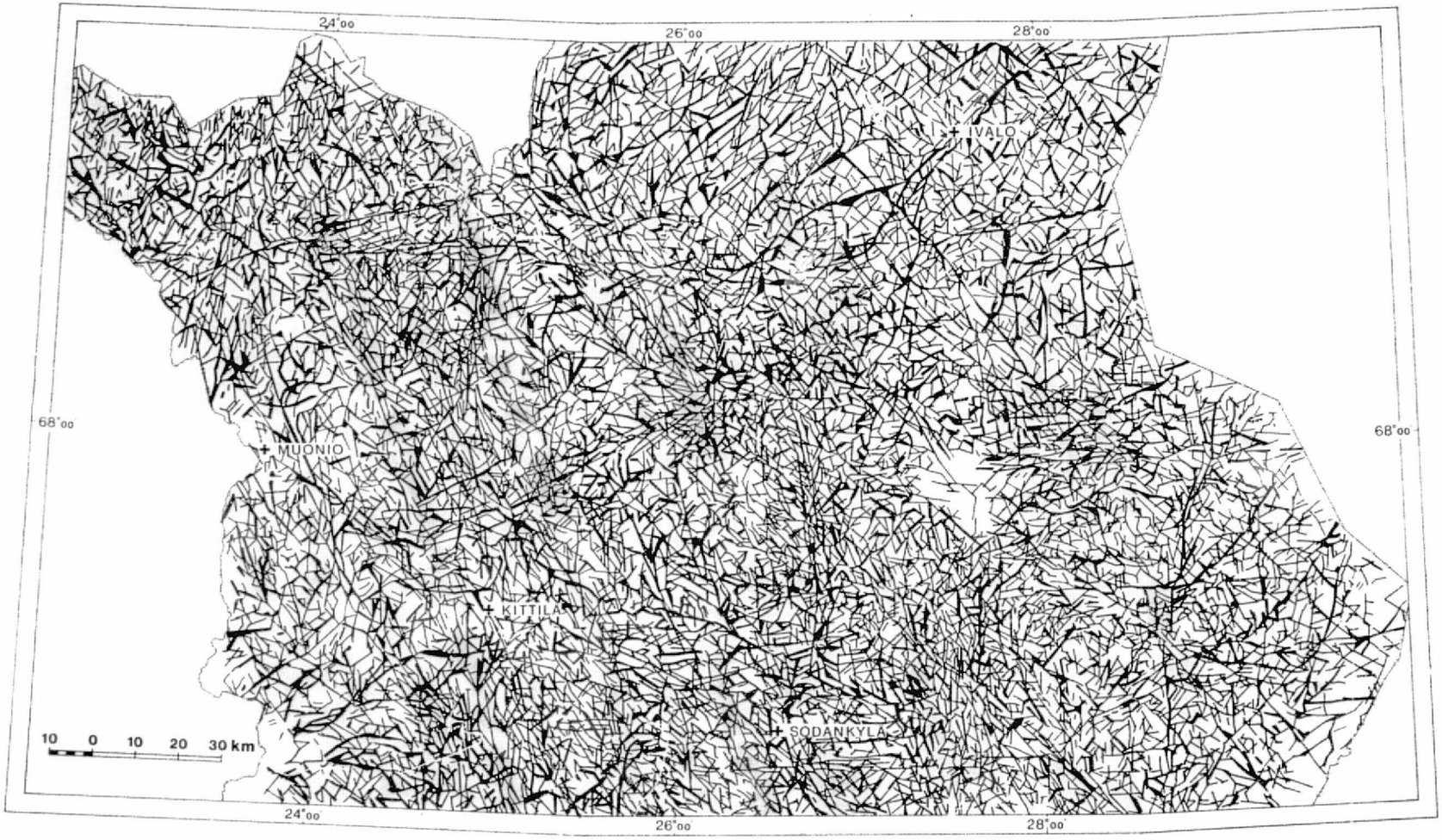

Fig. 15. Map of linears in central Finnish Lapland.

foliation of bedrock, dikes and joints. However, the dense network of linears clearly reveals some characteristic patterns. Several wider zones of subparallel linears, as well as lines of discrete short linears, can be traced over long distances, in some cases through the whole area studied. For example, there is an obvious zone of subparallel linears running through the Sodankylä, Kittilä and Muonio areas. Another clear zone runs from north of Muonio ENE towards Ivalo. On the other hand, some areas of distinctive linear patterns and densities can be discerned. In many cases these areas seem to be confined to some major rock units of the region (compare Figs. 15 and 27). For instance, NE of Muonio there is a roughly triangular area of higher linear density, which coincides with an area of granite gneiss.

3.2.3 LANDSAT-linears discarded

To see to what extent the LANDSAT-linears found in scene 1039-09315 (Fig. 9) have been included in the final map of linears (Fig. 15), the LANDSAT-linears, or parts of them, not included in the final map were drawn on a separate map (Fig. 16 a). Comparing Fig. 8 with 16 a, one will notice that most of the LANDSAT-linears have been detected also either in the aerial photos or in the bog and water map. Only a few of the longer LANDSAT-linears or their segments have been left out of the final map of linears.

The strike-frequency analysis of the discarded LANDSAT-linears (Fig. 16 b) shows that they are mainly oriented in three directions, 65^{o} - 90^{o}, 350^{o} - 05^{o} and 320^{o} - 330^{o}. Moreover, there occur three minor peaks in the 340^{o} - 345^{o}, 30^{o}, and 40^{o} - 45^{o} ranges. The highest peak in the 65^{o} - 90^{o} range is obviously due to the illumination effect (see p. 33). The azimuth of the sun has been 167^{o} and the elevation 30^{o}.

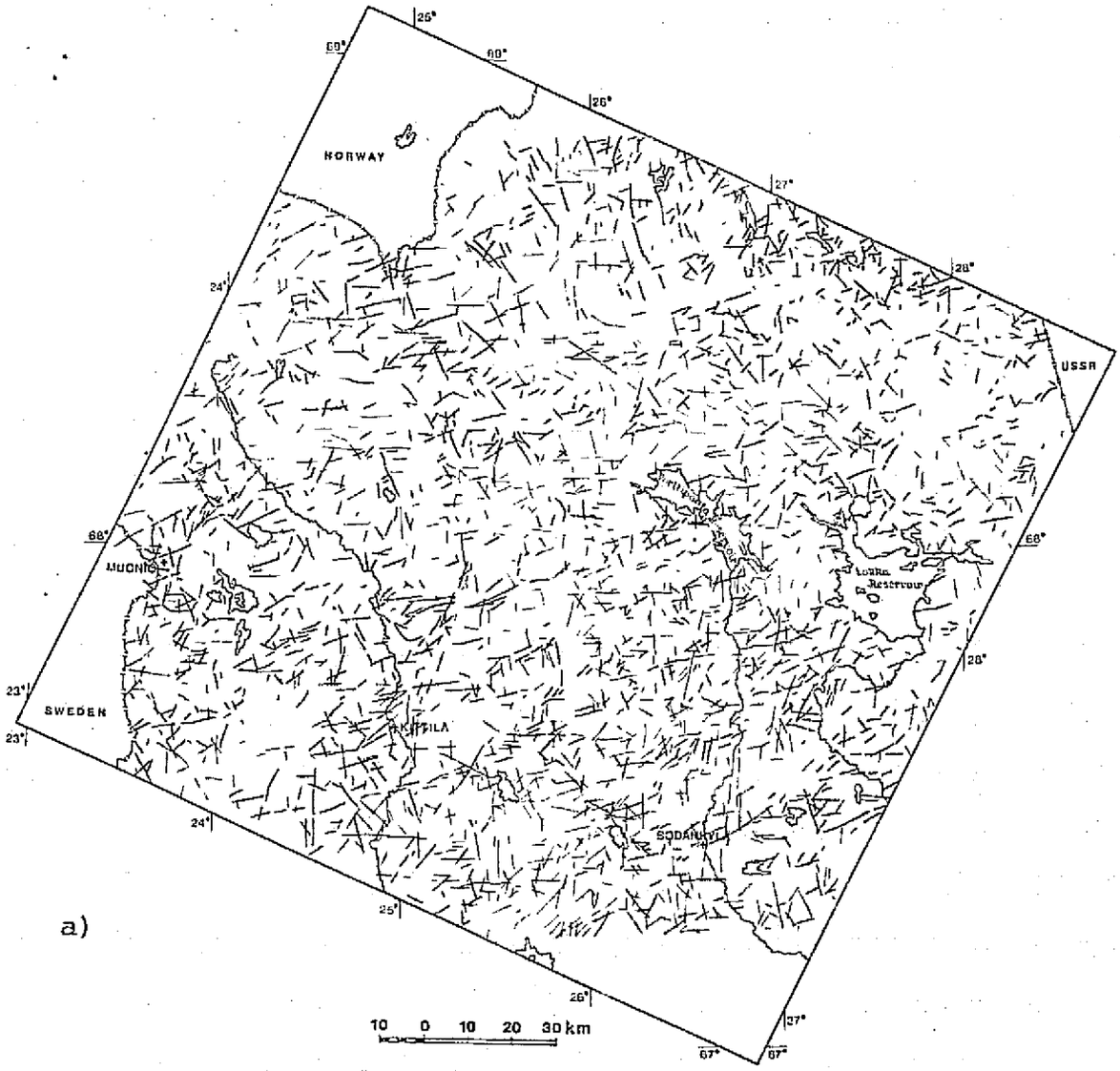

a)

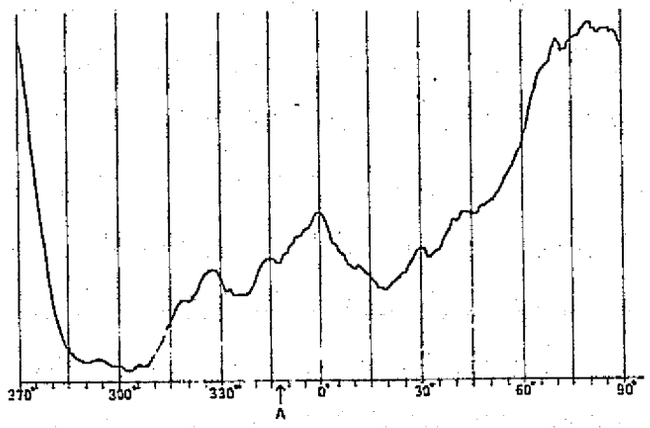

b)

Fig. 16. a) LANDSAT-linears of scene 1039-09315, or parts of them, not included in Fig. 15.

b) The relative strike-frequency curve of the LANDSAT-linears shown in (a). Obtained by optical filtering. The azimuth of the sun at the imaging time is marked A.

Features roughly perpendicular (77°) to this direction tend to show up clearly on the image and have thus been easily overemphasized in the interpretation. The peaks 320° - 330° and 350° - 05° coincide roughly with corresponding maxima in Fig. 12, b and c, as do the minor peaks at 30° and 40° - 45°. Thus they evidently indicate true prevailing linear trends of the area. Linears of these trends have been detected relatively more often or as longer linears from LANDSAT imagery than from aerial photos or the bog and water map. The reason for this might be that the linears in the directions of 320° - 330° and 350° - 05° are at a small angle to the incident light (167° or 347°, marked A in Fig. 16b) and may, if composed of valleys or slopes, be well revealed in a low angle illumination by sharp, narrow shadows on one slope and illuminated areas on the other (cf., Wise 1968). On the other hand, the overemphasis of linears in the 320° - 330° range is also due to glaciogenic features, since the general flow direction of the Quaternary ice sheet in the southwestern parts of the scene area was from about 320° - 330°.

As a whole, considering the use of LANDSAT imagery in the analysis of linears, it seems possible to obtain essentially the same results rather than by doing, for instance, time-consuming aerial photo interpretations of large areas. Moreover, satellite imagery often seems to reveal linear features better over their whole length than does stereographic study of large-scale aerial photos piece by piece. However, the specific illumination effects caused by the nearly polar sun-synchronous orbit of LANDSAT should be kept in mind in the search for linears or lineaments from the images and especially in the strike-frequency studies of these features.

3.2.4 Classification and trend analysis of the linears

As the different types of linears were not differentiated in Fig. 15, the network became quite dense; linears representing significant fault or fracture zones, or their components, are difficult to distinguish from other linears.

It is well known that sudden changes in aeromagnetic anomalies, such as disruptions, dislocations, systematic bends, steep gradients, changes in the pattern of anomalies, etc., frequently indicate faults and fracture zones, while narrow anomalies mostly reflect magnetized horizons and thus bedrock trends. The main bedrock trends are also indicated by small-scale geological maps. Aeromagnetic (1 : 400 000) and geological maps (1 : 400 000) were therefore used in the classification of the linears.

A criterion used in many of the definitions of linears and lineaments is the observed length. Different authors have used different length classes but generally the lower limit adopted for a linear has been one or a few miles (e.g, Lattman 1958 and Hoppin 1974).

In the present work, with a few exceptions, linears 5 km and more in length have been considered significant. Thus the linears shown in Fig. 15 were placed into the following three classes:

- Class I: Significant linears, representing fault and fracture zones (Fig. 17); length $\geq$ 5 km, visible on aeromagnetic maps as sudden disruptions, dislocations, systematic bends, sudden drops of intensity, etc., of anomalies. Further ,certain shorter linears have been accepted as significant if they are obvious parts of longer significant linears or zones of them.

- Class II: Linears representing bedrock trends (Fig. 18); parallel or subparallel to elongated aeromagnetic anomalies or anomaly belts, or to the general bedrock trends shown by geological maps.

- Class III: Minor linears, representing minor faults, fractures, jointing, dikes, etc., as well as superficial features attributable to, for instance, glaciogenic effects (Fig. 19); no observable correlations with aeromagnetic anomalies or geological maps.

In Figs. 17, 18 and 19, certain differences can be noticed in the areal distribution of the linears of each class. These differences seem to correlate roughly with the main rock distribution of the linears (Fig. 27). Class III linears are more frequent in the areas of granitoid rocks and parts of the Pre-Svecokarelian basement than in the schist areas where linears of Classes I and II are relatively more abundant. The schist areas generally have a higher and more complicated magnetic relief (Figs. 27 and 31). For this reason, linears of Classes I and II are more easily found in them than in the areas of granitoid rocks and parts of the basement. As the magnetic relief in the latter areas is mainly smooth, linears of Class III tend to be observed at the expense of those of Classes I and II.

According to observations made by Autio (1975) in central Finland, differences in the type and distribution of magnetic linears show a regular correlation with differences in the bedrock type. As studied in the present work, the rates of occurrence of linears correlating differently with the magnetic bedrock properties may also be used as a criteria of the nature of the bedrock (see also p. 42 and Fig. 15).

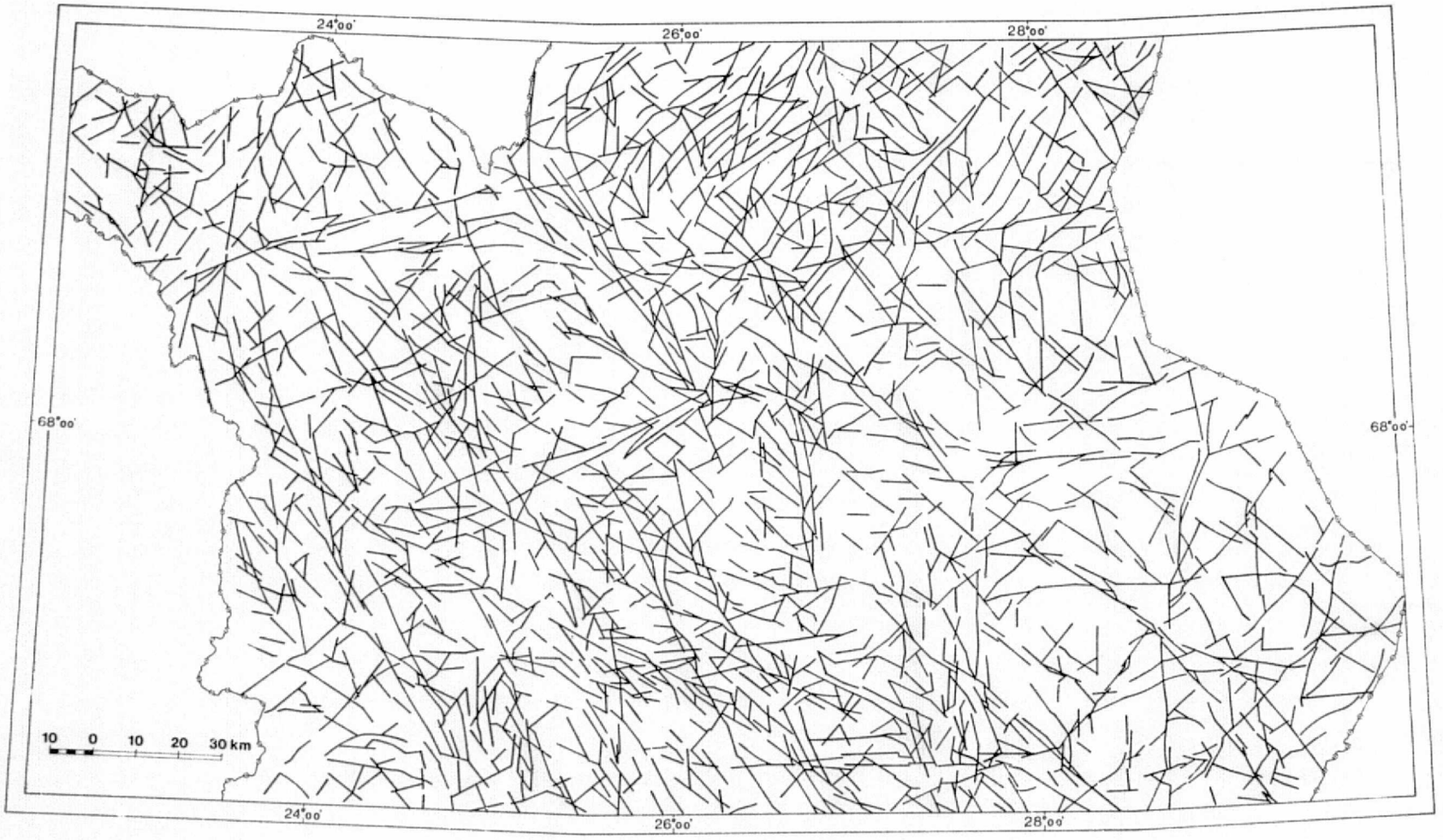

Fig. 17. Class I linears, representing fracture and fault zones.

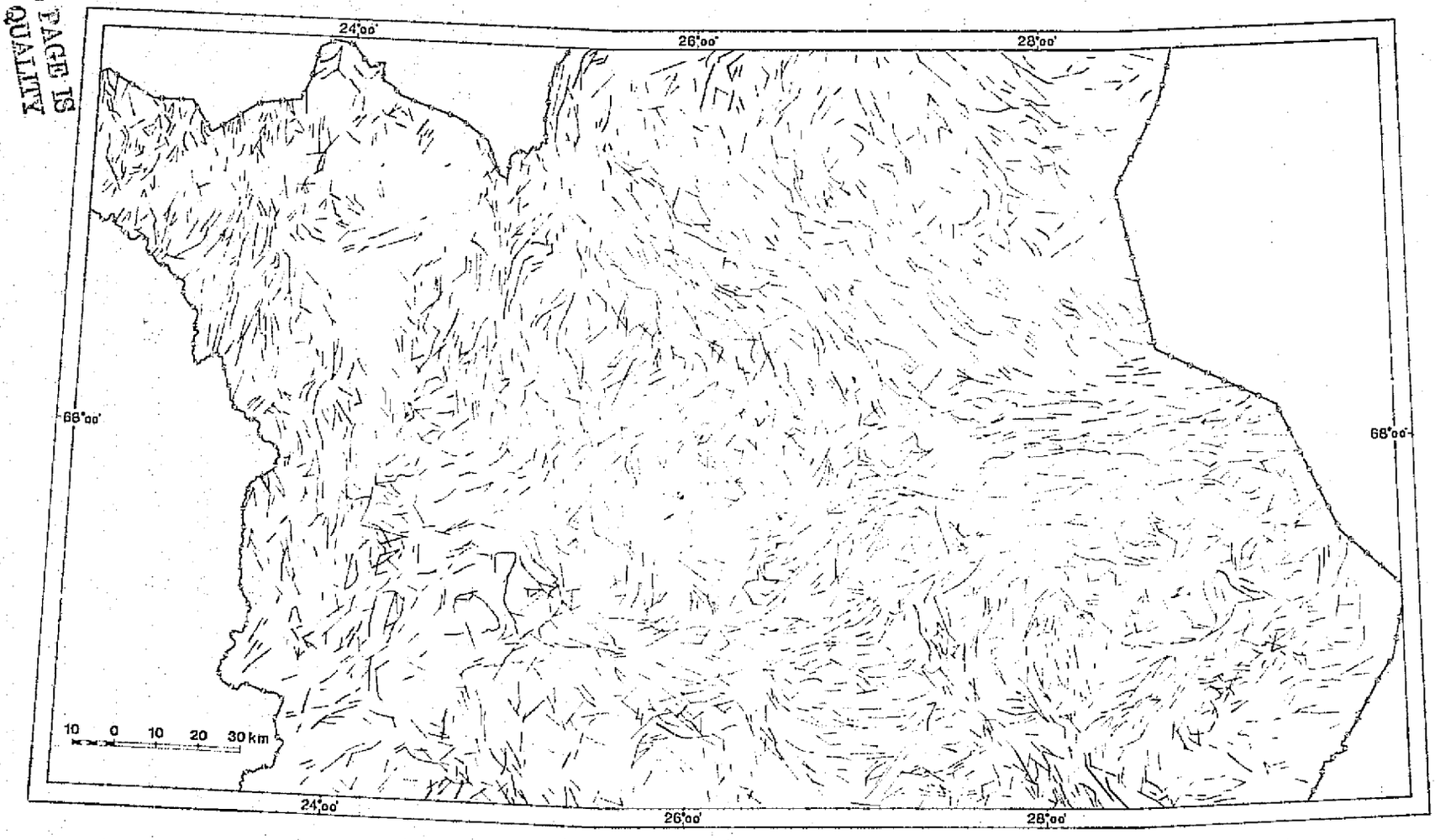

Fig. 18. Class II linears, representing bedrock trends.

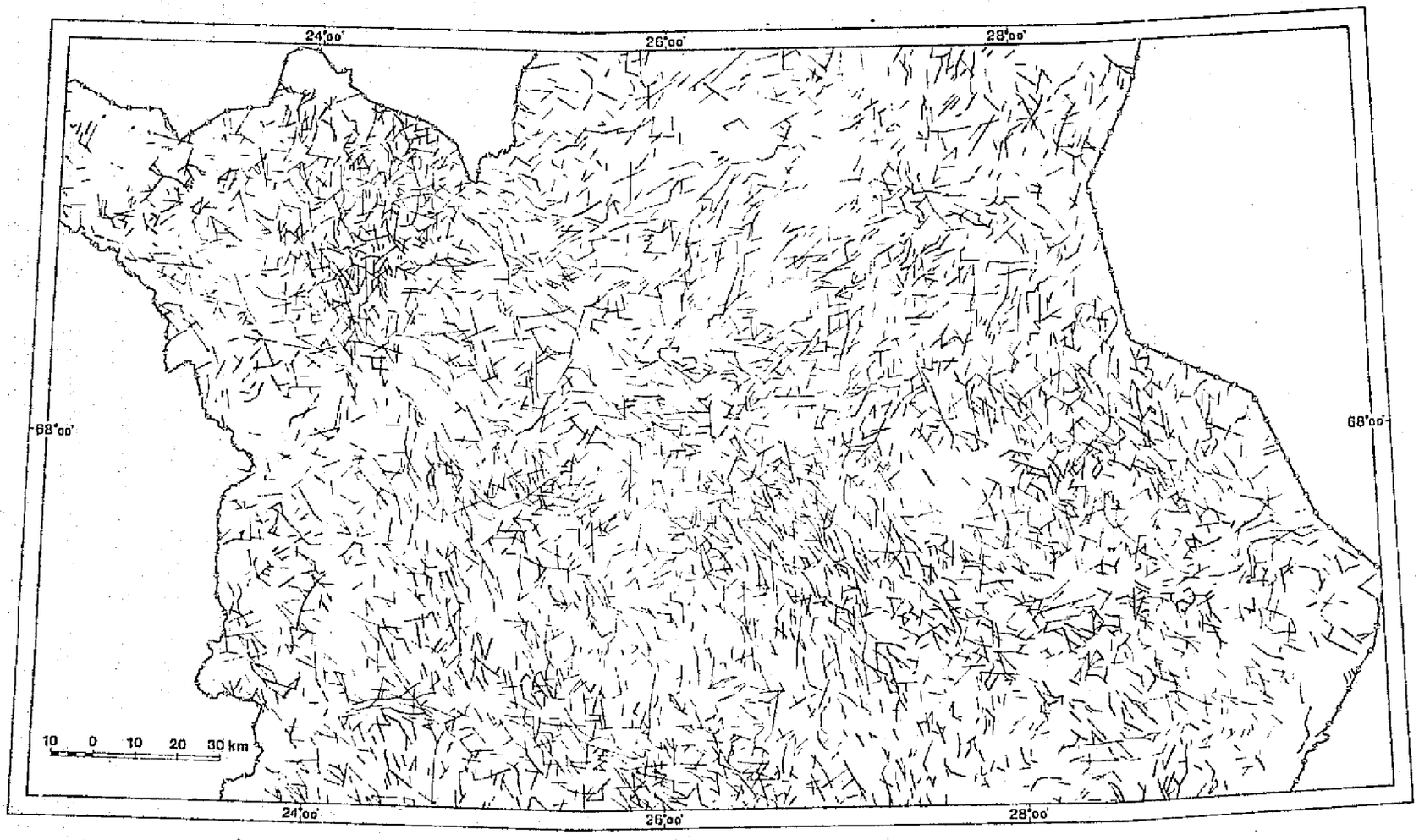

Fig. 19. Class III linears, representing minor faults, fractures, jointing, dikes, etc.

Tuominen et al. (1973) report the crustal shear in the central Baltic Shield to have followed eight main trends. This conclusion was drawn from a strike-frequency analysis of foliation, gravity isolines and fracture lines (Fig. 21B) from areas of Finland south of 67th parallel. To see whether the same main trends occur also in the linears of central Lapland, a strike-frequency analysis was performed on each of the three classes of linears (Figs. 17, 18 and 19) by optical filtering (see p. 33).

The resulting strike-frequency curves are seen in Fig. 20. The general strike frequency distribution of Class I (Fig. 20a) differs clearly from those of Classes II and III (Fig. 20, b and c), the latter two showing rather similar general distributions. However, certain correlations can be noticed between the separate peaks of each curve, although the peaks in Classes II and III are mostly rather small or mere bulges on the slopes of the curves. The maxima of the strike frequency curve for Class I (Fig. 20a) are numbered from 1 to 10 and those of the other curves (Fig. 20b and c), which are considered analogous to them, are numbered respectively. The Class I linears (Figs.17 and 20a) seem to follow ten main trends, six of which (320^{o}-325^{o} , 328^{o}-335^{o}, 350^{o}-05^{o}, 38^{o}-45^{o}, 50^{o}-60^{o} and 80^{o}-90^{o}) coincide with Class II and III linears (Fig. 20b and c). Three of the main trends of Class I (307^{o}-315^{o}, 25^{o}-30^{o} and 65^{o}-75^{o}) seem to coincide only with those of Class III.

One of the maxima of Class I (298^{o}-303^{o}) does not form peaks in Class II or III, but may be reflected as slight bulges in the slopes of these curves (Fig. 20b and c). There are also two other obvious maxima, one common to Classes II and III (09^{o}-18^{o}) and one occuring in Class III only (275^{o}-285^{o}), which fall within frequency lows of Class I.

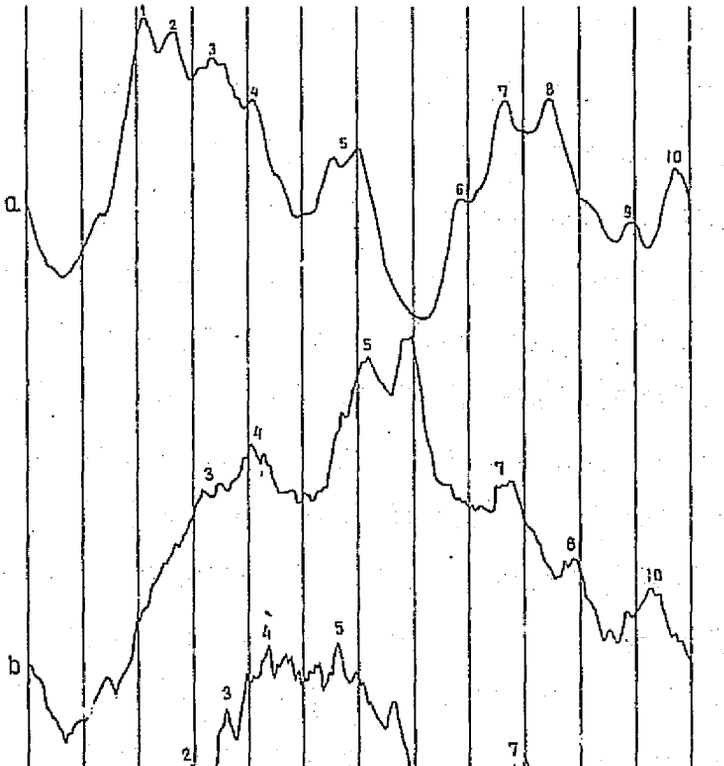

Fig. 20 Strike-frequency analysis of different classes of linears: a) Class I linears, b) Class II linears, and c) Class III linears. Obtained by optical filtering. The curves are not normalized and may contain some instrumental drift. Numbers 1 through 10 indicate the maximum trends of Class I linears and respective peaks in the other curves.

The relative strike-frequency maxima (Fig. 20) of Figs. 17, 18 and 19 correlate fairly well with the results of the trend analysis of photolinears, LANDSAT-linears and the corresponding LANDSAT-image (Fig. 12 and p. 36 The differences result obviously from the different

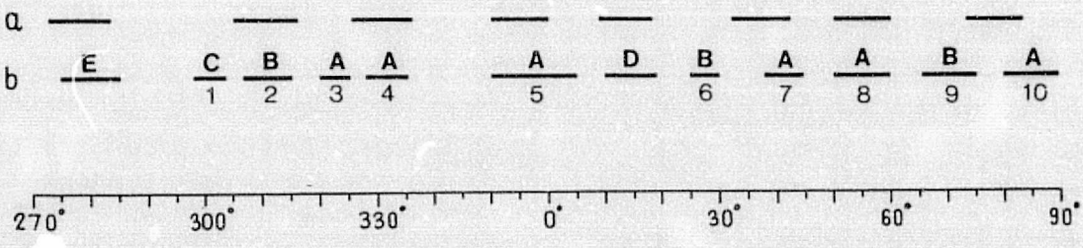

Fig. 21A Main trends of crustal shear in the central Baltic Shield as recalculated from Tuominen et al. (1973, Fig. 4) (a), and the main trends of the linears of different Classes (b). The trends in (b) are numbered respectively as in Fig. 20 and categorized according to their occurrences in different Classes of linears:

A maximum present in each of the three Classes
B " " in Classes I and III
C " " in Class I only
D " " in Classes II and III
E " " in Class III only

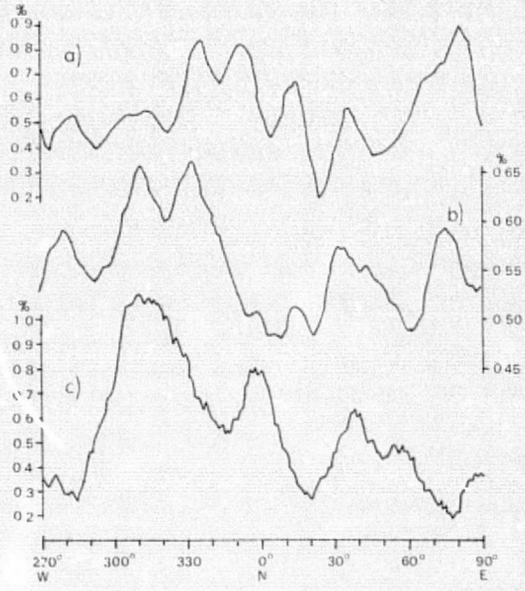

Fig. 21B. Strike-frequency distribution for: (a) foliation , (b) Bouguer gravity isolines, (c) fracture lines; from Finland between 60th and 67th parallels (Tuominen et al. 1973, Fig. 4.)

sample areas (Figs. 11, 17, 18 and 19) and from the procedure used in the compilation of the map of linears (fig. 15). The curves in Fig. 12 have been obtained from samples of the bulk data (Fig. 11), which evidently include linears of superficial (glaciogenic ?) origin. These have been removed, at least partly, from the map of linears (Fig. 15) and thus also from Figs. 17, 18 and 19.

Fig. 21A shows the main trends of linears obtained in the present study (b) and the main trends of crustal shear (a) recalculated from Tuominen et al. (1973, Fig. 4.). This recalculation was made by using the azimuthal means and standard deviations of each maximum of their strike frequency curves (Fig. 21B) for foliation, gravity isoline and fracture line trends, respectively. Then the number of maxima present in each one-degree intervals as defined by the aforementioned quantities, was counted. The azimuthal means^{+} standard deviations of the maxima thus obtained were used as representing the main trends.

In Fig. 21A (b) the main trends of the linears are categorized according to their occurrence in the different classes of linears. Five of the trends of category A correlate rather well with the trends recalculated from Tuominen et al. (1973). One, possibly two, of the category B trends correlate with the trends reported by Tuominen et al. (op.cit.). Only two of the trends of Tuominen et al. (op.cit.) do not have respective maxima in the strike frequency distribution of Class I linears (Figs. 17, 20a and 21A), but occur as maximum trends for Class II and/or Class III linears (categories D and E) (Figs. 18, 19, 20b and c, 21A).

In addition, there are four trends for the Class I linears that do not correlate directly with the trends derived from Fig. 21B.

They are numbered 1, 3, 6 and 9 in Fig. 20a and belong to categories A through C in Fig. 21A(b). Their position, as compared to the other maximum trends, however, show a remarkable analogy. All of them are about 5^{o} to 10^{o} to the left from the main trends of Tuominen et al. (op.cit.) and of the corresponding maxima of the present study. Moreover, they are all of the same, or one degree lower, category as the respective neighbouring maxima to the right. Drawing on these analogies, they may actually belong to the corresponding trends of Tuominen et al. (op.cit.). As a matter of fact, even the maximum 5 (Fig. 20 a) seems to be a double maximum, with peaks some 5^{o} apart. The differences of this kind might be explained in three ways:

1. They may reflect rotation of some structures 5^{o} to 10^{o} to the left at some stage of the geological evolution and later rejuvenation of the corresponding structure in their original positions.

2. They may reflect a 5^{o}-10^{o} deflection (cf., Newhouse 1942, pp. 11-12) of the corresponding structures at the boundaries of some lithologic units or major blocks.

3. They may reflect slightly different patterns of the corresponding structures within different lithologic units or major blocks.

Anyhow, at this stage they are assumed to belong to the same main trends of crustal shear (Tuominen et al. 1973) as the neighbouring peaks to the right.

It seems obvious that the patterns of crustal shear found in southern and central Finland have played an important role also in the evolution of central Lapland. However, judging from the data analyzed, the different

trends evidently differ in nature and occur differently in different parts of the area. In certain parts of the area, some of them may even be lacking (cf., Nanyaro 1975).

As the linears obtained in this study are considered to represent the structures mentioned in their classification (p. 45), the significance of their trends can be deduced. The trends (320°-325°)+(328°-335°), 350°-05°, (25°-30°)+(38°-45°), 50°-60° and (65°-75°)+(80°-90°) are evidently the most significant, since they are reflected in bedrock trends as well as in trends of significant fault and fracture zones, and in the trends of minor fractures, jointing, dikes, etc. The trend (298°-303°+(307°-315°) seems to come from fracture and fault zones. Two of the main trends of Tuominen et al. (op.cit.) have obviously played a minor role in central Lapland, since they are reflected only in bedrock trends (09°-18°), on in minor fractures, jointing, dikes, etc. (275°-285°).

To see how the Class I linears, representing significant fracture and fault zones, are distributed over the study area, the map of these linears (Fig. 17) was filtered optically in seven different azimuthal sectors. The filtration was performed with a 25° sector-pass filter so that each maximum trend of the linears falls within at least one of the azimuthal sectors (Figs. 20, 22 and 23). Each filtration was photographed and the linears belonging to each azimuthal sector thus obtained were redrawn using the photos and the original map. The approximate boundary between the Svecokarelidic formations and their basement complex (according to Simonen 1971, Fig. 2) was drawn on each filtered map.

The results of filtration show several characteristic features in the distribution of linears of different

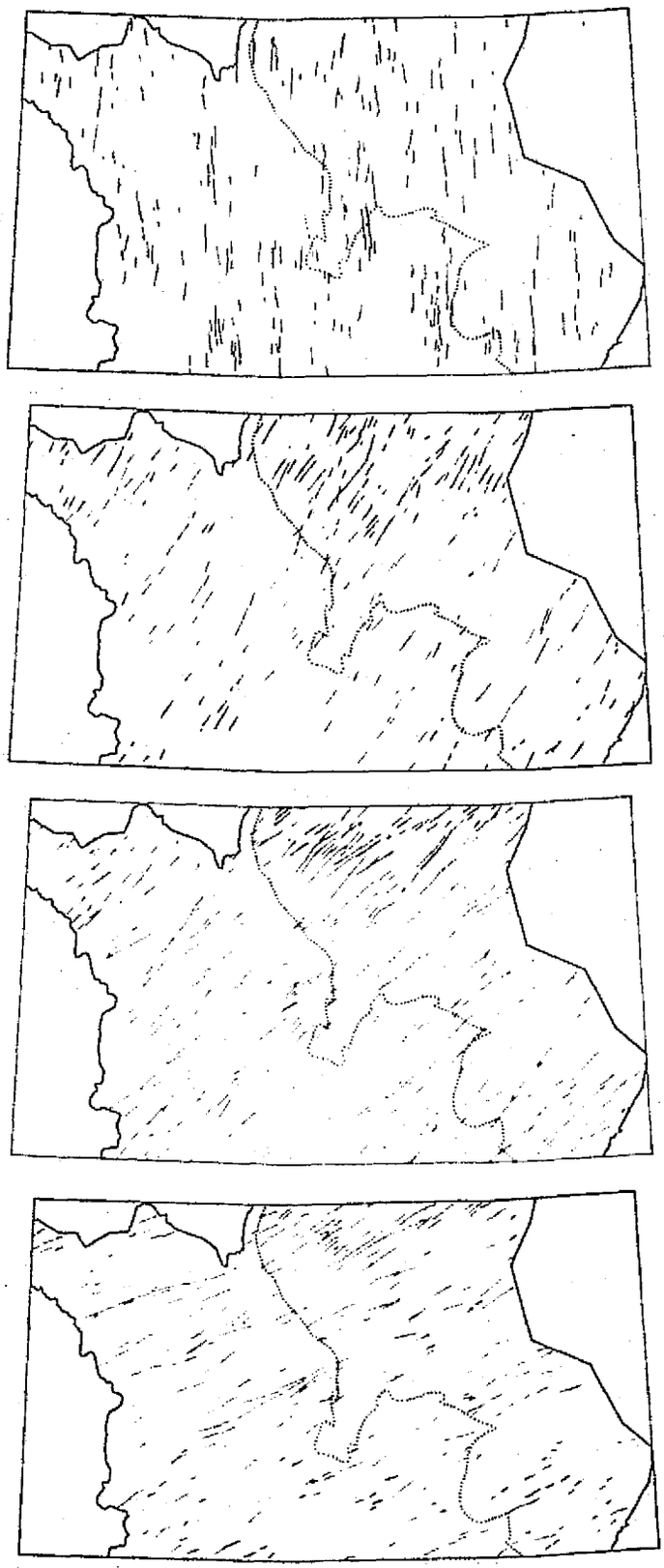

Azimuthal sector	Maximum trends included
351°-16°	350°-05°
15°-40°	25°-30°
33°-58°	38°-45° 50°-60°
48°-73°	50°-60° 65°-78°

Fig. 22a. Areal distribution of Class I linears of different trends in central Finnish Lapland, northeasterly trends. Obtained by optical filtering (25°-sector-pass filter) of linears in Fig. 17. The boundary of the Svecokarelidic formations (W-side) and their basement complex (E-side) is marked with dotted line.

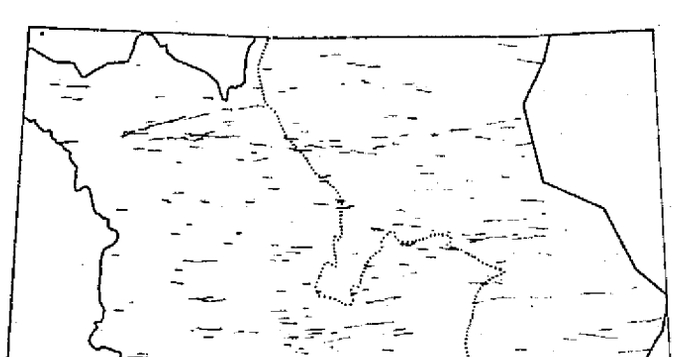

Azimuthal sector	Maximum trends included
77^{o}-282^{o}	80^{o}-90^{o}

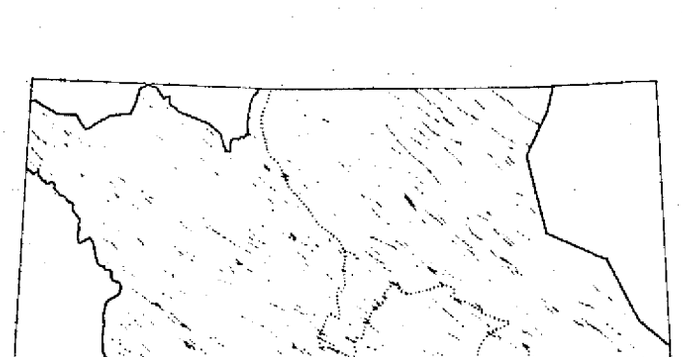

294^{o}-319^{o}	296^{o}-303^{o} 307^{o}-315^{o}

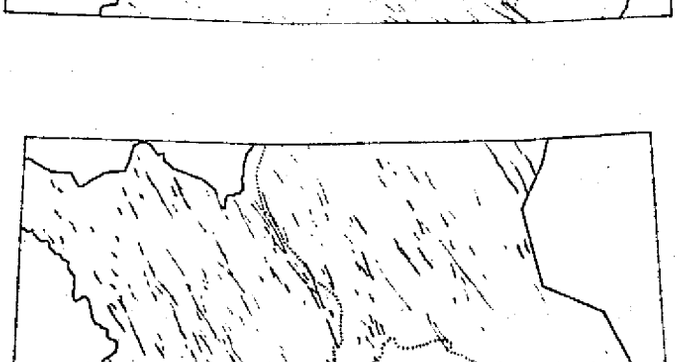

318^{o}-343^{o}	320^{o}-325^{o} 328^{o}-335^{o}

Fig. 22b. Areal distribution of Class I linears of different maximum trends in central Finnish Lapland, northwesterly trends. Obtained bu optical filtering (25^{o}-sector-pass filter) of the linears in Fig. 17. The boundary of the Svecokarelidic formations (W-side) and their basement complex (E-side) is marked with dotted line.

trends (Fig. 22). Especially the linears in sectors 351^{o}-16^{o} and 77^{o}-282^{o} seem to be arranged in zones, but also the other sectors reveal zones of longer, sub-parallel linears extending in some cases through the map area (e.g., the sectors 48^{o}-73^{o}, 294^{o}-319^{o} and 318^{o}-343^{o}). In the area of Svecokarelidic formations, the northwesterly linears appear to be more abundant and generally longer than the northeasterly ones. The linears in sector 318^{o}-343^{o} are clearly more abundant in the Svecokarelidic formations than in their basement complex. Northeasterly linears are most frequent in the northern parts of the basement complex. In sector 294^{o}-319^{o} (Fig. 22), a slight difference in the trends of the linears within the two main lithologic units can be noted: within the Svecokarelidic formations, these linears appear to be oriented more westerly than within the basement complex.

To study the differences observed in the patterns of linears between the Svecokarelidic formations and their basement complex, a relative strike-frequency analysis of the Class I linears (Fig. 17) was performed separately for the eastern and western parts of the area in two ways. In the first, the map was divided into the two parts along the approximate formation boundary (Fig. 22), and in the second, along the line A-A shown in Fig. 24 The results are shown in Fig. 23 together with the relative strike-frequency curve of the whole map. The filter sectors used for Fig. 22 are indicated along the top of the picture. The strike-frequency analysis confirms clearly that the orientational patterns of the linears in the Svecokarelian formations and their basement complex are different. However, there is no essential difference between the two ways of separating the areas. This could mean that the border of the basement complex is actually a zone where the pattern of linears changes. In the area of Svecokarelidic formations, the strikes of

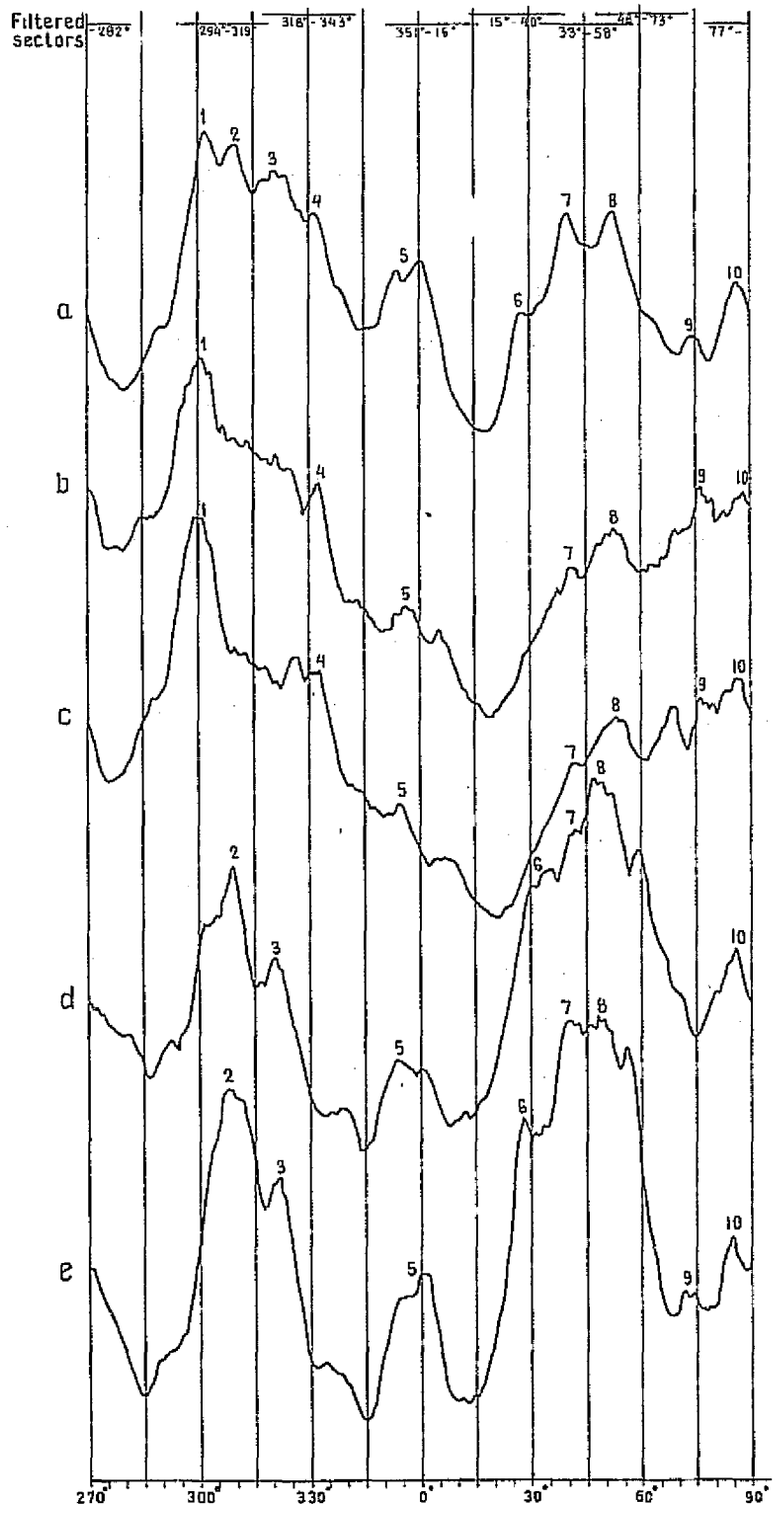

Fig. 23. Strike-frequency analysis of Class I linears for W and E parts of the study area separately.
a) whole area (as in Fig. 20a),
b) area west of the boundary of the Svecokarelidic formations,
c) area west of line A-A shown in Fig. 24,
d) area east of the boundary of the Svecokarelidic formations,
e) area east of line A-A shown in Fig. 24.

the linears are concentrated into two wide maximum ranges (Fig. 23, b and c). In the basement complex, they form four main ranges of maxima (Fig. 23 d and e). Further, obvious shifts in the positions of the peaks can be noticed between the two areas.

The peaks are numbered according to the respective peaks in the curve for the whole area (Fig. 23 a). As noted earlier (p. 54), the Class I linears (Figs. 20a, 21 A(b) and 23 a), have four maxima, 1, 3, 6 and 9, which are related similarly to the nearest maxima to the right, i.e., 2, 4, 7 and 10, respectively, and to the corresponding main trends of the crustal shear (Tuominen et al. 1973) (Fig. 21 A). Trends 1, 4 and 9 seem to prevail in the Svecokarelidic formations and trends 2, 3 and 6 in the basement complex. Trends 7 and 10 are found in both areas. The curves of both areas show minor maxima, which do not exist in the curves of the other area, or have shifted 5^{o}-10^{o}.

The foregoing analysis indicates that the two main lithologic units of the area, the Svecokarelidic formations and their basement complex, both have their own characteristic patterns of linears. The trends of the linears correlate in a general way with the main shear trends reported by Tuominen et al. (1973) but show distinct deviations in detail. This suggests that the patterns of crustal shear are also different in the two areas.

In Fig. 24 a and b, the azimuthal sectors (Fig. 22) containing the characteristic trends of Class I linears obtained for these areas are combined into two maps to demonstrate the difference between the patterns of the linears in the Svecokarelidic formations and their basement complex. Fig. 24 c shows the linears of the maximum trends common to both areas. In Fig. 24 a, the basement complex is clearly characterized by one set of long linears with a northwesterly

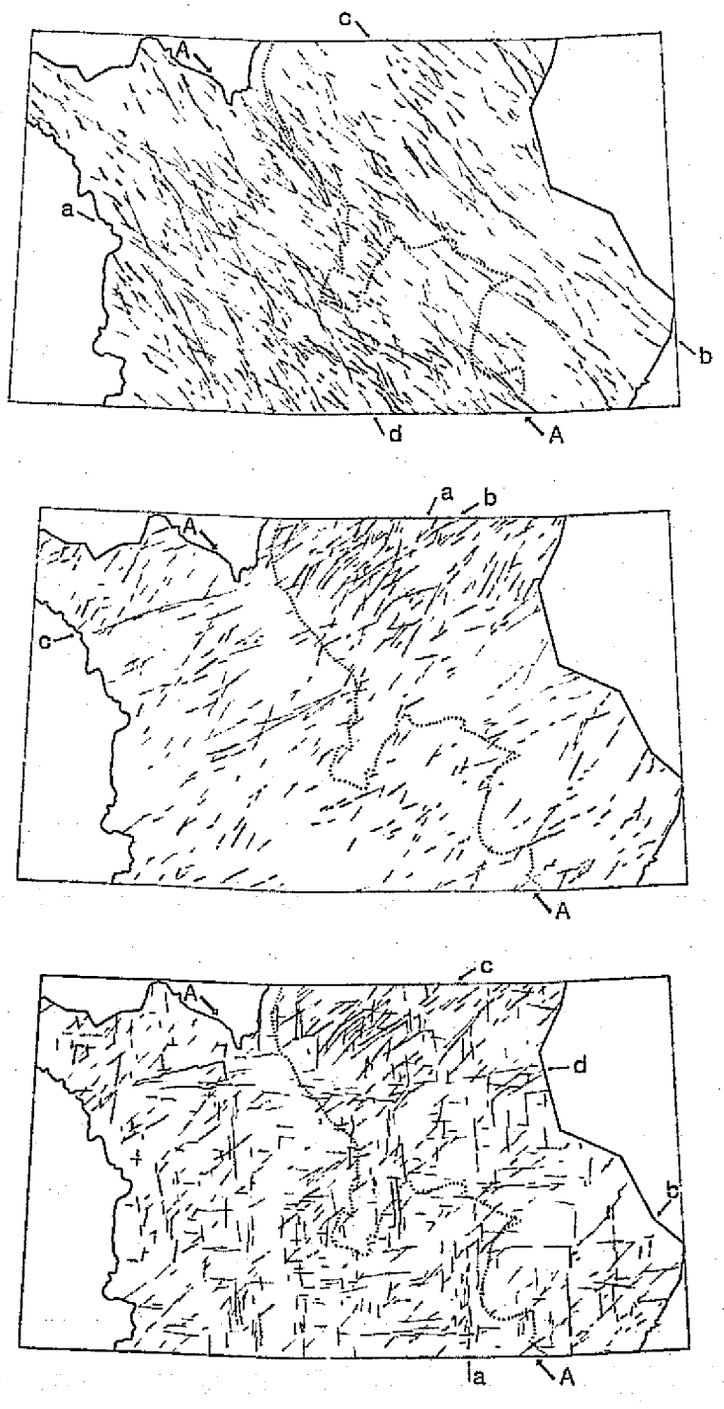

Maximum trends included

a) 296°-303°(a), 307°-315°(b), 320°-325°(c), 328°-335°(d)

b) 25°-30°(a), 50°-60°(b), 65°-78°(c)

c) 350°-05°(a), 38°-45°(b), 50°-60° (c), 80°-90°

Fig. 24. a) and b): Azimuthal sector combinations from Fig. 22 revealing different patterns of Class I linears in the Svecokarelidic formations (W-side) and their basement complex (E-side).

c) Trends common to both areas.

The boundary of the Svecokarelidic formations and their basement complex is marked with dotted line. A-A: divide line for the second strike-frequency analysis.

trend or zones of linears with strikes fluctuating between the maximum trends 307°-315° and 320°-325°. The Svecokarelidic formations, again, are characterized by two distinct sets of linears, trending 298°-303° and 328°-335°. Of linears trending northeasterly (Fig. 24 b), on the other hand, the set trending 25°-30° is apparently the most frequent in the northern parts of the basement, which is occupied by the granulite complex (see Fig. 27). The set trending 65°-78° forms a few distinct zones of linears within the Svecokarelidic formations. These zones seem to deflect to the north at the boundary zone of the basement complex and may continue there as sets of linears trending 38°-45° or 50°-60°.

The same kind of deflection of fracture zones at the boundary of the Karelidic metasediments and their basement has been noticed by Talvitie and Paarma (1973) in Koillismaa, south of the area of the present study. There the boundary is reported by them to be a block boundary formed by deep fractures. On the other hand, different basement blocks identified in the eastern parts of the Baltic Shield and in the Russian platform are characterized by different trends and intensities of geophysical anomalies and by different trends of faulting (Zhdanov and Sprygina 1968, Simonenko and Tolstikhina 1968) and, according to Salop (1971), by different trends of folding.

It seems possible that the boundary between the Svecokarelidic formations and their basement complex follows the boundary between two major blocks separated by a deep fracture zone (cf., Perevoztsikova, 1974, Fig. 1),

3.3 Fracture zones of central Finnish Lapland

The Baltic Shield is known to consist of a mosaic of blocks separated by numerous faults and fractures of

Fig. 25. Trends of the aeromagnetic anomalies in central Finnish Lapland.

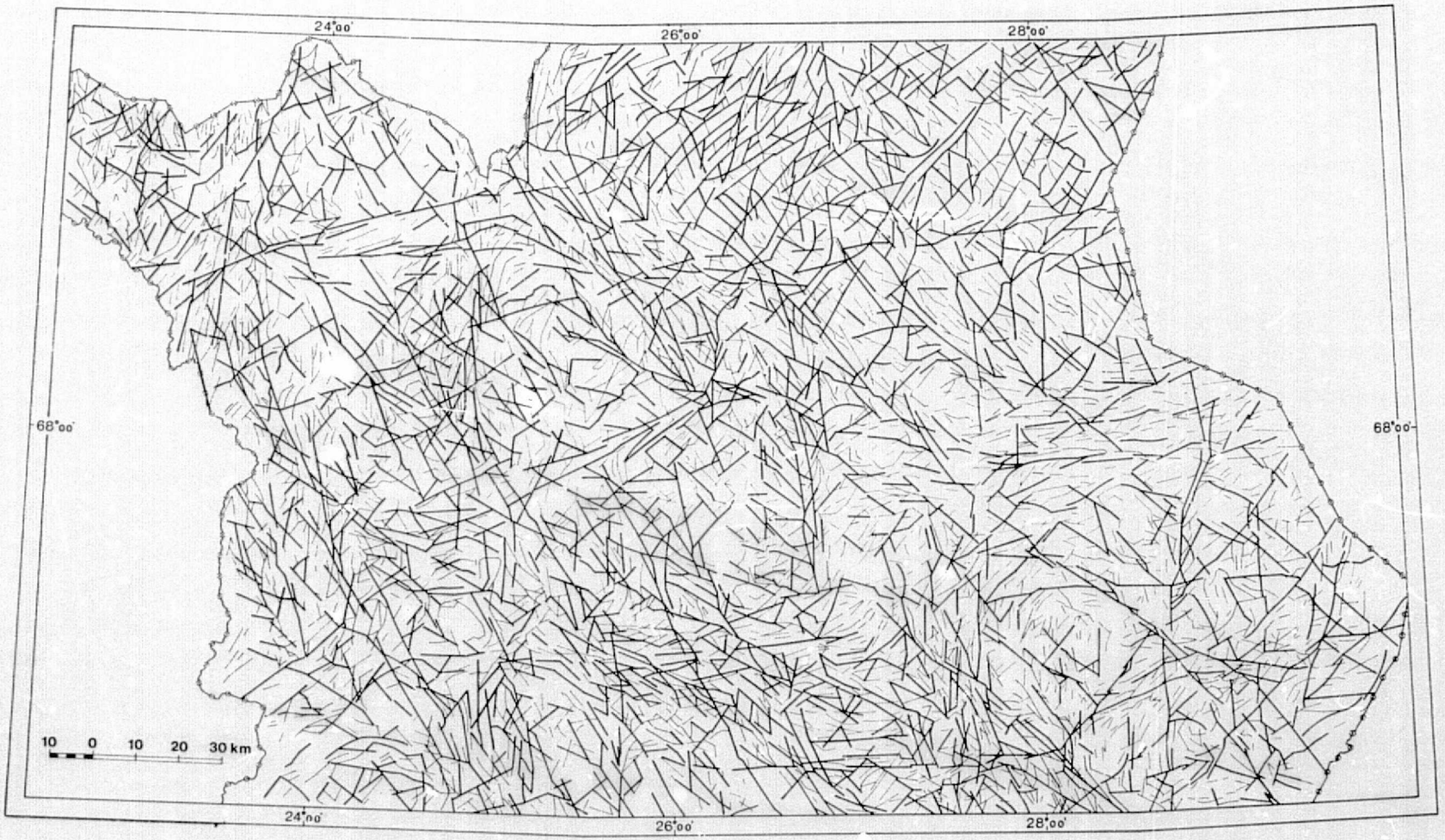

Fig. 26. Class I linears (heavy lines) combined with Class II linears (thin lines) representing bedrock trends in central Finnish Lapland.

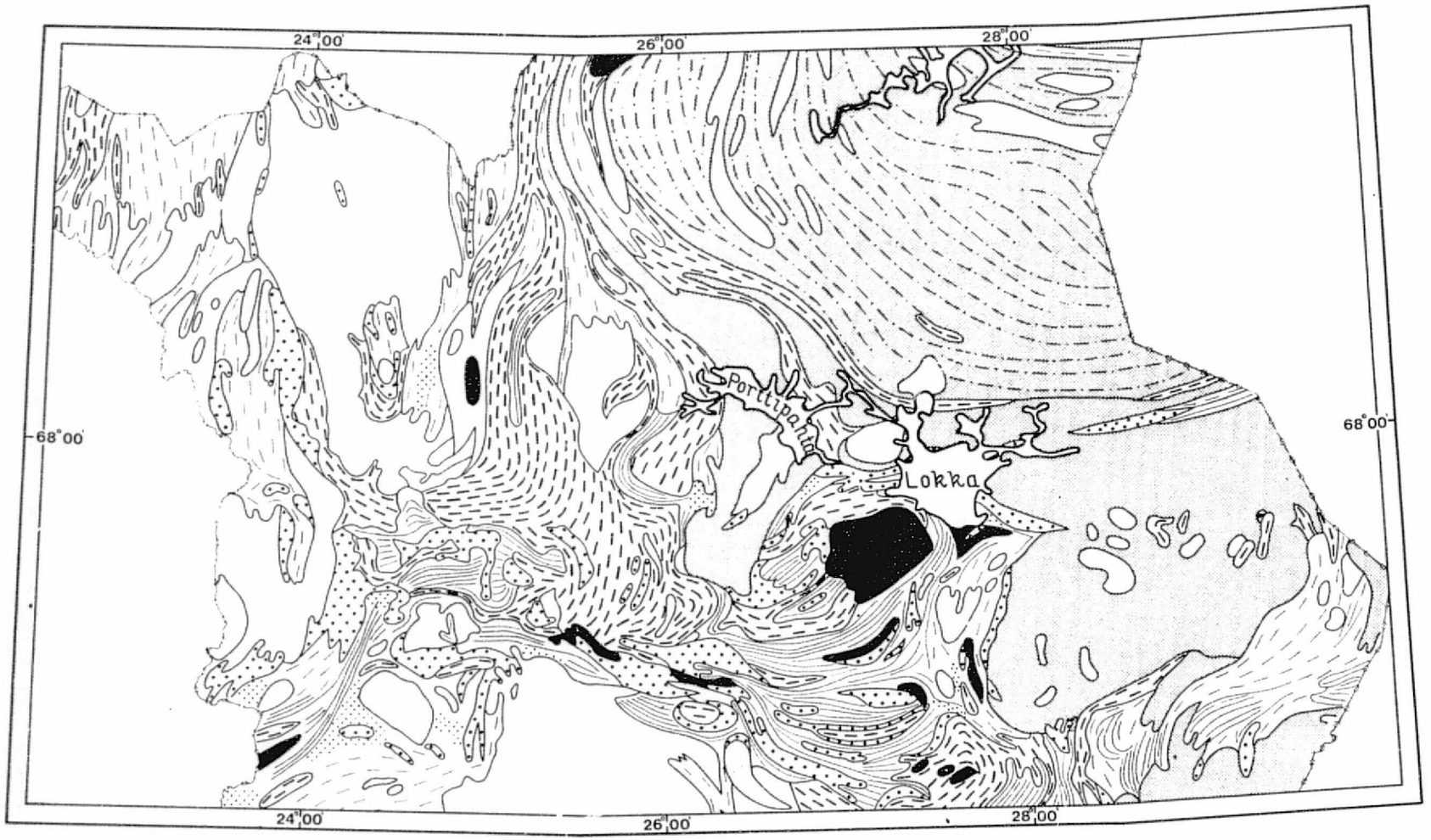

Fig. 27. Generalized bedrock map of central Finnish Lapland, mainly after Simonen (1960). Later mappin 's by Outokumpu Oy, Exploration, are added. For explanation of rock types, see Fig. 32.

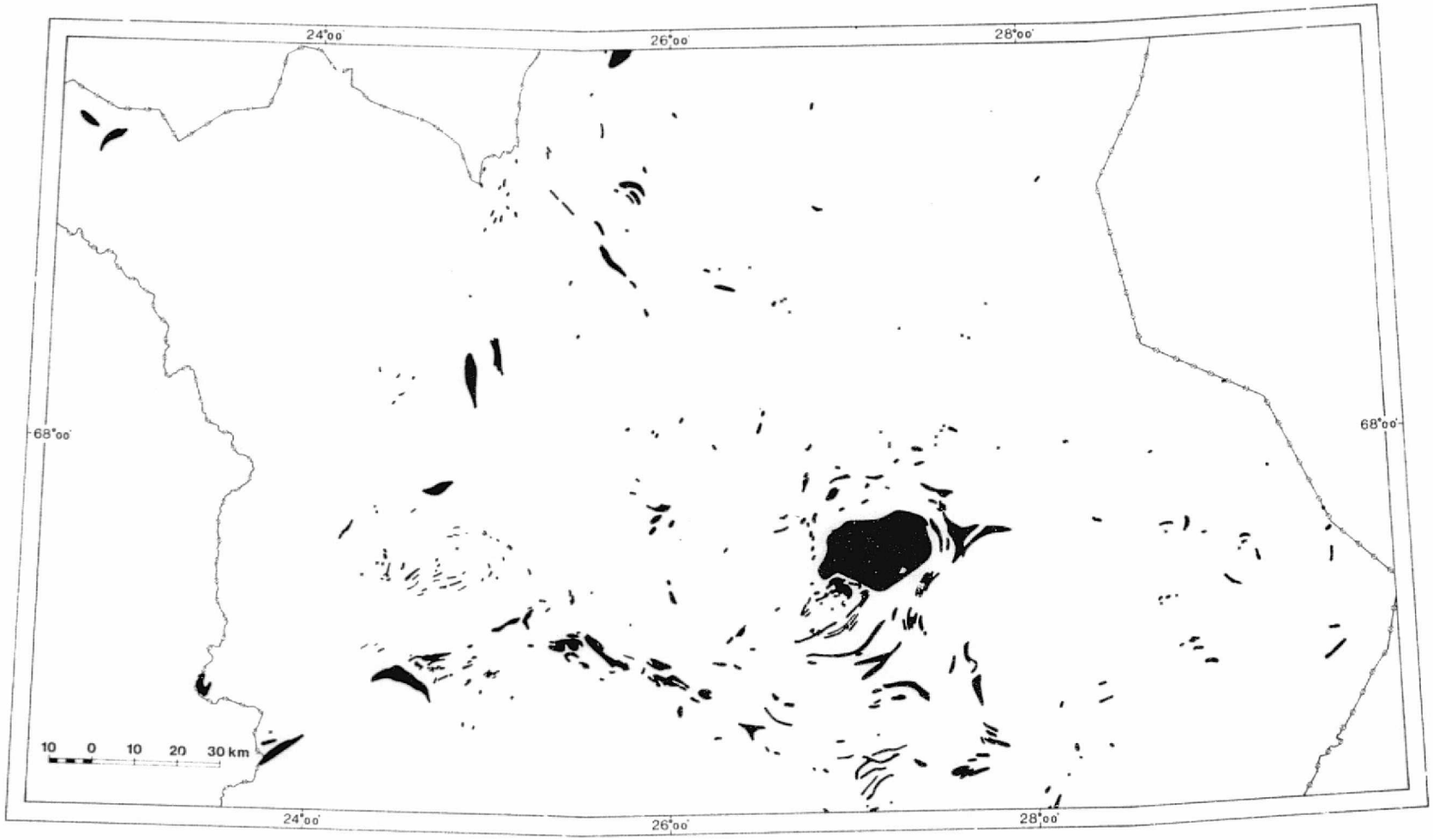

Fig. 28. Basic and ultrabasic rocks of central Finnish Lapland. Compiled from the general geological maps (Mikkola 1936 a, 1936 b, 1937, Meriläinen 1965 and Matisto 1959) and from the mappings of Outokumpu, Exploration. Crosses indicate bodies the sizes of which are not known.

different sizes (e.g., Tuominen 1957, Paarma and Marmo 1961, Paarma 1963, Härme 1966, Bogdanov and Khodotov 1967, Zhdanov and Sprygina 1968, Simonenko and Tolstikhina 1968, Mikkola and Niini 1968, Petrov 1970, Talvitie 1971, Tuominen et al. 1973). Repeated movements of the blocks along the deep fractures and faults have played an important role in the evolution of the Shield by controlling the formation of sedimentation basins, the distribution of igneous rocks and the various phases of folding and faulting (e.g., Mikkola and Niini 1968, Petrov op.cit., Gaál 1972, Tuominen et al.,op.cit., Mikkola and Vuorela 1974, Perevoztšikova 1974). The fractures and faults are therefore traceable also in geophysical maps (e.g., Paarma and Marmo 1961, Paarma 1963, Simonenko and Tolstikhina 1968, Krutikhovskaya et al. 1973, Talvitie and Paarma 1973).

The nature of Class I linears as traces of fractures and faults can be observed by superposing Plate I (same as Fig. 17) on Fig. 25, which shows the trends of aeromagnetic anomalies in the study area. It can be noticed further that the bedrock trends as revealed by the trends of these anomalies as well as by Class II linears (Fig. 26) are generally subparallel to some of the nearby Class I linears. The zones of subparallel Class I linears frequently coincide with the boundaries of different rock formations (Fig. 27 and Plate I) and surround areas of distinctive patterns of bedrock orientation (Figs. 25, 26, 27 and Plate I). Also the basic intrusions tend tc be distributed along these zones (Fig. 28 and Plate I).

It seems evident that the Class I linears and zones composed of them are surface manifestations of major fractures and faults dividing the bedrock into a mosaic of blocks. These fractures and faults follow, in general, the main trends of crustal shear characteristic of the Baltic Shield, but have different patterns in the areas of Svecokarelidic formations and their basement complex.

Plate II shows schematically the most prominent fractures of the study area. The major block boundary between the Svecokarelidic formations and their basement complex seems to consist of several fractures running along the transition zone between the areas of different shear patterns (see p. 58 and Fig. 24). According to v. Gaertner (1962) and Salop (1971), the southern boundary of the granulite complex (Fig. 27) is also a major block boundary.

3.4 Major fracture zones of northern Finland

To obtain a wider view of the fracture patterns described, the study was extended to cover most of northern Finland. The lineament study needed for this purpose was made on LANDSAT-1 imagery obtained mostly in the winter of 1973 (Fig. 29). The search for lineaments was made on the scale of 1 : 1 000 000 since only the more regional features were to be detected and the interpretation scale has been seen to influence the results (Tchalenko and Ambraseys 1970, Vuorela 1973 and Kuosmanen 1975). Lineaments were sought first from each LANDSAT-1 image separately. Then the interpretation overlays were placed together on a mosaic of the images (Fig. 29) to show the lineaments continuing from one image to another. Fig. 30 shows the result of the procedure. The network of lineaments is rather dense, although partly discontinuous owing to the cloud cover. It shows a number of long continuous lineaments or zones consisting of them, which in many cases can be traced through the entire area, extending several hundreds of kilometers. Longer lineaments seem to be concentrated especially in northwesterly directions, but some clear northeasterly lineament zones can also be observed.

The prominent fractures detected in the more detailed analysis of central Finnish Lapland were added to the lineament map (Fig. 30) to complement it in the cloud-covered areas. The resulting map was then compared with the aeromagnetic map of the area, reduced to the same scale (Fig. 31). The lineaments coinciding with disruptions, systematic bends and deep gradients, etc., of the aeromagentic anomalies, as well as with pattern variations and zonal disturbances in the magnetic field, were redrawn on an overlay (Plate III). Other lineaments were discarded.

A comparison of Plate III with the general geological map (Fig. 32) and the geophysical maps reveals the following. The schist belts are commonly parallel to, and the areas of different rocks and major lithologic units bordered upon, the lineaments. In the gravity map (Fig. 33), the gradiental, disruption or discontinuity zones of the anomalies frequently coincide with the lineaments.

It seems obvious that the lineaments shown on Plate III, being discernible in the LANDSAT-imagery, aeromagnetic maps and gravity maps, as well as in the distribution and orientation of different rock units, are traces of major fractures. The changes in the character of the rocks and the geophysical configurations across the fracture zones suggest considerable displacements. Blocks distinguishable on the basis of differences in geophysical and geological configuration and lithology are shown schematically in Plate IV.

The blocks are separated by long continuous fractures or fracture zones. Some of these zones, indicated by letters on Plate IV, have been described as block boundaries also in earlier literature. The blocks are transected by many other fracture zones, extending in some cases over the whole area. They divide the main blocks into numerous smaller ones.

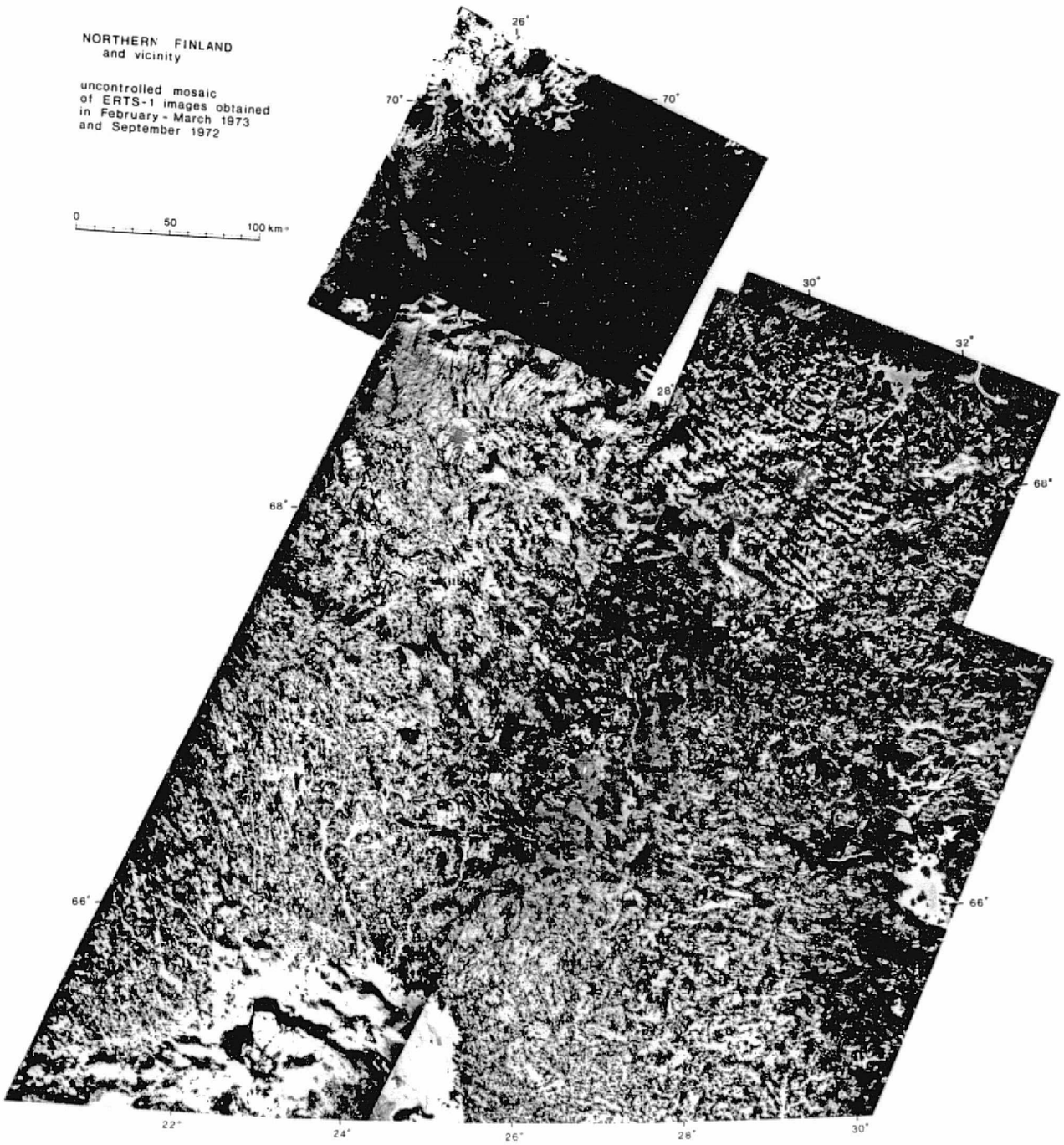

Fig. 29. Uncontrolled mosaic of LANDSAT-1 (former ERTS-1) images obtained over northern Finland and vicinity in the winter of 1973 and September 1972.

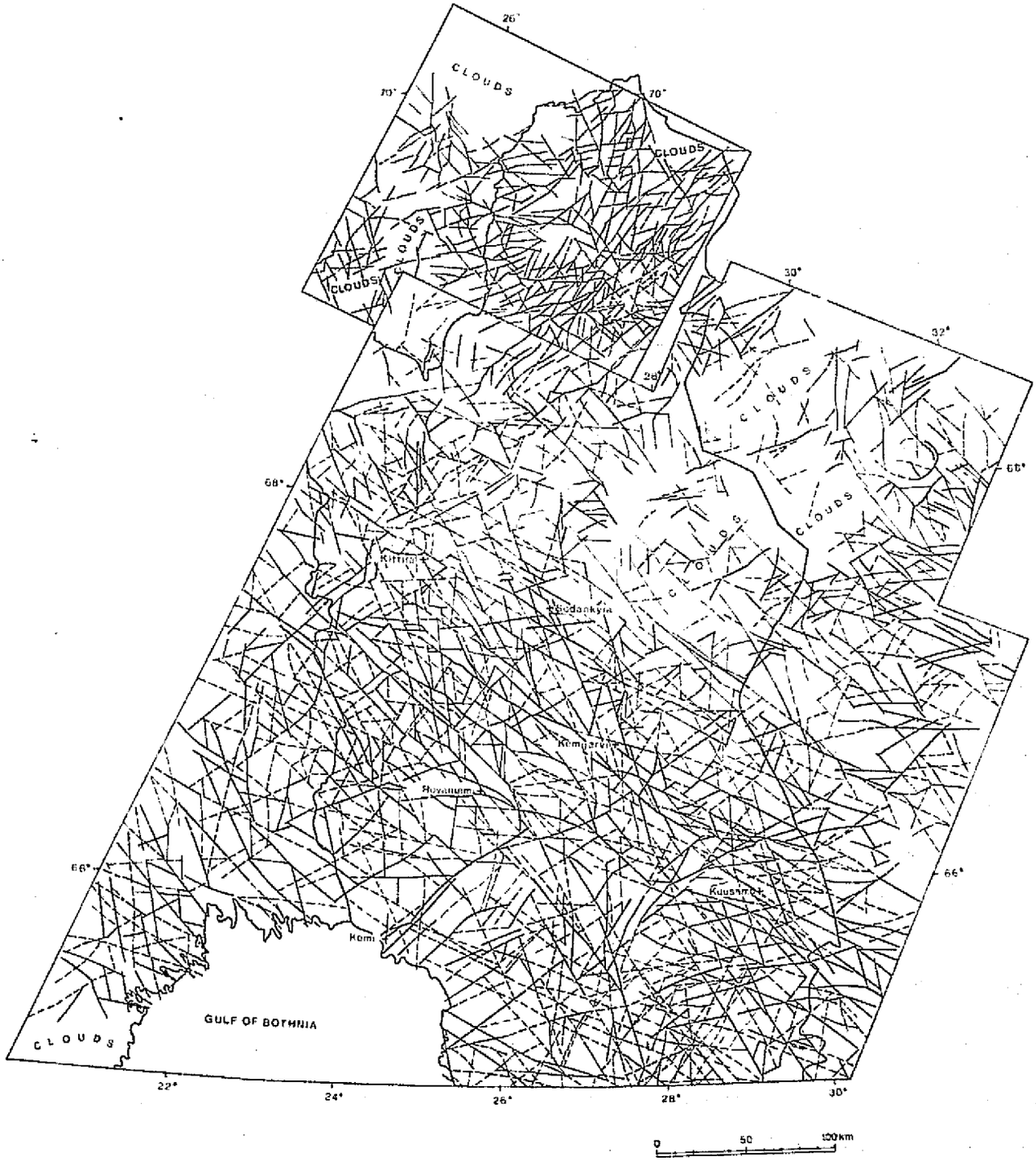

Fig. 30. Lineaments derived from LANDSAT imagery shown in the mosaic of Fig. 29.
~~ Border of Finland.
---- Lineaments, indicated by dashes where weakly detectable.

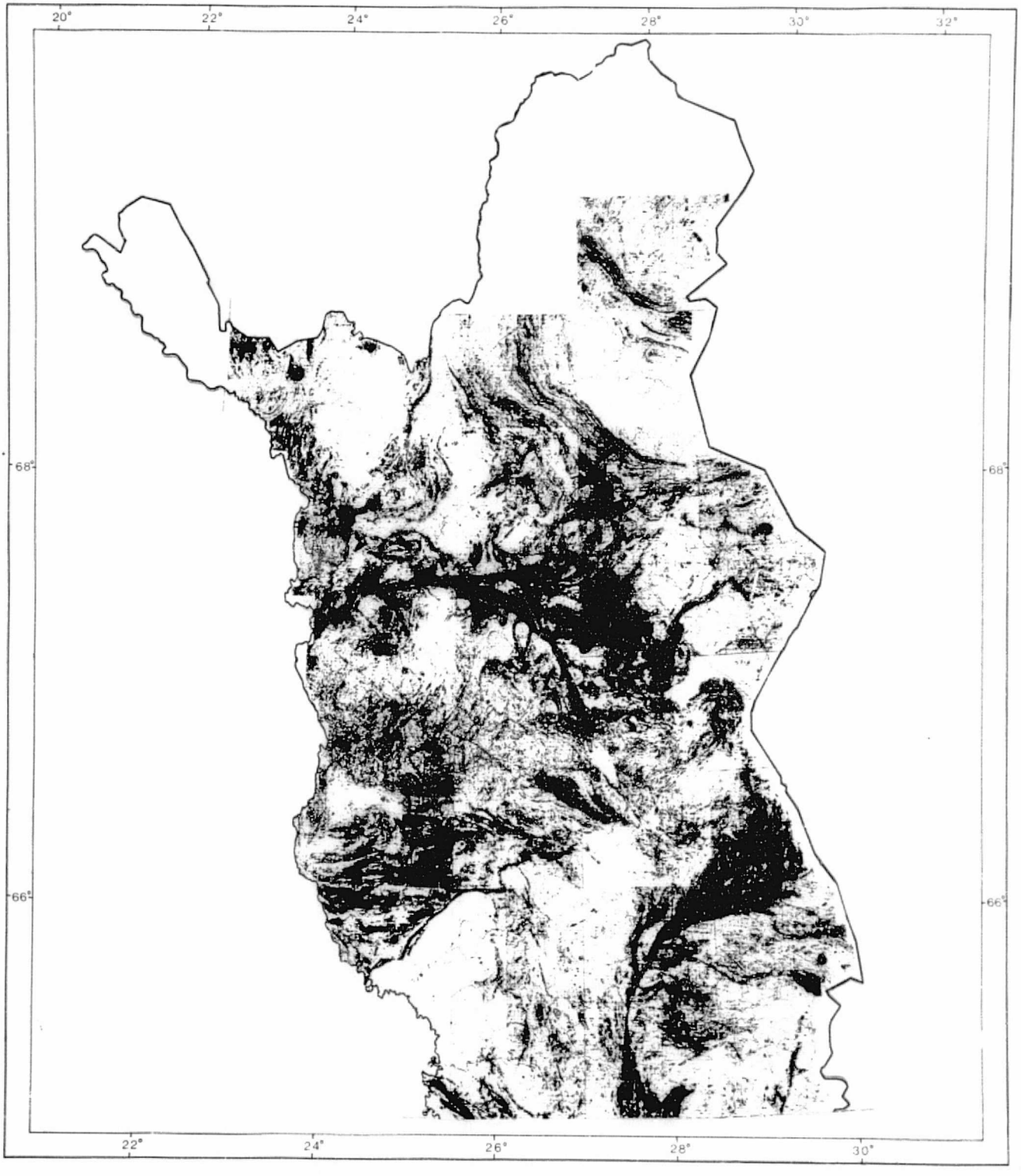

Fig. 31. Aeromagnetic anomalies of northern Finland. Compiled from 1 : 400 000 map sheets published by the Geological Survey of Finland.

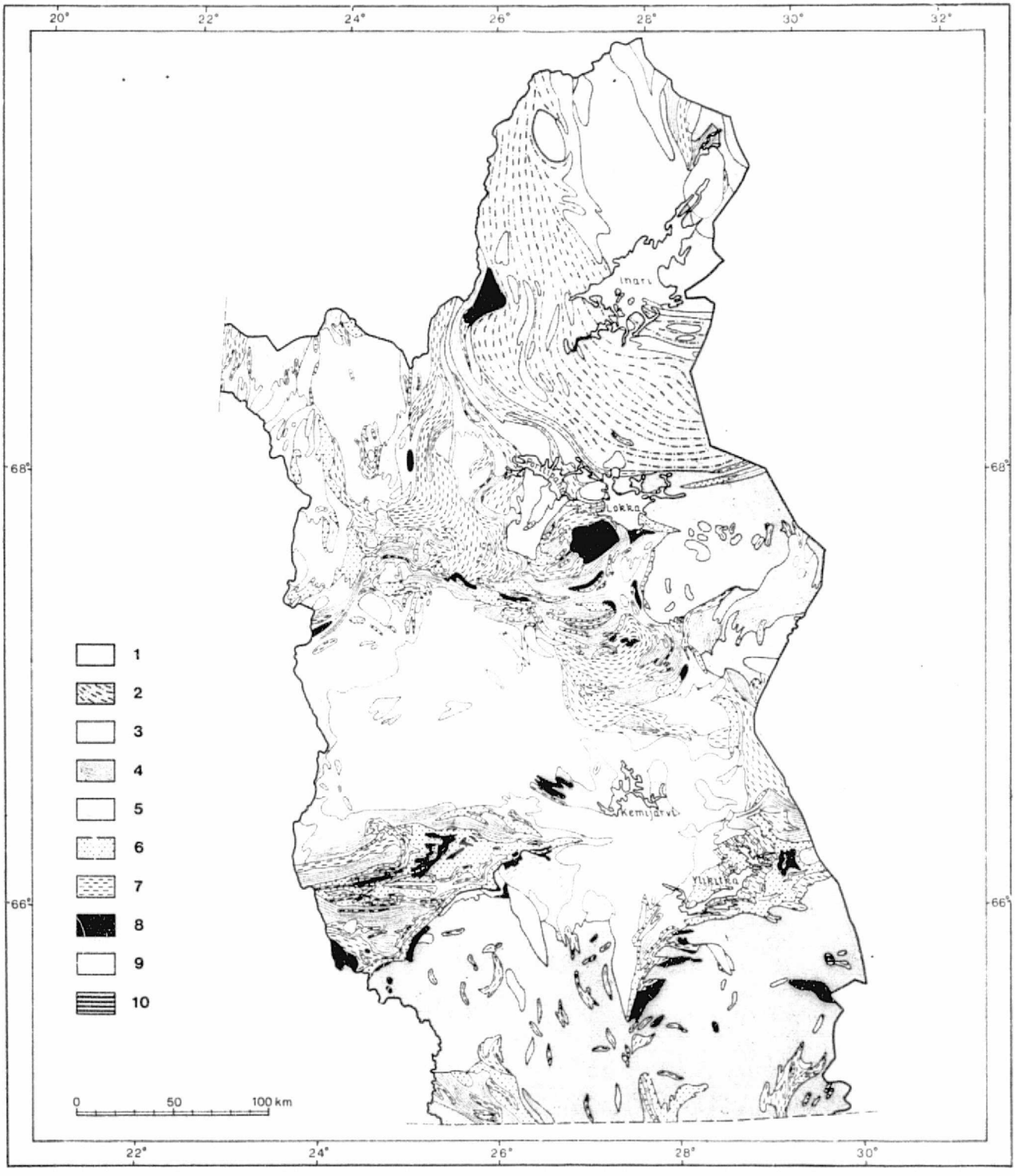

Fig. 32. Generalized geological map of northern Finland, mainly after Simonen (1960). Later mappings by Outokumpu Exploration are added.
1 granite gneiss, 2 granulite, 3 quartz-feldspar schist, 4 phyllite and mica schist, 5 migmatite, 6 quartzite, 7 metabasalt, amphibolite and hornblende gneiss, 8 gabbro, anorthosite, diabase and ultrabasic rocks, 9 granite, acid plutonic rocks in general, 10 alkaline rocks.

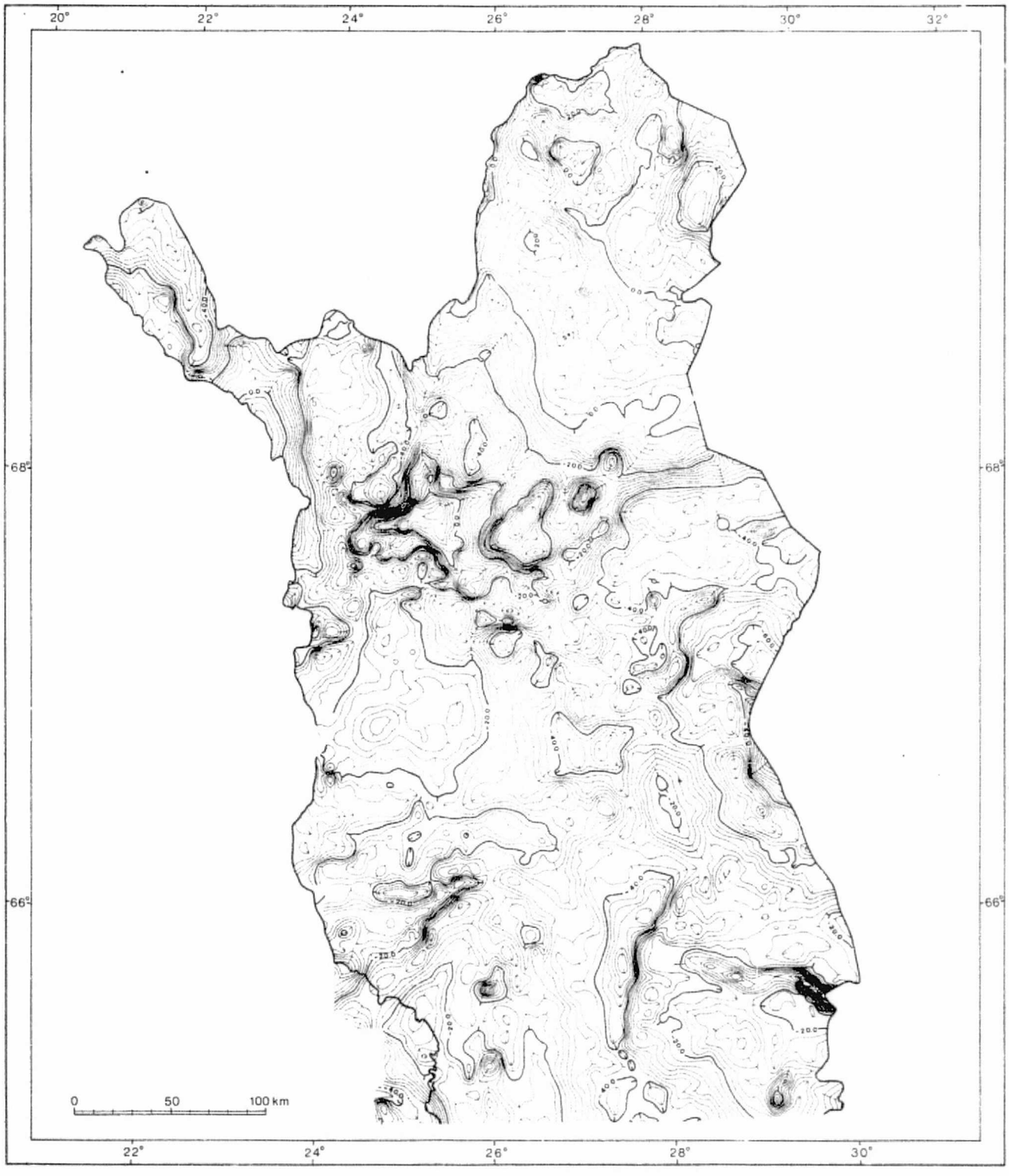

Fig. 33. Gravimetric map of northern Finland. Bouguer-anomalies. Redrawn from gravity maps made by the Geodetic Survey of Finland (Honkasalo 1975).

The fracture patterns seem to vary slightly from block to block. The greatest changes occur across the block boundaries bordering the main rock units of the area (Plate IV and Fig. 32). Some fractures are deflected or terminate at the block boundaries (e.g., at A-A and B-B in Plate IV). These results support further the conclusions reached in central Lapland (p.).

3.5 Mineralizations and major fracture zones

The relations between ore deposits and lineaments or fracture zones have for a long time attracted the attention of researchers (e.g., Mayo 1958, Landhwer 1967, Gorzhevskiy 1965, Kutina 1969 and 1971). In general, a positive correlation has been proposed to exist between them. In Finland the problem has been studied by, among others, Mikkola and Niini (1968), Talvitie and Paarma (1973), Gaál (1972) and Mikkola and Vuorela (1973).

To determine whether such correlations might exist in northern Finland, a map of known base metal deposits and mineralizations (Fig. 34) was compiled from data contained in various sources [1]. Since the

---

1) Mikkola and Niini (1968),
Professor Aimo Mikkola's personal data file on the mineralizations of Finland,
Mikkola and Vuorela (1973),
Metallogenic Map of Finland (Kahma 1973),
Ore Data File Project presently in progress in northern Finland.

source data include adequate genetic information in only a few cases, the ore deposits and mineralizations were divided into three broad groups: oxides, except Cr, sulphides, ecept Ni, and Ni and Cr. Especially the oxide group is heterogeneous, since it obviously includes mineralizations of both magmatic (Fe, Ti, V) and sedimentary (Fe, Mn) origin. Besides, most of the oxide mineralizations are marked only as Fe mineralizations in the source data. So it was not possible to classify them into more homogeneous groups. According to Mikkola and Niini (1968) the sulphide mineralizations (Cu, Zn, Pb, Fe and Mo) originated or, at least, were deformed under hydrothermal conditions or are of pegmatitic-pneumatolytic origin . The Ni and Cr mineralizations are associated with basic igneous rocks and belong to early magnatic ores (Mikkola and Niini, op.cit.).

The positions of altogether 142 mineral occurrences were plotted on the map, Fig. 34. Seventy-eight of them are oxides, except Cr, 45 sulphides, except Ni, and 19 Ni or Cr mineralizations. By superposing the map of fracture zones (Plate III) on Fig. 34, close relations between the fractures and the mineral occurrences can be perceived. Many of the occurrences seem to be situated directly in the fracture zones, that is, on the lines symbolizing these zones. Several others fall at a distance of only about two kilometers or less from a nearby line, which in many cases actually represents a wide zone of fracturing. When these distances are compared with the lengths - tens or even hundreds of kilometers - of the respective fracture zones, and with the spaces between the zones, it seems obvious that also these occurrences are related to the fracture zones. A summary of these relationships for each group of mineralizations separately is presented in Table 1.

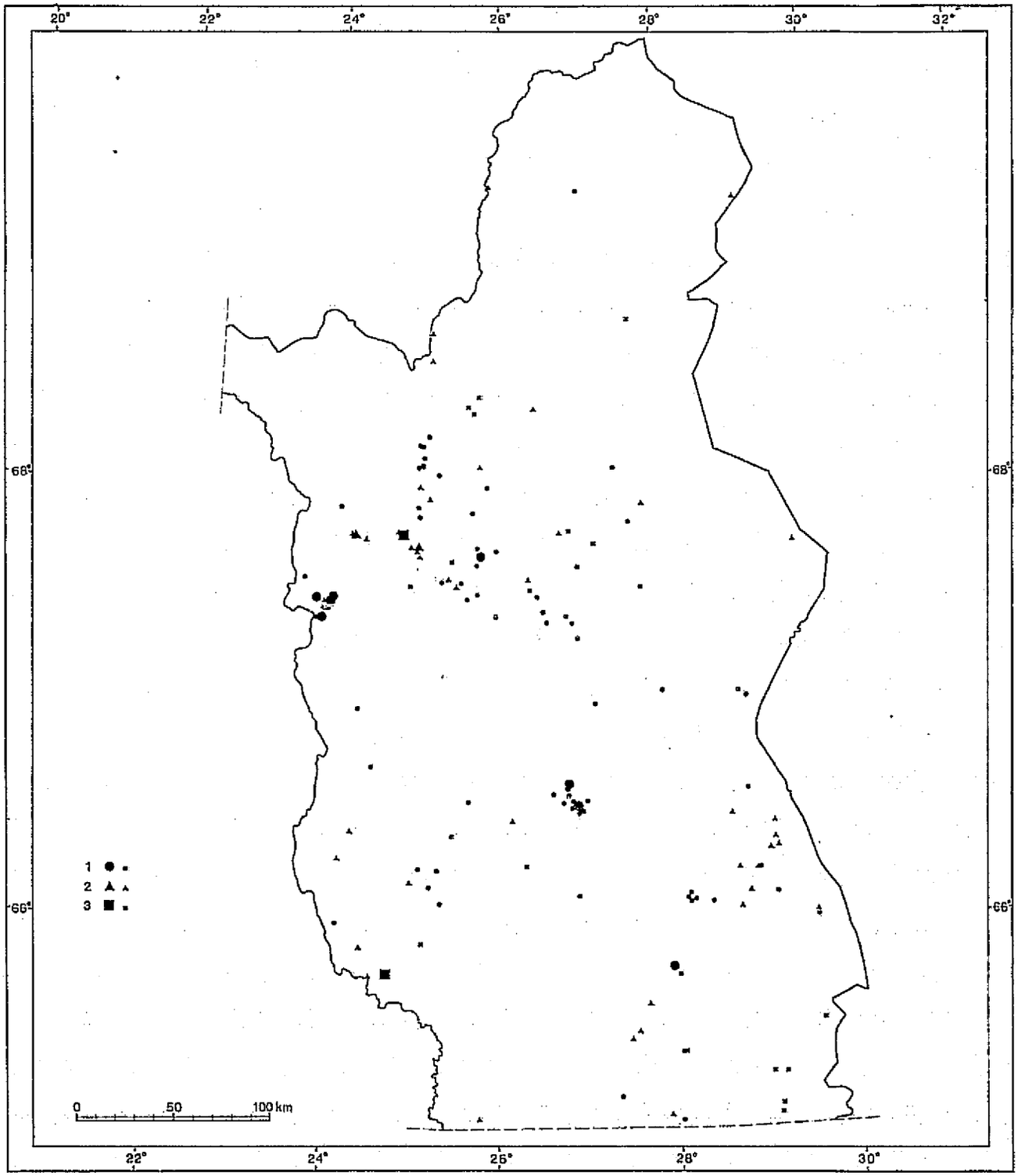

Fig. 34. Base metal deposits (large symbols) and mineralizations (small symbols) in northern Finland.
1: Oxides (Fe, Ti, V, Mn), 2: Sulphides (Cu, Zn, Pb, Fe, Mo), 3: Ni and Cr.

	1	2	3	4
Oxides (Fe, Ti, V, Mn)	78	30	27	21
Sulphides (Cu, Zn, Pb, Fe, Mo)	45	20	14	11
Ni and Cr	19	6	11	2
Total	142	56	52	34

Table 1. Summary of the relationships of the mineral occurences shown in Fig. 34 with the fracture zones of northern Finland (Plate III). 1: Number of occurrences, 2: number of occurrences situated within a fracture zone, 3: number of occurrences situated at a distance of about two kilometers or less from a line indicating fracture zone, 4: number of occurrences not correlating with the observed fracture zones.

It appears from Table 1 that 34 or 24 % of the mineral occurrences do not show any correlations with the fracture zones, 52 or 37 % are situated in the immediate vicinity of the zones, and finally 56 or 39 % are situated clearly within the observed fracture zones. Altogether 108, or 76 %, of the occurrences seem to have some correlation with the fracture zones and 33 or 24 % do not. Especially the Ni and Cr occurrences, associated with basic igneous rocks, seem to be situated within or near the fracture zones, but also sulphides and oxides show a clear tendency to concentrate along the zones.

An interesting question is whether the mineralizations are concentrated in fractures of certain trends or not. This kind of information could also be used in evaluating the different fracture trends for exploration purposes. Mikkola and Vuorela (1973) have studied this matter by tracing two main fractures from all the known ore

deposits or showings in Finland and compiling strike frequency rosettes with a 30° grouping from this data (Fig. 35). They conclude that the most important direction in this respect seems to be NW-SE all over Finland, but that in Lapland SW-NE trends are more frequently found associated with the ore deposits or showings than in other parts of the country.

To see whether this applies to the data used in the present study, the trends of all the fractures possibly associated with a mineral occurrence were observed. The results were then grouped at 10° intervals for each three types of mineralizations and plotted as rose diagrams (Fig. 35). A summary rosette was plotted for all the mineralizations combined.

The strike-frequency rosette for fractures associated with all the mineral occurrences (Fig. 35) correlates well with the results obtained by Mikkola and Vuorela (1973). The division of the NW-SE trending maximum of Mikkola and Vuorela into two separate maxima in this study is evidently due merely to the different grouping of the data. Judging from these data, it seems obvious that in northern Finland ore deposits and mineralizations are associated mostly with fracture zones trending 300°, 330° and 40°-50° on the average. A small maximum occurs also in the 0° direction. On the other hand, the mineral occurrences are evidently not generally concentrated along the fractures trending about 80°-100° (or-280°), and 10°-30°.

The strike-frequency rosettes for the fractures associated with each different group of mineral occurrences reveal a good correlation of oxide and sulphide occurrences with fractures trending 300° on the average. These rosettes have a smaller maximum in common also along the 50° trend. The

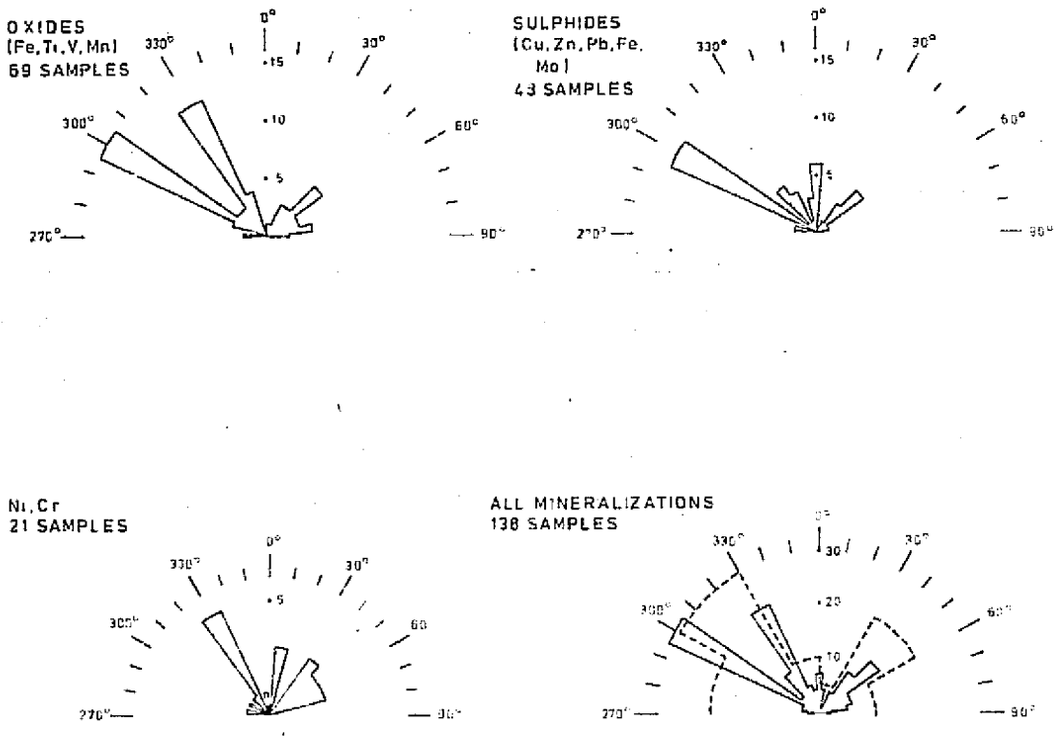

Fig. 35. Strike frequency rosettes of the fractures associated with ore deposits and mineralizations of different groups in northern Finland. Broken line in the rose diagram for all mineralizations indicate the strike frequency rosette for Lapland obtained by Mikkola and Vuorela (1973). It is not on the same scale as the rosette for all the mineralizations. The number of observed fractures in each 10^{o} group is shown in the N-S axis of the diagrams.

oxide occurrences are clearly associated also with fractures trending 330^{o}, but sulphide occurrences have only a minor maximum in this direction. They show, on the contrary, a tendency to concentrate rather along fractures with a northerly trend.

The strike frequency rosette for fractures associated with Ni and Cr occurrences is markedly different. The

300° trend, which is the most prominent in the two other rosettes, is nearly completely missing. A wide maximum area occurs in the 40°-70° range, with the highest peak at 40°, and a maximum in the 10° direction.

The number of observations of Ni and Cr occurrences is small. However, the absence of the maximum with a 300° trend could be of considerable importance, since it indicates that in northern Finland mineralized basic and ultrabasic intrusions may not be associated with fractures of this trend, but are rather concentrated in the fractures trending 330°, 40°-70°, and perhaps 10°, or roughly northward. This might also lead to age and genesis problems involving the fractures. Nevertheless, if this kind of difference is found also in further, more detailed studies, it could evidently be used as an exploration tool for Ni and Cr deposits.

4.0 CONCLUSIONS

The following conclusions and suggestions may be made about the use of LANDSAT-1 imagery in the analysis of geological features:

- The imagery has proven useful in mapping Quaternary glaciogenic features.

- Precambrian schist belts can be discerned from areas occupied by their basement rocks or major plutons. The major formations are easily located, but in detail the run of their boundaries tends to remain obscure. Masking enhancement pictures processed from bands 5 and 7 seem to provide a tool for more detailed studies.

- Different structural features can be discerned from

LANDSAT imagery. Large-scale layering, folds, fractures and faults have been identified in the study area.

- LANDSAT-1 imagery provides a rapid tool for the analysis of major bedrock structures. Moreover, these analyses are evidently far less expensive than the time-consuming aerial-photo interpretations of large areas. Simultaneous use of different remote sensing and geophysical material (e.g., aerial photos, aerogeophysical maps, gravimetric maps with LANDSAT imagery seems to provide the best results in these analyses.

- The interpretation of lineaments, representing fracture and fault zones, from the LANDSAT imagery is shown to have both advantages and disadvantages when compared with photolinear studies. The sets of linears with northeasterly to easterly trends are shown clearly in LANDSAT imagery because of the low-angle illumination effects and near-polar, sun-synchronous orbit. On the other hand, linear features trending near the scanning direction of the MSS-system have obviously been neglected in the interpretation of LANDSAT imagery, as is shown by the trend analysis of the linear maps. This is possibly due to the fact that the scanning lines form a line raster the direction of which has been apt to be avoided in the search for linears. These characteristics of the appearance of linear features in LANDSAT imagery should be kept in mind when studying them.

- In latitudes where the seasonal variation is great, a simultaneous study of winter and summer imagery is useful in detecting geological structures.

- It seems possible that optical filtering might provide a quick method to analyze LANDSAT imagery for linear geological structures and structural patterns in wide areas, such as the different shields or even continents. Statistical studies of this magnitude might produce new information related to plate tectonics.

The present analysis of LANDSAT imagery and geophysical data from northern Finland has revealed many zones of fracturing, which obviously represent surficial manifestations of major fractures dividing the bedrock into a mosaic of polygonal blocks. The fractures follow, in general, the eight main trends of crustal shear characteristic of the Baltic Shield; but they have different patterns within several of the main rock units, or main blocks, of the area. The major fracture zones, and blocks separated by them, have obviously played an important role in the evolution of the Shield. They have controlled the development of sedimentation basins and later deformations of the sediments, thus affecting the present distribution of the ancient supracrustal rocks. The deep fractures are zones of greater permeability in the crust, into which basic and ultrabasic rocks have been able to intrude. Thus they have controlled the locations of the ores associated with these intrusions. They have evidently also offered channels for volcanism and so controlled the distribution of volcanics and the ore deposits associated with them. The movements along the fractures and the higher permeability of these zones have also offered favorable conditions for the mobilization and migration of ore-bearing fluids, and for their concentration in chemically and physically favorable places.

REFERENCES

Aarnisalo, J. (1973) ERTS-tekokuututkimukset Suomessa ("ERTS-satellite studies in Finland". English abstract). Geofysiikan päivät Helsingissä 29-30.05.1973 (Ed. E Jatila). Helsinki.

_____(1974) ERTS-kuvia Suomesta (Summary: ERTS-scenes of Finland). Geologi 26, 8, 73-81.

_____and Mikkola, A.K. (1975) Fracture patterns of Finnish Lapland and their relation to ore deposits. Meeting of European Geological societies, Reading, U.K. Sept.,1975. Abstracts of keynote addresses and short communications. Univ. Reading. Reading, U.K.

Autio, H (1975) Aeromagneettisen anomalikentän suuntausanalyyttinen tulkinta (Trend analytical interpretation of aeromagnetic anomaly field; in Finnish). Ph.Lic. thesis. Ms. Arch. Techn. Helsinki Univ.

Bogdanov, V.I. and Khodotov, Yu.D. (1967) Some patterns of the block structure of the Baltic crystalline Shield. Geotectonics, 1, 53-55.

Brock, B.B. (1957) World patterns and lineaments. Trans. Geol.Soc. South Africa, 60, 127-160.

Gaâl, G. (1972) Tectonic control of some Ni-Cu deposits in Finland. Int. Geol. Congr. 24th session, Montreal, Sect. 4, 215-224.

von Gaertner, H.R. (1962) Gedanken zur Tektonik des "Lappländischen Granulite". Bull. Comm. Géol. Finlande, 204, 207-221.

Gorzhevskiy, D.I. (1965) About the metallogenetic importance of deep fractures. (in Russian). Geolog. sbornik Lvovsko geolog. abshtsh.9, 19 p.

Haman, P.J. (1961) Lineament analysis on aerial photographs. Examplified in the North Sturgeon Lake area, Alberta. W. Can. Res. Publ. Geol. and rel. Sci, 2,1, 23 p.

Hobbs, W.H. (1911) Repeating patterns in the relief and in the structure of land. Bull. Geol. Soc. Am 22, 123-126.

Honkasalo, T. (1975) Gravity measurements. In Geodetic operations in Finland 1971-1974, 23 p. Geodetic Survey,Helsinki.

Hoppin, R.A. (1974) Lineaments: their role in tectonics of central Rocky Mountains. Am. Ass. Petrol. Geol. Bull., 58, 11, 2260-2273.

Härme, M. (1966) On the block character of the Finnish Precambrian basement. Ann. Acad. Sci. Fennicae A III 90, 133-134.

Kahma, A. (1973 The main metallogenic features of Finland. Geol. Surv. Finland, Bull. 265, 28 p.

Krutikhovskaya, Z.A., Pashkevich, I.K. and Simonenko, T.N. (1973) Magnetic anomalies of Precambrian shields and some problems of their geological interpretation. Can. J. Earth Sci. 10, 629-636.

Kuittinen, R. (1973) Demonstrating applicability of satellite data to hydrology: a brief report on the usability of satellite images in Hydrology and limnology. NASA-CR-130524, U.S. Dept. of Commerce. Publ. E73-10101, NTIS, Springfield, Va. 22151.

Kuosmanen, V. (1975) Pohjois-Suomen Bouguer-anomaliat ja kallioperän suurrakenteet (Bouguer-anomalies and major bedrock structures in northern Finland; (in Finnish). M.Sc. thesis,Ms. Arch. Dept. Geol. Min., Univ. Helsinki.

Kutina, J. (1969) Hydrothermal ore deposits in the western United States: A new concept of structural control of distribution. Science, 165, 12, 1113-1119.

_____ (1971) A contribution to the correlation of structural control of ore deposition between North America and Western Europe. Proc. IMA-IAGOD Meetings "70", Tokyo, 70-75.

Kuusela, K. (1973) Demostration of the applicability of satellite data to forestry. NASA-CR-130553, U.S. Dept.of Commerce.Publ. E 73-10297, NTIS, Springfield, Va 22151.

Landhwer, W.R. (1967) Belts of major mineralization in Western United States. Econ. Geol. 62, 4, 494-501.

Lathram, E.H. (1972) Nimbus IV view of the major structural features of Alaska. Science 175, 1423-1427.

Lattman, L.H. (1958) Technique of mapping geologic fracture traces and lineaments on aerial photographs. Photogr. Eng. 24, 568-576.

Matisto, A. (1959) (Map of Pre-Quaternary rocks), sheet B 8 Enontekiö. General Geological Map of Finland, 1 : 400 000.

Mayo, E.B. (1958) Lineament tectonics and some districts of the southwest. Min. Eng. 10, 11, 1169-1175.

Meriläinen, K.I. (1965) (Map of Pre-Quaternary rocks), sheet C 8-9 Inari-Utsjoki. General Geological Map of Finland, 1 : 400 000.

Mikkola, A. and Niini, H. (1968) Structural position of the ore-bearing areas in Finland. Bull. geol. Soc. Finland, 40, 17-33.

_____ and Vuorela, P. (1974) Ore-bearing areas and linearity in Finnish bedrock. Abstract.XI Nordiska Geologiska Vintermötet, Oulu/Uleåborg 1974 Jan. 3-5, B. Abstracts, program, deltagarlista och allmänna intructioner. Univ. Oulu, Oulu.

Mikkola, E. (1936 a) (Map of Pre-Quaternary rocks), sheet B 7 Muonio. General Geological Map of Finland, 1 : 400 000.

_____ (1936 b) (Map of Pre-Quaternary rocks), sheet D 7, Tuntsajoki, General Geological Map of Finland, 1 : 400 000.

_____ (1937) (Map of Pre-Quaternary rocks), sheet C 7 Sodankylä, General Geological Map of Finland, 1 : 400 000.

Nanyaro, J.T. (1975) On the geology and lineaments of northern Finnish Lapland, with special reference to the Lemmenjoki and Ivalo gold districts. M.Sc. thesis. Ms. Arch. Dept. Geol. Min., Univ. Helsinki.

NASA/GSFC (1972) Data user's handbook. Greenbelt, Maryland.

NDPF/NASA User Services (1972) Earth resources technology satellite, Non-U.S. standard catalog, Vols. of Aug. 18, 1972, through Dec. 31. 1972.NASA/ GSFC, Greenbelt, Maryland.

NDPF/NASA User Services (1973) Earth resources technology satellite, Non-U.S. standard catalog, Vols. of Jan. 31, 1973,through Oct. 31, 1973. NASA/ GSFC, Greenbelt, Maryland.

Newhouse, W.H. (1942) Structural features associated with the ore deposits descriped in this volume (In:Ore deposits as related to structural features.Ed. W.H. Newhouse). Princeton Univ. Press, Princeton, N.J.

Paarma, H. (1963) On the tectonic structure of the Finnish basement, especially in the light of geophysical maps. Fennia 89, 1, 33-36.

_____ Aarnisalo, J.and Talvitie, J. (1974) On the tectonic control of weathered iron formations in Finnish Lapland. Abstract. XI Nordiska Geologiska Vintermötet, Oulu/ Uleåborg 1974 Jan. 3-5. B. Abstracts, program, deltagarlista och allmänna instruktioner. Univ. Oulu, Oulu.

_____ and Marmo, V. (1961) Eräistä suurrakenteista Suomen geologiaan sovellettuina. Summary: On some large structures with an application to geology of Finland. Terra, 73, 2, 78-86.

Perevoztšikova, V.A.,Ed. (1974) Tectonics of the eastern parts of the Baltic Shield (in Russian). 287 p. Nedra, Leningrad.

Petrov, A.J. (1970) Old faults in the eastern part of the Baltic Shield. Am. Geol. Inst., 191 (transl.) 56-62.

Sabatini, R.R., Rabehevsky, G.A. and Sissala, J.E. (1971) Nimbus Earth resources observations. Techn. Rep. 2. Prep. for NASA, GSFC, Greenbelt, Md. (Contr. No. NAS 5-21617). Allied Res. Assoc., Inc., Concord, Mass., 256 p.

Sahama, Th.G. (1933) Die Regelung von Quarz und Glimmer in den Gesteinen der Finnisch-Lappländischen Granulit formation. Bull. Comm. Geol. Finlande 113, 90-113.

Salop, L.I. (1971) The main features of the stratigraphy and tectonics of the Precambrian of the Baltic Shield (in Russian). (In Problemy geologii dokembrija Baltijskogo Shchita i pokrova Russkoj Platformy.) Trudy VSEGEI, 175, 6-87.

Simonen, A. (1960) (Map of Pre-Quaternary Rocks in Finland,1:2 000 000.) Pre-Quaternary rocks in Finland, Bull. Comm. Géol. Finlande 191, 49 p.

_____ (1971) Das Finnische Grundgebirge (English abstract). Geol. Rundsch. 60, 4, 1406-1421.

Simonenko, T.N. and Tolstikhina, M.M. (1968) Block structure of folded basement in the European USSR, Geotectonics 4, 222-229.

Talvitie, J. (1971) Seismotectonics of the Kuopio region, Finland. Bull. Comm. Géol. Finlande 248, 41 p.

_____(1974) ERTS winter imagery as a tool for tectonic and tectonophysical studies in the Baltic Shield, Finland. Photogramm. J. Finland, 6, 2, 174-184.

_____ and Paarma, H. (1973) Reconnaissance prospecting by photogeology in northern Finland. (In:Prospecting in areas of glacial terrain. Ed. M.J. Jones), 73-81. The Inst. Mining and Metallurgy. London.

Tchalenko, J.S. and Ambraseys, N.N. (1970) Structural analysis of the Dasht-e Bayaz (Iran) earthquake fractures. Geol. Soc. Am. Bull., 81, 41-60.

Tuominen, H.V. (1957) The structure of an archean area: Orijärvi, Finland. Bull. Comm. Géol. Finlande 177, 32 p.

_____ (1973) Major crustal fractures in the Baltic Shield. NASA-CR-132189. U.S. Dept. of Commerce Publ. E74-10682, NTIS, Springfield, Va. 22151.

_____ Aarnisalo, J. and Söderholm, B. (1973) Tectonic patterns in the central Baltic Shield. Bull. Geol. Soc. Finlande 45, 205-217.

Wilson, J.T. (1941) Structural features in the Northwest Territories. Am. Jour. Sci., 239-502.

Wise, D.U. (1968) Regional and sub-continental sized fracture systems detectable by topographic shadow techniques. (In: Research in tectonics. Ed. Baer, A.J. and Norris, D.K.) Geol. Surv. Canada, Paper 68-52, 175-199.

Vuorela, P. (1973) Ruhjevyöhykkeet ja niiden suhde malmiesiintymiin ja malmeihin Suomessa (Fracture zones and their relation to ore showings and deposits in Finland; in Finnish), 53 p. Ph:Lic. thesis. Ms. Arch. Helsinki. Univ. Techn.

Zhdanov, V.V. and Sprygina, T.V. (1968) Block structure of the Baltic Shield. Geotectonics 3, 171-176.

NOTES ON THE PLATES

PLATE

I Class I linears representing fracture and fault zones. Same as Fig. 17.

II Most prominent fractures of central Finnish Lapland - dashes where inferred. Thickness of the line indicate the prominence of the zones.

III Significant lineaments of northern Finland representing major fractures, or component parts of them.

IV Schematic map of the main blocks in northern Finland. Fracture zones separating the blocks are shown as shaded areas. Dark shading: major block boundaries, usually separating blocks differing in their internal fracture patterns. Light shading: other important block boundaries. The zones described in earlier literature are indicated by letters:

A-A Sahama (1933), v. Gaertner (1962),

B-B Salop (1971),

C-C Talvitie and Paarma (1973).

PLATE I

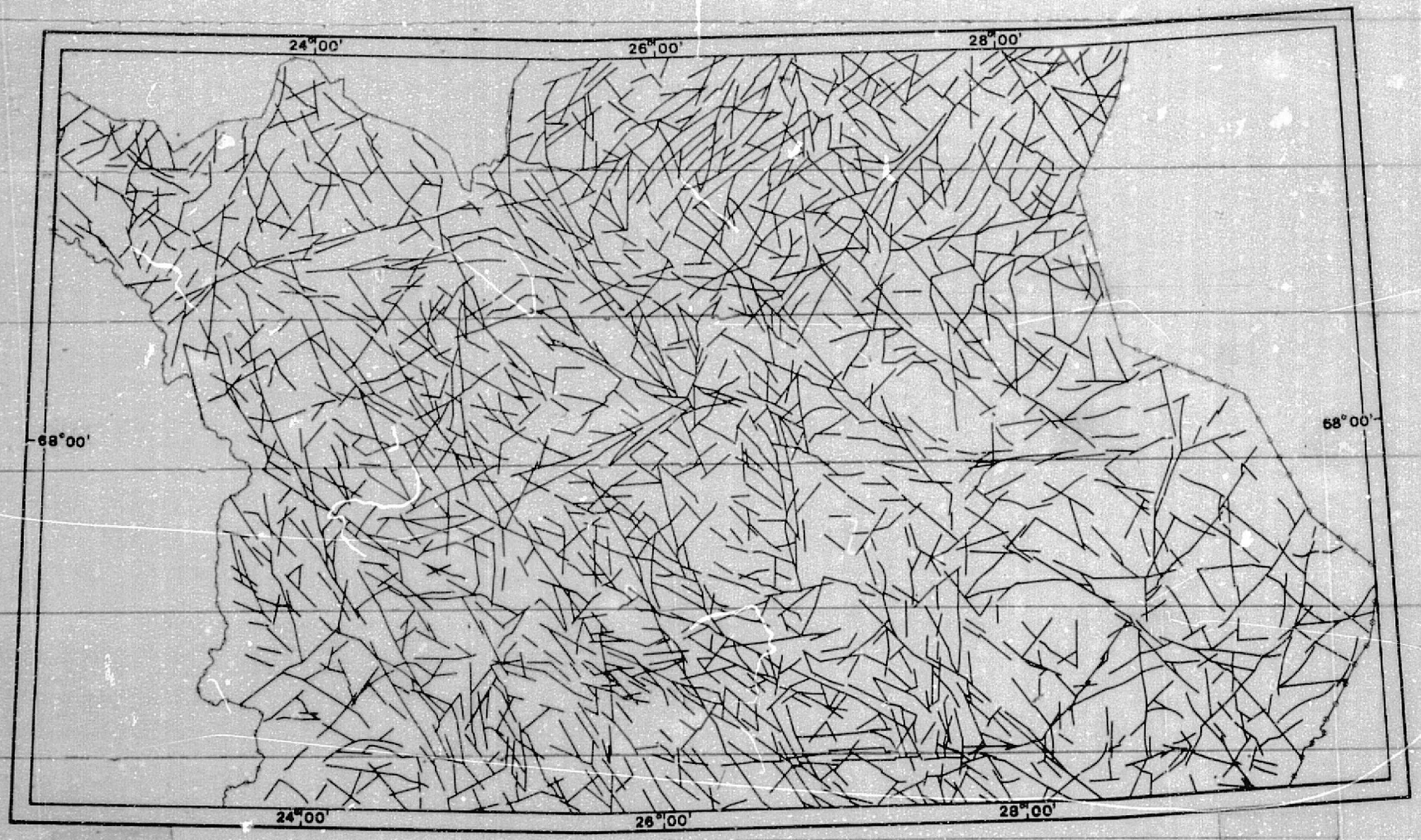

Jussi Aarnisalo: Use of satellite pictures for determining major shield fractures relevant for ore prospecting, northern Finland. SR 580-03, Type III Report, Sept. 1976.

PLATE II

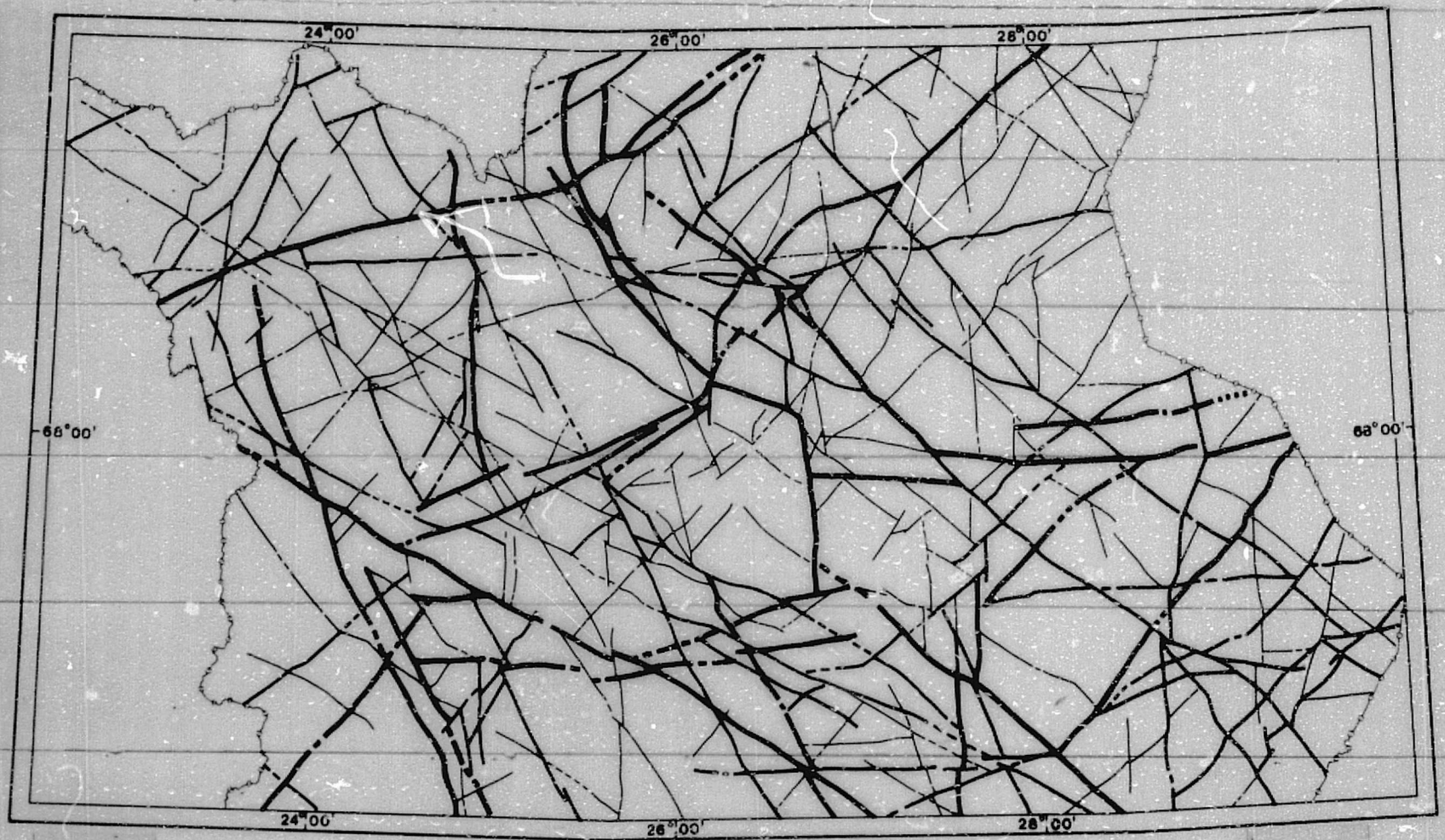

Jussi Aarnisalo: Use of satellite pictures for determining major shield fractures relevant for ore prospecting, northern Finland. SR 580-03, Type III Report, Sept. 1976.

PLATE III

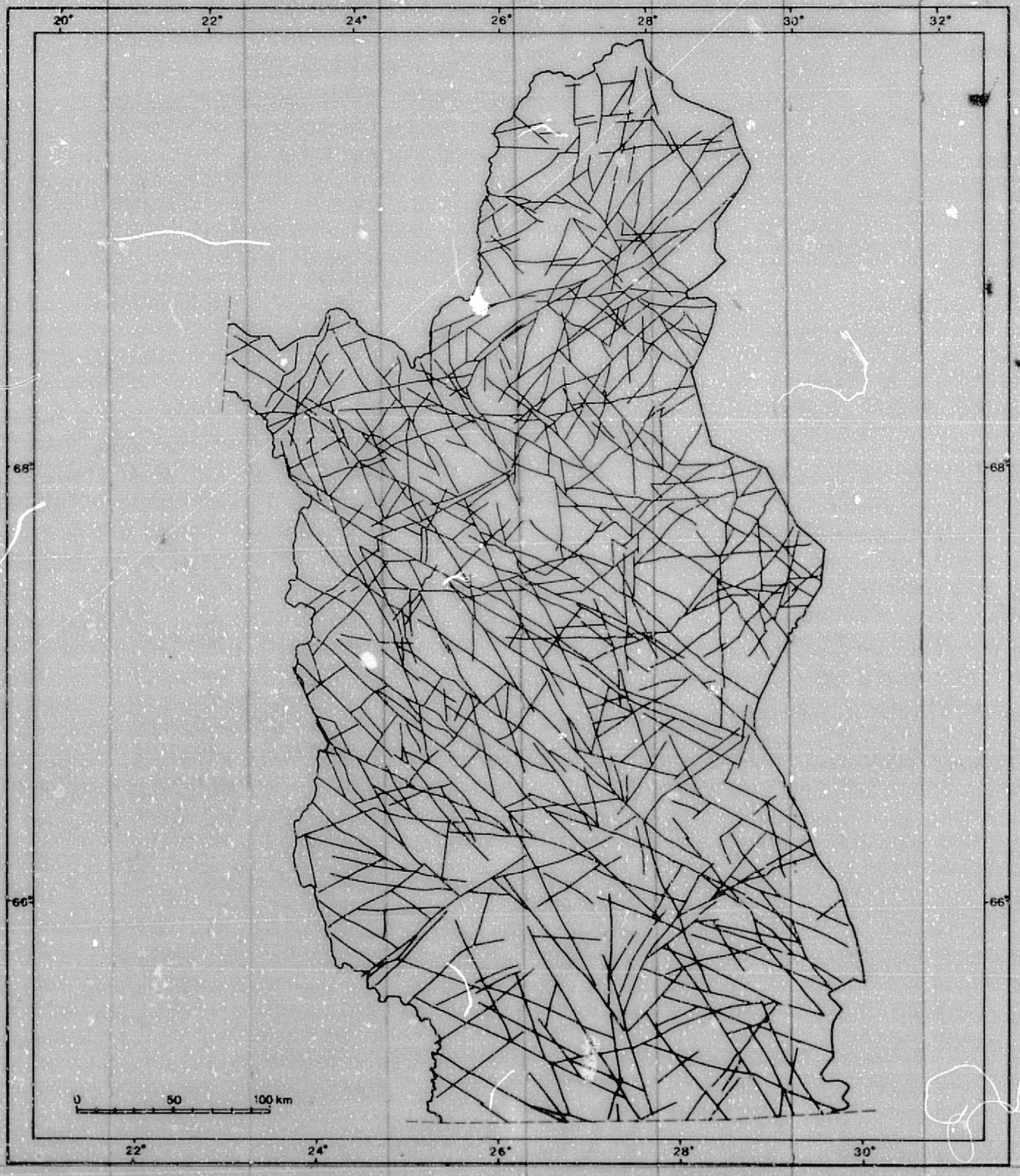

Jussi Aarnisalo: Use of satellite pictures for determining major shield fractures relevant for ore prospecting, northern Finland. SR 580-03, Type III Report, Sept. 1976.

PLATE IV

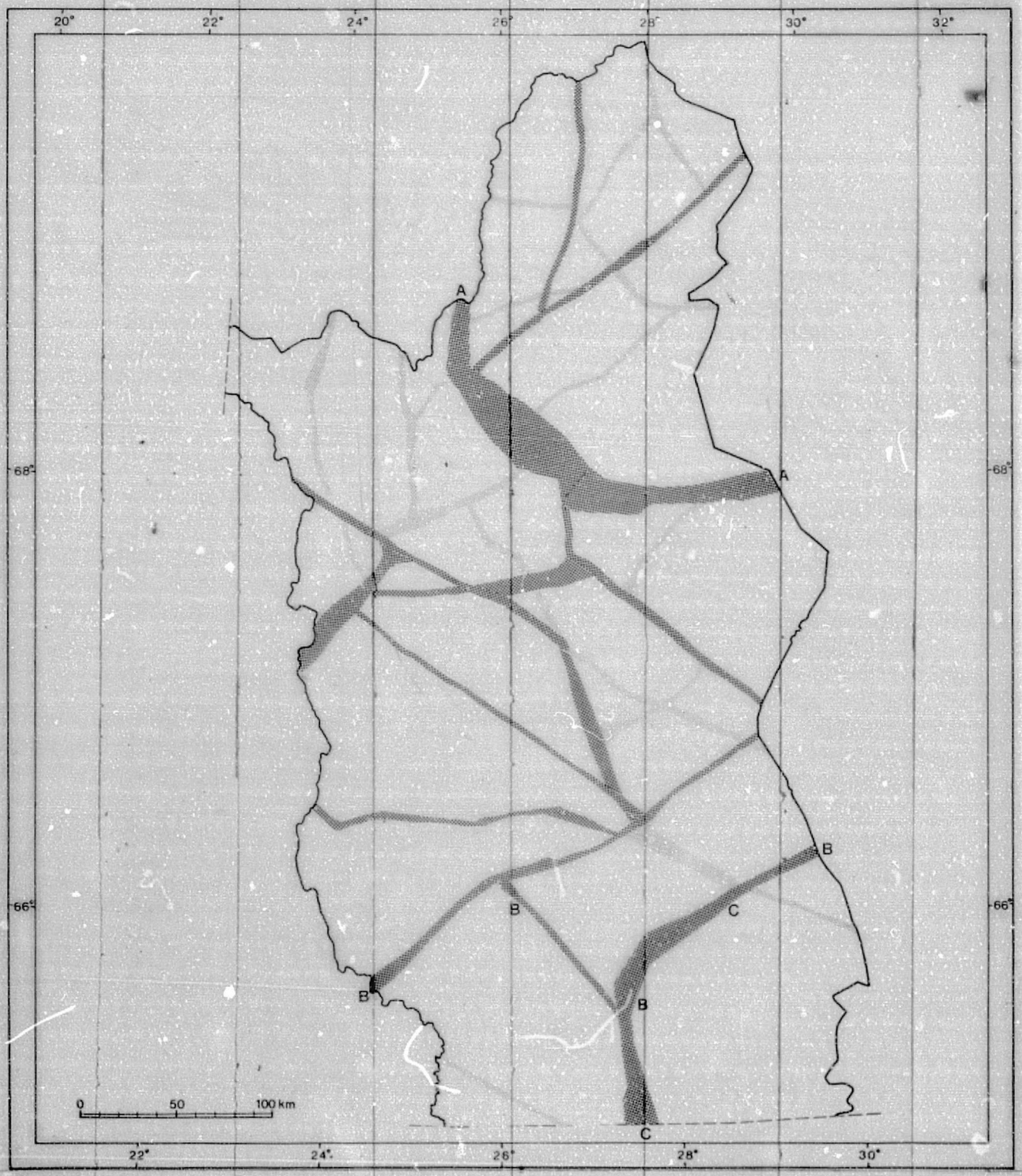

Jussi Aarnisalo: Use of satellite pictures for determining major shield fractures relevant for ore prospecting, northern Finland. SR 580-03, Type III Report, Sept. 1976.